

Overcoming Limitations in Dual Photoredox/Nickel catalyzed C–N Cross-Couplings due to Catalyst Deactivation

Sebastian Gisbertz, Susanne Reischauer, [Bartholomäus Pieber](#)

Submitted date: 13/11/2019 • Posted date: 25/11/2019

Licence: CC BY-NC-ND 4.0

Citation information: Gisbertz, Sebastian; Reischauer, Susanne; Pieber, Bartholomäus (2019): Overcoming Limitations in Dual Photoredox/Nickel catalyzed C–N Cross-Couplings due to Catalyst Deactivation.

ChemRxiv. Preprint. <https://doi.org/10.26434/chemrxiv.10298735.v1>

Dual photoredox/nickel catalyzed C–N cross-couplings are an attractive alternative to the palladium catalyzed Buchwald-Hartwig reaction, but are limited to aryl halides containing electron-withdrawing groups. We show that the formation of catalytically inactive nickel-black is responsible for this limitation. Deposition of nickel-black further deactivates heterogeneous photocatalysts restricting their recyclability. We demonstrate that catalyst deactivation can be avoided by the combination of nickel catalysis and a carbon nitride semiconductor. The broad absorption range of the organic, heterogeneous photocatalyst enables a wavelength dependent reactivity control to prevent nickel-black formation. A second approach is to run the reactions at high concentrations to increase the formation of nickel-amine complexes that reduce nickel-black formation. This allows reproducible, selective C–N cross-couplings of electron-rich aryl bromides.

File list (2)

manuscript.pdf (1.56 MiB)

[view on ChemRxiv](#) • [download file](#)

SI.pdf (8.70 MiB)

[view on ChemRxiv](#) • [download file](#)

ARTICLE

Overcoming Limitations in Dual Photoredox/Nickel catalyzed C–N Cross-Couplings due to Catalyst Deactivation

Sebastian Gisbertz,^{1,2} Susanne Reischauer^{1,2} & Bartholomäus Pieber^{1*}

¹*Department of Biomolecular Systems, Max-Planck-Institute of Colloids and Interfaces, Am Mühlenberg 1, 14476 Potsdam, Germany*

²*Department of Chemistry and Biochemistry, Freie Universität Berlin, Arnimallee 22, 14195 Berlin, Germany*

**Corresponding author*

Email: bartholomaeus.pieber@mpikg.mpg.de

Abstract

Dual photoredox/nickel catalyzed C–N cross-couplings are an attractive alternative to the palladium catalyzed Buchwald-Hartwig reaction, but are limited to aryl halides containing electron-withdrawing groups. Here we show that the formation of catalytically inactive nickel-black is responsible for this limitation and causes severe reproducibility issues. Deposition of nickel-black further deactivates heterogeneous photocatalysts restricting their recyclability. We demonstrate that catalyst deactivation can be avoided by the combination of nickel catalysis and a carbon nitride semiconductor. The broad absorption range of the organic, heterogeneous photocatalyst enables a wavelength dependent reactivity control to prevent nickel-black formation. A second approach, that is applicable to a broader set of substrates, is to run the reactions at high concentrations to increase the formation of nickel-amine complexes that reduce nickel-black formation. This allows reproducible, highly selective C–N cross-couplings of electron rich aryl bromides and enables efficient reactions of aryl chlorides.

MAIN

The palladium-catalyzed formation of carbon–nitrogen bonds (Buchwald-Hartwig) ranks among the most widely applied reactions in synthetic chemistry.¹ Nickel is an attractive alternative to palladium due to its higher abundance, but the air-sensitive Ni(0) complexes, sophisticated ligands, strong reductants, and bases required for C–N bond formations have hampered its use.²⁻⁴ Air-stable nickel pre-catalysts have been developed, but require harsh conditions and have a limited substrate scope (Figure 1, a).⁵⁻⁸ In combination with electrochemistry, ligated Ni(II) salts catalyze the C–N cross-coupling under mild conditions (Figure 1, b).^{9,10} Ligand-free Ni(II) salts were used together with UV light (365 nm),¹¹ or visible light photoredox catalysis (PRC)¹²⁻¹⁶ in a similar approach (Figure 1, c). Although synthetically attractive, electro- and photochemically mediated, nickel-catalyzed C-N couplings are limited to electron-poor aryl halides. Aryl halides that do not contain electron withdrawing groups are usually either unreactive,¹⁵ or give low yields,^{10-12,16} and only a few examples with a good isolated yield are reported (for a detailed analysis, see the Supplementary Information).^{13,17} Electro- and photochemically mediated methods rely on the initial reduction of the Ni(II) catalyst to a low valent (Ni⁰ or Ni^I) species, followed by oxidative addition that is slow for electron-rich aryl halides.^{10,18} This potentially leads to the accumulation of nickel(0) species that aggregate, resulting in catalyst deactivation. In the electrochemically driven, nickel-catalyzed aryl amination, nickel-black deposition was observed on the cathode and could be avoided by using Ni(bpy)₃Br₂ (bpy = 2,2' bipyridine) instead of a 1:1 mixture of NiBr₂·glyme and dtbbpy (4,4'-di-tert-butyl-2,2'-bipyridine), thereby expanding the scope to a few electron-rich heteroaryl halides.¹⁰ Stabilizing ligands are unsuitable for light mediated, nickel-catalyzed C–N cross-couplings,¹¹⁻¹⁶ but catalyst deactivation or nickel-black formation was not reported. It is, however, well known that Ni(II) salts – in presence of amines as sacrificial electron donors (SED) – can be used intentionally for the photochemical preparation of Ni(0) nanoparticles (Figure 1, d).¹⁹⁻²¹

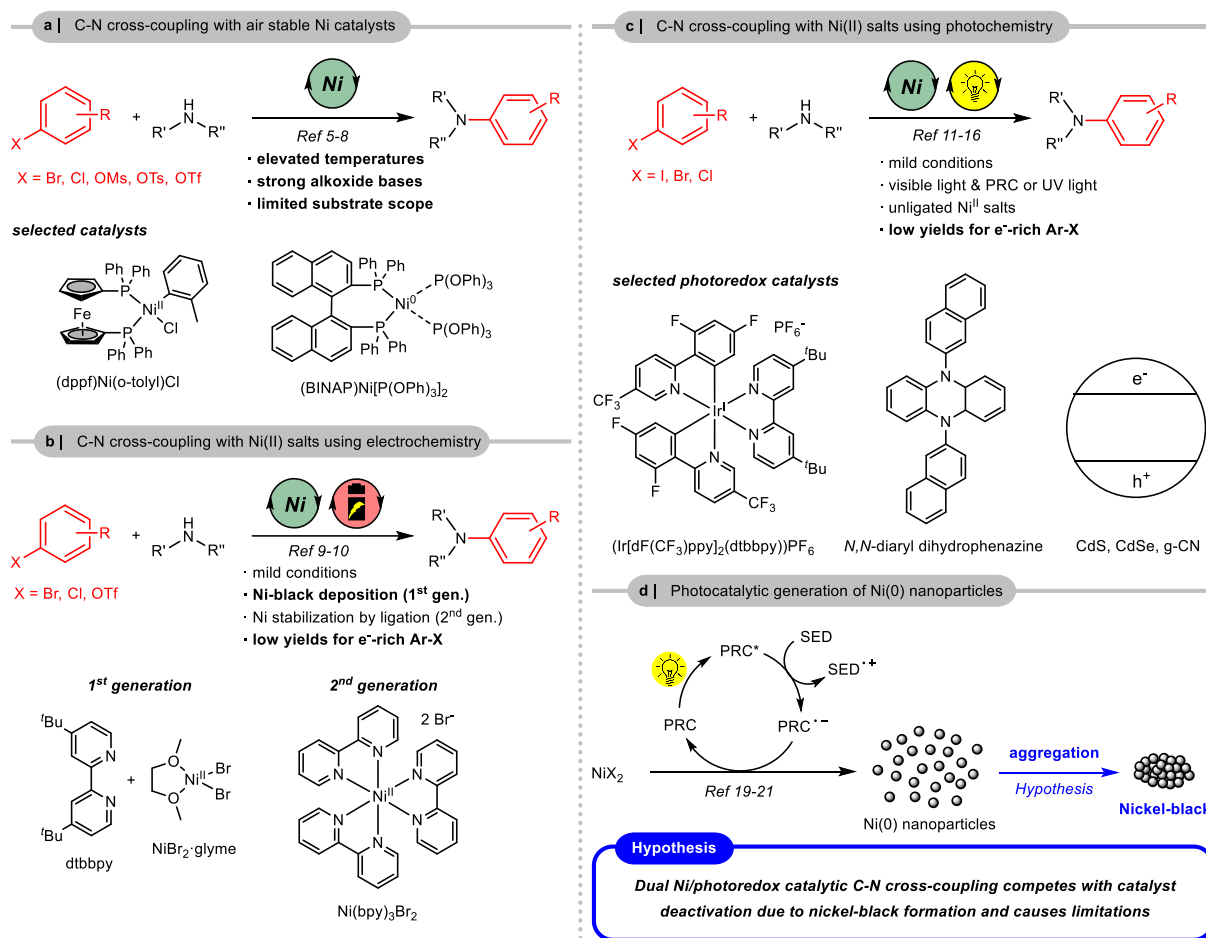


Figure 1 | Nickel catalyzed C–N cross-coupling reactions. **a**, air stable Ni precatalysts require harsh conditions. **b**, electrochemically enabled Ni-catalyzed aminations and; **c**, photochemically driven Ni-catalyzed aminations are limited to electron-poor aryl halides. **d**, photocatalytic reduction of Ni(II) salts for is used for nanoparticle formation potentially leads to nickel-black formation in catalysis.

Here, we show that catalyst deactivation via nickel-black formation is responsible for low yields for electron-rich aryl halides in dual photoredox/nickel catalyzed C–N cross-couplings. Deposition of the catalytically inactive, low-valent nickel species further deactivates a heterogeneous photocatalyst, hampering its recyclability. We demonstrate that nickel-black formation can be avoided by controlling the reactivity of a carbon nitride photocatalyst, or the reduction of catalyst-solvent interactions. The resulting protocols enable selective and reproducible couplings of electron-rich aryl halides, efficient reactions using aryl chlorides, and allow recycling of the heterogeneous photocatalyst.

Results

Our investigations started by optimizing the dual nickel/photoredox catalyzed amination of methyl 4-bromobenzoate with pyrrolidine using CN-OA-m, a carbon nitride derivative prepared from urea and oxamide (see Supplementary Information for details).²²⁻²⁴ Nearly quantitative formation of the desired alkyl aryl amine (**1**) was obtained within 8 h when CN-OA-m (3.33 mg mL⁻¹), NiBr₂·3H₂O (2.5 mol%) and three equivalents of the amine were used without any additional base in dimethylacetamide (DMAc) as solvent (Table 1, Entry 1-2).¹⁷ The reaction was easily scaled up by increasing the reaction time, affording **1** on a gram scale within 14 hours (see Supplementary Information). Aside from aryl bromides, aryl iodides coupled with similar efficiency and selectivity (Entry 3). The optimized protocol further enabled C–N couplings using aryl chlorides and aryl triflates, but these reactions did not go to completion (Entry 4-5).

Table 1 | Optimized conditions and control experiments using white LEDs (RGB)^[a]

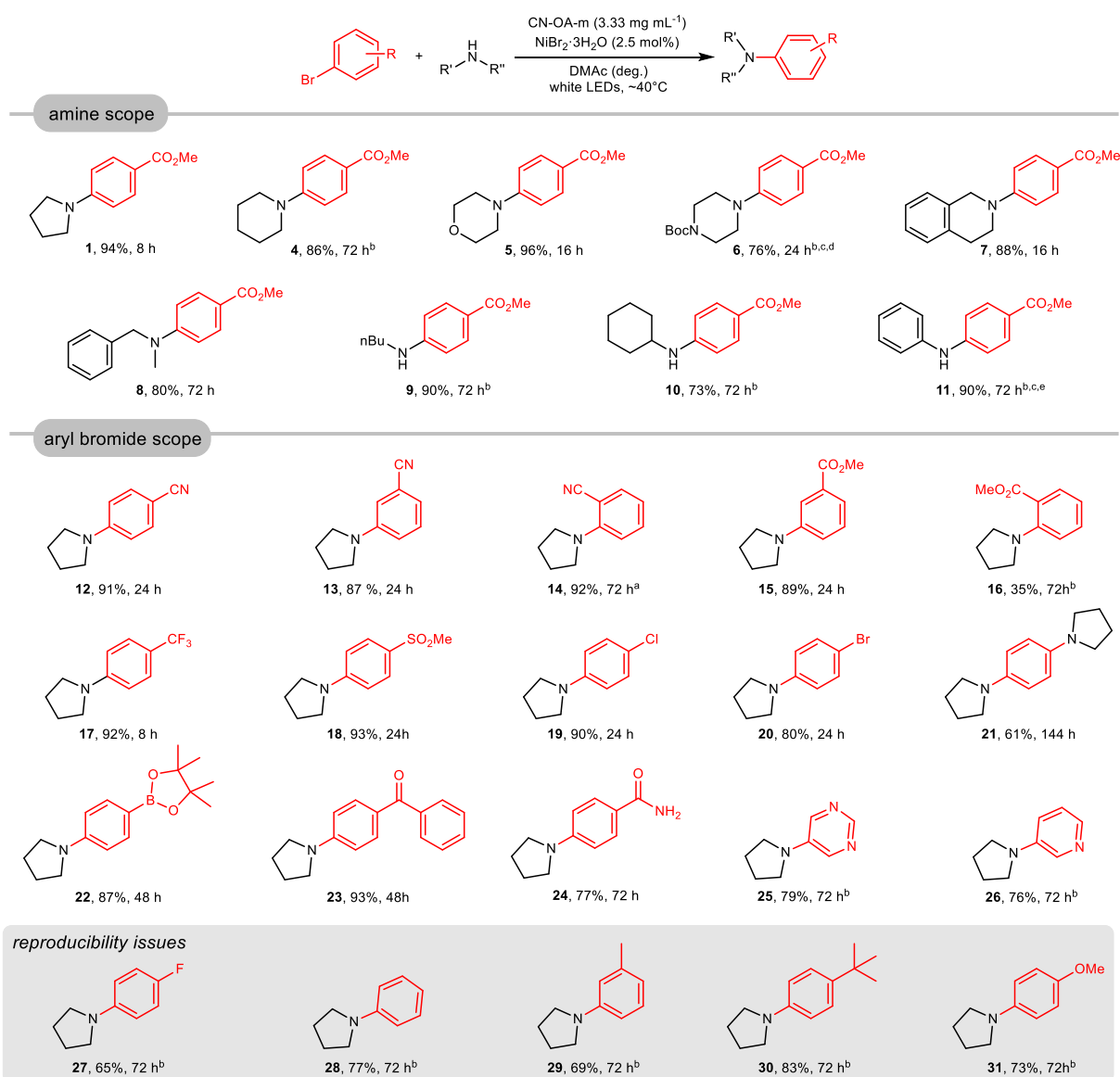
Entry	X	Conditions	Conversion [%] ^b	1 [%] ^c	2 [%] ^c	3 [%] ^c
1	Br	as shown	quant.	98	2	n.d.
2	Br	1.66 mg mL ⁻¹ CN-OA-m	quant.	96	2	1
3	I	as shown	quant.	99	1	n.d.
4	Cl	168 h	76	72	4	n.d.
5	OTf	72 h	75	67	5	2
6	Br	no CN-OA-m	5	n.d.	2	1
7	Br	no NiBr ₂ ·3H ₂ O	5	n.d.	n.d.	n.d.
8	Br	no light	<1	n.d.	n.d.	n.d.
9	Br	no degassing	10	10	n.d.	n.d.

^aReaction conditions: methyl 4-bromobenzoate (1.2 mmol), pyrrolidine (3.6 mmol), NiBr₂·3H₂O (2.5 mol%), CN-OA-m (20 mg), DMAc (anhydrous, 6 mL), white LEDs (RGB) at 40 °C for 8 h. ^bConversion aryl halide determined by ¹H-NMR using 1,3,5-trimethoxybenzene as internal standard. ^cNMR yields were determined by ¹H-NMR using 1,3,5-trimethoxybenzene as internal standard. n.d. = not detected. dtbbpy = 4,4'-di-*tert*-butyl-2,2'-bipyridine

With the optimized conditions in hand, the versatility of the semiheterogeneous catalytic system was evaluated (Table 2). The reaction of methyl 4-bromobenzoate with cyclic secondary amines generally gave high yields for the corresponding aryl amines (**1**, **4-7**). A secondary amine with low steric hindrance also resulted in the desired aryl amine (**8**), but the majority of acyclic secondary amines did not react under these conditions (see Supplementary Information). Aliphatic and aromatic primary amines reacted efficiently (**9-11**). Aryl halides containing electron-withdrawing groups coupled with high selectivity; Nitriles (**12-14**), carbonyl groups (**1**, **15**, **23-24**), trifluoromethyl- (**15**) as well as methylsulfonyl-groups (**16**), halides (**17-18**), boronic acid pinacol esters (**22**), and heteroaromatic bromides (**25**, **26**) were tolerated in the dual catalytic amination. 1,4-dibromobenzene can undergo selective mono- (**20**) or diamination (**21**) by varying the reaction time and stoichiometry of the amine coupling partner. Similar to related C–O bond formations,^{22,23} a carbonyl-group in the 2-position only gave moderate yield (**16**).

Although good isolated yields were obtained for 1-bromo-4-fluorobenzene (**27**),²⁵ bromobenzene (**28**), and aryl bromides with electron donating substituents (**29-31**), these values are not representative and these substrates suffered from severe reproducibility issues. The reactions frequently resulted in low yields and the heterogeneous PRC became black. High amounts of deposited nickel were detected on the recovered carbon nitride by ICP-OES analysis, indicating nickel-black formation (see Supplementary Information). Deactivation of metal catalysts via deposition is a common problem in palladium catalysis (Pd-black formation) and can be addressed by avoiding high concentrations of Pd(0) species that agglomerate.²⁶ In light-mediated, nickel catalyzed C–N cross-couplings, a Ni(0) complex was proposed to be the catalytically active species that is *i*) initially formed via a photoredox-catalyzed hydrogen atom transfer (HAT), and *ii*) regenerated in the last step of the catalytic cycle via a SET reduction of a Ni(I) intermediate by the PRC.¹⁸ Consequently, we assumed that controlling the reactivity of the photocatalytic system could enable us to decrease the accumulation of unstabilized Ni(0)

Table 2 | Scope of the semi-heterogeneous amination of amines and aryl bromides.^[a]



^aReaction conditions: aryl bromide (1.2 mmol), amine (3.6 mmol), CN-OA-m (20 mg), NiBr₂·3H₂O (30 μmol), DMAc (anhydrous, 6.0 mL), white LEDs at 40 °C. ^b5 mol% NiBr₂·3H₂O were used. ^c10 mol% pyrrolidine were added. ^dThe reaction was carried out on a 0.6 mmol scale. ^e3 equivalents *N*-*tert*-butylisopropylamine were added. Isolated yields are reported. For experimental details, see the Supplementary Information.

species, avoiding their aggregation. We hypothesized that this can be achieved using higher wavelengths as CN-OA-m has an extended visible light absorption that enables catalytic cross-couplings using green light.²³ The coupling of pyrrolidine and 1-bromo-4-fluorobenzene was indeed highly selective and reproducible using 520 nm LEDs (Method B), and the desired compound (**27**) was obtained in 85-91% in six parallel experiments (Figure 2, a). The same set of experiments using blue LEDs (~450 nm, Method A) exhibited large variations in yield. While

five experiments gave 60-70% of **27**, only 5-6% of the desired amine were formed for two reactions where the reaction mixture turned black. Careful analysis of the heterogeneous material recovered from the low yielding reactions identified the nature and quantity of the deposited Ni species (see Supplementary Information). ICP-OES analysis showed a Ni concentration of 126 mg g⁻¹ for the reaction irradiated with blue light and only 36 mg g⁻¹ for the material after an experiment using green LEDs. Elemental analysis via energy-dispersive X-ray spectroscopy (EDX) is in agreement with these results. X-ray powder diffraction (XRD) confirmed the deposition of low valent nickel species, with a significantly higher concentration on the material irradiated with blue light. High resolution X-ray photoelectron spectroscopy (XPS) for core levels of Ni2p_{3/2} spectrum of the recovered CN-OA-m from experiments using 450 nm LEDs (Method A) showed two main deconvoluted peaks located at 853.7 (±0.02) eV and 852.5 (±0.02) eV that can be assigned to the binding energy of Ni(II) and Ni(0) species, respectively. Only Ni(II) was detected on the material recovered from experiments using 520 nm LEDs (Method B) by XPS. Scanning transmission electron microscopy (STEM) was used to visualize nickel particles on the surface of the recovered CN-OA-m from both methods. High-angle annular dark-field (HAADF) images show a high amount of nickel particles that agglomerated (nickel-black) on the CN-OA-m recovered from experiments using 450 nm LEDs (Method A), whereas the material from experiments using 520 nm LEDs (Method B) contained almost no agglomerates (Figure 2, a).

Nickel-black formation was also shown to be responsible for low yields using other light-mediated protocols for the same model reaction (Figure 2, b). Using 1 mol% of the homogeneous PRC (Ir[dF(CF₃) ppy]₂(dtbbpy))PF₆,¹² resulted in low selectivity towards the desired coupling product (**25**, 33% yield), and small amounts of a black precipitate were formed during the reaction. Decreasing the amount of (Ir[dF(CF₃) ppy]₂(dtbbpy))PF₆ to 0.02 mol% increased the yield of **27** significantly (77%) and no particle formation was observed. Here, the

amount of the PRC plays a crucial role to avoid nickel-black formation and the optimal catalyst loading needs to be determined for each substrate individually. The PRC-free, UV light-

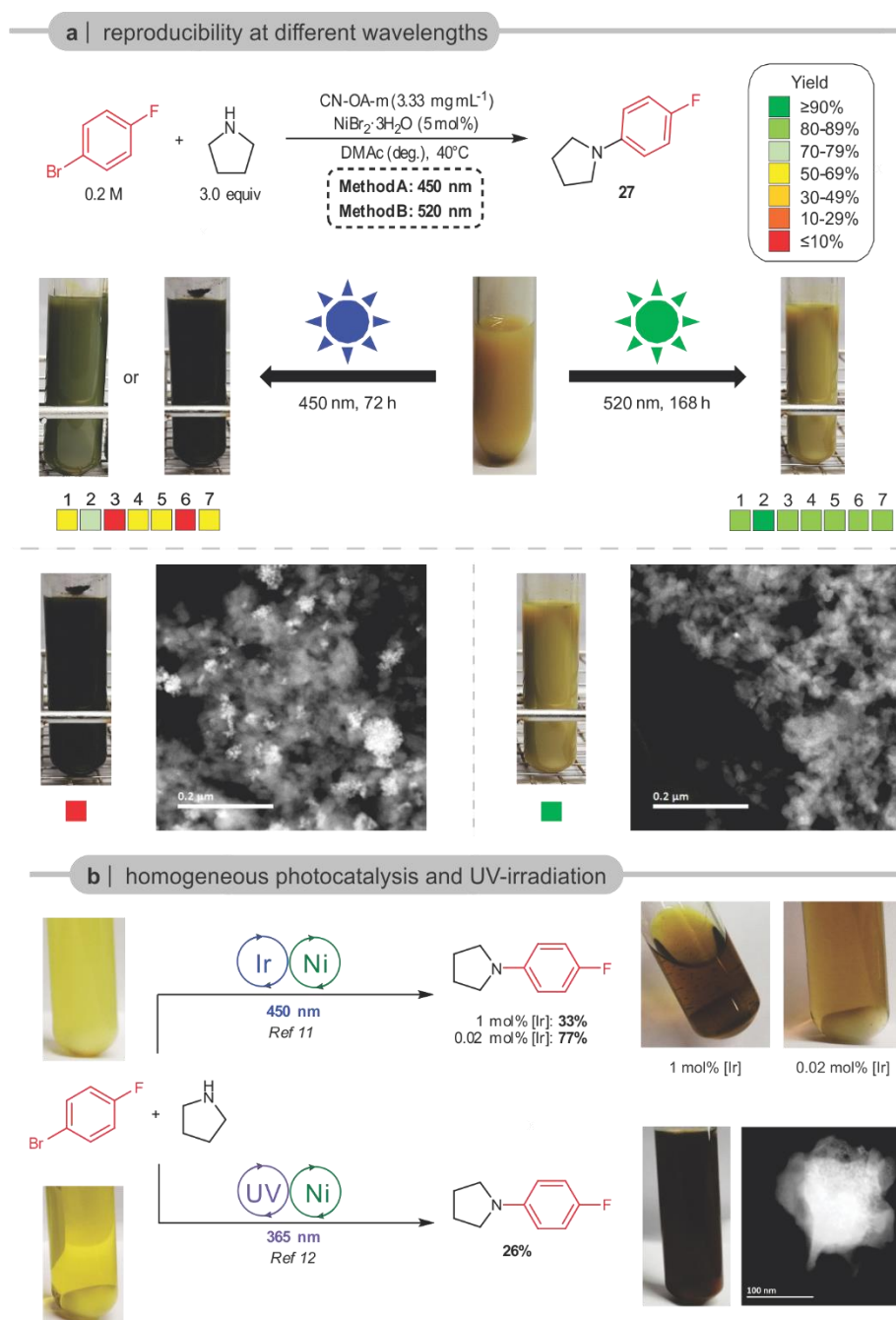


Figure 2 | Catalyst deactivation during the reaction of 4-bromofluorobenzene with pyrrolidine. a, Reproducibility using blue (450 nm) and green (520 nm) LED irradiation. The reaction mixture turned dark green or black and suffered from severe reproducibility issues at 450 nm, whereas almost no color change and reproducible results were obtained at 520 nm. HAADF-STEM images show nickel particle agglomerates (bright spots) on CN-OA-m recovered the experiment using blue light and almost no agglomerates when 520 nm were used. **c,** Nickel-black formation was also observed using the homogeneous (Ir[dF(CF₃)ppy]₂(dtbbpy))PF₆ (= [Ir]) photocatalyst and in the PRC-free reaction using UV light. For experimental details, see the Supplementary Information.

mediated protocol¹¹ resulted in no more than 26% of **27** and a black precipitate was formed in high amounts (Figure 2, c). STEM imaging and EDX spectroscopy confirmed that these solids consist of nickel and organic matter that is presumably resulting from substrate/product degradation by the high-energy light source (see Supplementary Information for details).

The dual carbon nitride/nickel catalyzed protocol using green light (520 nm, Method B) did also enable selective, reproducible C–N cross-couplings of bromobenzene (**26**), and 3-bromotoluene (**27**) with pyrrolidine, but did not eliminate catalyst deactivation issues in the cases of 1-bromo-4-*tert*-butylbenzene (**28**), and 4-bromoanisole (**29**) (Figure 3, a). Although almost quantitative product formation was observed in some cases, the reactions sometimes gave low yields and black reaction mixtures. In the case of 1-bromo-4-*tert*-butylbenzene, for example, six parallel reactions using 450 nm (Method A) gave 52-70% of the desired product (**28**), whereas up to 92% as well as only 28 % were obtained under identical conditions using 520 nm (Method B). Efforts to increase the reproducibility and to minimize the nickel-black formation by changing the light intensity, distance between the reaction mixture and light source, varying the amount of both catalysts, changing the solvent or nickel catalyst, and adding MTBD¹² or dtbbpy to stabilize intermediate nickel species were not successful. We hypothesized that the formation of Ni(0) agglomerates is not only caused by the photon energy and activity of the photocatalyst but also results from competitive binding of the amine and the solvent (DMAc) with the nickel salt. In palladium catalyzed cross couplings, for example, PdArylXL_n intermediates, are known to form complexes with various solvents, including DMAc, that undergo β-hydride elimination followed by the formation of Pd(0) and Aryl-H.²⁷ Although pyrrolidine was shown to be the most favorable ligand in light-mediated, nickel catalyzed aminations,¹⁸ the high excess of DMAc likely leads to a significant amount of solvent-catalyst complexes. Indeed, running the reaction at 1.2 M instead of 0.2 M resulted in reproducible reactions and the desired products (**28-31**) were obtained in high yields even at 450 nm (Method C). These results could not be further improved using 520 nm irradiation,

suggesting that the photochemical nickel-black formation can be outpaced at high concentrations independent of the photon energy in our semiheterogeneous catalytic system (see Supplementary Information).²⁸

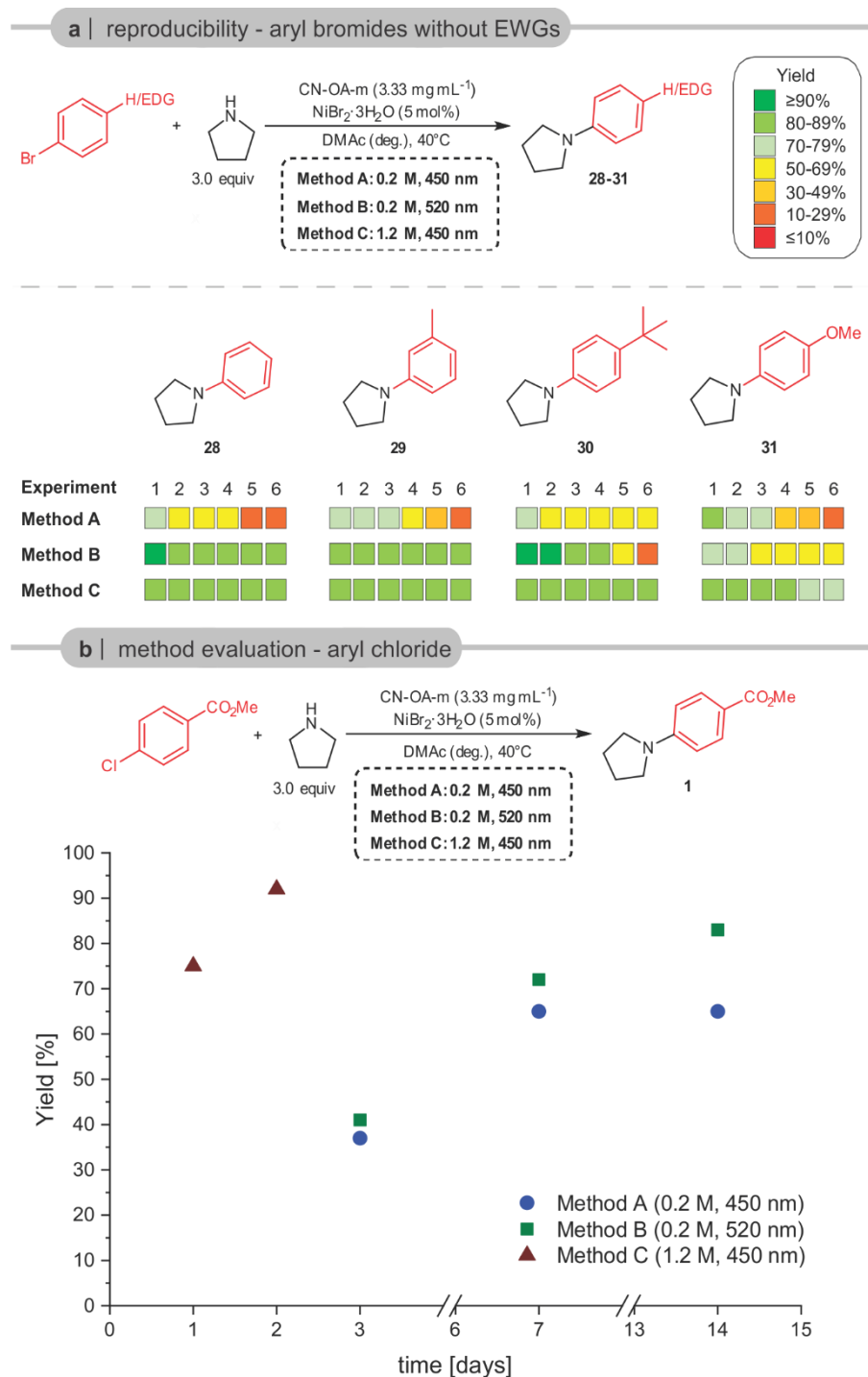


Figure 3 | Evaluation of different coupling protocols for non-activated aryl bromides and an aryl chloride. a, Reproducibility study for aryl bromides without electron withdrawing groups using different C–N coupling protocols **B,** Comparison of the different coupling protocols for the reaction of methyl 4-chlorobenzoate and pyrrolidine.

A reinvestigation of the coupling of methyl 4-chlorobenzoate with pyrrolidine was carried out using all protocols (Figure 3, b), as this reaction did not go to completion using the initially optimized conditions (Table 1, Entry 3). The standard protocol (Method A) afforded the desired coupling product (**1**) in 65% within seven days. Longer irradiation did not result in higher yields and only increased the amount of the dehalogenated side product, indicating complete catalyst deactivation (see Supplementary Information). With green light (Method B), 83% of **1** were obtained within 14 days. The optimized method using 450 nm LEDs and a lower amount of solvent (Method C) significantly enhanced the C–N coupling and resulted in 92% of **1** within two days.

Finally, we sought to study if the deposition of nickel-black also affects the recyclability of CN-OA-m by altering its photocatalytic activity. During the coupling of pyrrolidine with methyl 4-bromobenzoate using white (RGB) LEDs, the reaction mixture became greenish-brown (Figure 4, a). ICP-OES analysis of the heterogeneous material showed a nickel content of $\sim 14 \text{ mg g}^{-1}$. The product formation decreased significantly when the heterogeneous PRC was recycled (Figure 4, b).²⁹ Further, the yellow PRC turned dark green to black and the amount of deposited Ni rose to $\sim 61 \text{ mg g}^{-1}$ over five recycling experiments. At higher wavelengths (520 nm, Method B), the model reaction required 48 h instead of 8 h for full conversion (Figure 4, a). Although the reaction mixture did not change its color, the amount of deposited Ni was similar to the white LED experiment ($\sim 14 \text{ mg g}^{-1}$). The photocatalyst did, however, not lose its catalytic activity during five recycling experiments and was recovered as a yellow solid that contained a lower amount of deposited nickel ($\sim 39 \text{ mg g}^{-1}$) compared to the white light experiment (Figure 4, b). Scanning transmission electron microscopy (STEM) of CN-OA-m from both recycling studies showed a significant amount of nickel agglomerates (nickel-black) for CN-OA-m from the experiments using white LEDs, whereas almost no agglomerates were detected on the semiconductor recovered from the recycling study using green LEDs (see Supplementary Information).

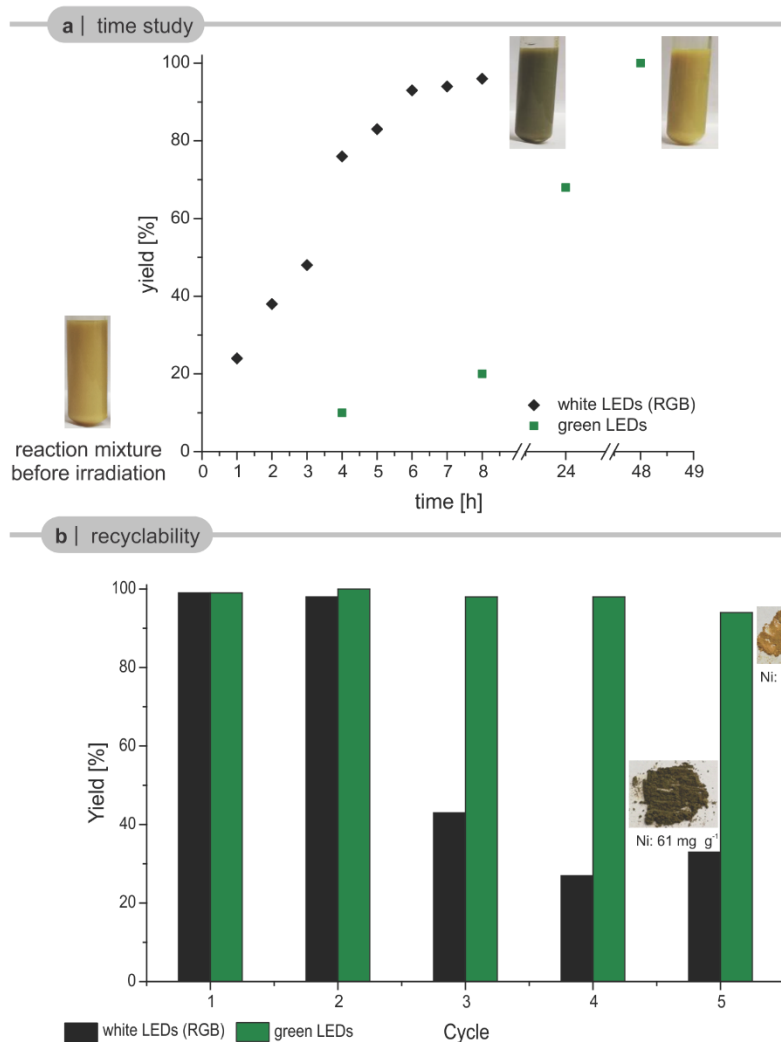
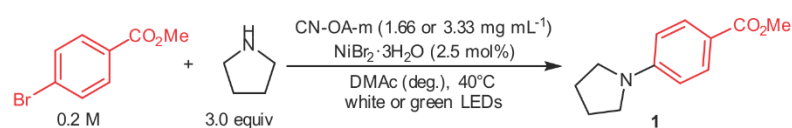


Figure 4 | Reduction of catalyst deactivation using higher wavelengths. **a**, Time study for the coupling of methyl 4-bromobenzoate and pyrrolidine using white (RGB) and green (~520 nm) LED irradiation. The heterogeneous photocatalyst turned green using white light (RGB) irradiation whereas no color change was observed when green light (~520 nm) was used. **b**, The recyclability of CN-OA-m is excellent using green (~520 nm) LEDs. Deactivation of the PRC by nickel-black depositions was observed using white (RGB) LEDs. For experimental details, see the Supplementary Information.

Conclusion

The formation of nickel-black limits the applicability of light-mediated, nickel catalyzed C–N cross-couplings. In particular, aryl halides lacking electron withdrawing groups suffer from reproducibility problems due to deactivation of the nickel catalyst. Deposition of agglomerated

nickel particles (nickel-black) not only deactivates the homogeneous nickel catalyst, but also the heterogeneous carbon nitride photocatalyst. Careful studies using dual carbon nitride/nickel catalysis showed that nickel-black formation can be avoided by wavelength dependent reactivity control to avoid agglomeration of low valent nickel species. For homogeneous PRCs this requires tedious screenings to identify a suitable stoichiometry of the photocatalyst. In case of carbon nitride materials the cross-couplings can be carried out at longer wavelengths due to their broad absorption spectrum. A second, more generally applicable approach is to run the reactions at higher concentrations. This increases the overall reaction rate and likely reduces the formation of nickel-solvent interactions that likely facilitate nickel-black formation. This method resulted in reproducible, highly selective C–N cross-couplings of aryl bromides and enables efficient reactions of aryl chlorides.

Methods

General procedure for light-mediated C–N cross-couplings using CN-OA-m and Ni catalysis. An oven dried vial (19 x 80 mm) equipped with a stir bar was charged with CN-OA-m (20 mg), aryl bromide (1.2 mmol, 1.0 equiv.) and NiBr₂·3H₂O (16.4 mg, 60 μmol, 5.0 mol%). Subsequently, pyrrolidine (256.0 mg, 295.6 μl, 3.6 mmol, 3.0 equiv.) and DMAc (anhydrous, Method A and B: 6 mL, Method C: 1 mL) were added and the vial was sealed with a septum and Parafilm. The reaction mixture was sonicated for 5-10 min until fine dispersion of the solids was achieved and the mixture was then degassed by bubbling N₂ for 10 min. The mixture was irradiated in the photoreactor (Method A and C: 450 nm, Method B: 520 nm, see Supplementary Information for details) at 40 °C. After the respective reaction time, one equivalent of 1,3,5-trimethoxybenzene (202.0 mg, 1.2 mmol, internal standard) was added. An aliquot (~300 μL) of the reaction mixture was diluted with DMSO-d₆ and subjected to ¹H-NMR analysis. After full consumption of the arene starting material, the liquid phase was diluted with H₂O (40 mL) and extracted with ethyl acetate (3 x 30 mL). The combined organic phases were washed with

H₂O (40 mL), NaHCO₃ solution (40 ml) and brine (40 mL), dried over Na₂SO₄ and concentrated. The crude product was purified by flash column chromatography (SiO₂, Hexane/EtOAc, dichloromethane/EtOAc or dichloromethane/MeOH) on a Grace™ Reveleris™ system using a 12 g cartridge to afford the desired product. The final product was characterized by ¹H-NMR, ¹³C-NMR, ¹⁹F-NMR and HRMS (ESI-TOF).

References

- 1 Roughley, S. D. & Jordan, A. M. The Medicinal Chemist's Toolbox: An Analysis of Reactions Used in the Pursuit of Drug Candidates. *J. Med. Chem.* **54**, 3451-3479 (2011).
- 2 Wolfe, J. P. & Buchwald, S. L. Nickel-Catalyzed Amination of Aryl Chlorides. *J. Am. Chem. Soc.* **119**, 6054-6058 (1997).
- 3 Ge, S., Green, R. A. & Hartwig, J. F. Controlling First-Row Catalysts: Amination of Aryl and Heteroaryl Chlorides and Bromides with Primary Aliphatic Amines Catalyzed by a BINAP-Ligated Single-Component Ni(0) Complex. *J. Am. Chem. Soc.* **136**, 1617-1627 (2014).
- 4 Tassone, J. P., England, E. V., MacQueen, P. M., Ferguson, M. J. & Stradiotto, M. PhPAd-DalPhos: Ligand-Enabled, Nickel-Catalyzed Cross-Coupling of (Hetero)aryl Electrophiles with Bulky Primary Alkylamines. *Angew. Chem. Int. Ed.* **58**, 2485-2489 (2019).
- 5 Kelly, R. A., Scott, N. M., Díez-González, S., Stevens, E. D. & Nolan, S. P. Simple Synthesis of CpNi(NHC)Cl Complexes (Cp = Cyclopentadienyl; NHC = N-Heterocyclic Carbene). *Organometallics* **24**, 3442-3447 (2005).
- 6 Park, N. H., Teverovskiy, G. & Buchwald, S. L. Development of an Air-Stable Nickel Precatalyst for the Amination of Aryl Chlorides, Sulfamates, Mesylates, and Triflates. *Org. Lett.* **16**, 220-223 (2014).

- 7 Kampmann, S. S., Skelton, B. W., Wild, D. A., Koutsantonis, G. A. & Stewart, S. G. An Air-Stable Nickel(0) Phosphite Precatalyst for Primary Alkylamine C–N Cross-Coupling Reactions. *Eur. J. Org. Chem.* **2015**, 5995-6004 (2015).
- 8 Shields, J. D., Gray, E. E. & Doyle, A. G. A Modular, Air-Stable Nickel Precatalyst. *Org. Lett.* **17**, 2166-2169 (2015).
- 9 Li, C., Kawamata, Y., Nakamura, H., Vantourout, J. C., Liu, Z., Hou, Q., Bao, D., Starr, J. T., Chen, J., Yan, M. & Baran, P. S. Electrochemically Enabled, Nickel-Catalyzed Amination. *Angew. Chem. Int. Ed.* **56**, 13088-13093 (2017).
- 10 Kawamata, Y., Vantourout, J. C., Hickey, D. P., Bai, P., Chen, L., Hou, Q., Qiao, W., Barman, K., Edwards, M. A., Garrido-Castro, A. F., deGruyter, J. N., Nakamura, H., Knouse, K., Qin, C., Clay, K. J., Bao, D., Li, C., Starr, J. T., Garcia-Irizarry, C., Sach, N., White, H. S., Neurock, M., Minter, S. D. & Baran, P. S. Electrochemically Driven, Ni-Catalyzed Aryl Amination: Scope, Mechanism, and Applications. *J. Am. Chem. Soc.* **141**, 6392-6402 (2019).
- 11 Lim, C.-H., Kudisch, M., Liu, B. & Miyake, G. M. C–N Cross-Coupling via Photoexcitation of Nickel–Amine Complexes. *J. Am. Chem. Soc.* **140**, 7667-7673 (2018).
- 12 Corcoran, E. B., Pirnot, M. T., Lin, S., Dreher, S. D., DiRocco, D. A., Davies, I. W., Buchwald, S. L. & MacMillan, D. W. C. Aryl amination using ligand-free Ni(II) salts and photoredox catalysis. *Science* **353**, 279-283 (2016).
- 13 Du, Y., Pearson, R. M., Lim, C.-H., Sartor, S. M., Ryan, M. D., Yang, H., Damrauer, N. H. & Miyake, G. M. Strongly Reducing, Visible-Light Organic Photoredox Catalysts as Sustainable Alternatives to Precious Metals. *Chem. Eur. J.* **23**, 10962-10968 (2017).
- 14 Caputo, J. A., Frenette, L. C., Zhao, N., Sowers, K. L., Krauss, T. D. & Weix, D. J. General and Efficient C–C Bond Forming Photoredox Catalysis with Semiconductor Quantum Dots. *J. Am. Chem. Soc.* **139**, 4250-4253 (2017).

- 15 Liu, Y.-Y., Liang, D., Lu, L.-Q. & Xiao, W.-J. Practical heterogeneous photoredox/nickel dual catalysis for C–N and C–O coupling reactions. *Chem. Commun.* **55**, 4853-4856 (2019).
- 16 Ghosh, I., Khamrai, J., Savateev, A., Shlapakov, N., Antonietti, M. & König, B. Organic semiconductor photocatalyst can bifunctionalize arenes and heteroarenes. *Science* **365**, 360-366 (2019).
- 17 Bulky, secondary amines such as *N*-tert-butylisopropylamine and 2,2,6,6-tetramethylpiperidine do not couple with aryl halides and can be used as a base if 1.5 equivalents of pyrrolidine are used (see Supplementary Information).
- 18 Qi, Z.-H. & Ma, J. Dual Role of a Photocatalyst: Generation of Ni(0) Catalyst and Promotion of Catalytic C–N Bond Formation. *ACS Catal.* **8**, 1456-1463 (2018).
- 19 Wang, C., Cao, S. & Fu, W.-F. A stable dual-functional system of visible-light-driven Ni(ii) reduction to a nickel nanoparticle catalyst and robust in situ hydrogen production. *Chem. Commun.* **49**, 11251-11253 (2013).
- 20 Rodríguez, J. L., Valenzuela, M. A., Pola, F., Tiznado, H. & Poznyak, T. Photodeposition of Ni nanoparticles on TiO₂ and their application in the catalytic ozonation of 2,4-dichlorophenoxyacetic acid. *J. Mol. Catal. A: Chem.* **353-354**, 29-36 (2012).
- 21 Indra, A., Menezes, P. W., Kailasam, K., Hollmann, D., Schröder, M., Thomas, A., Brückner, A. & Driess, M. Nickel as a co-catalyst for photocatalytic hydrogen evolution on graphitic-carbon nitride (sg-CN): what is the nature of the active species? *Chem. Commun.* **52**, 104-107 (2016).
- 22 Cavedon, C., Madani, A., Seeberger, P. H. & Pieber, B. Semiheterogeneous Dual Nickel/Photocatalytic (Thio)etherification Using Carbon Nitrides. *Org. Lett.* **21**, 5331-5334 (2019).

- 23 Pieber, B., Malik, J. A., Cavedon, C., Gisbertz, S., Savateev, A., Cruz, D., Heil, T., Zhang, G. & Seeberger, P. H. Semi-Heterogeneous Dual Nickel/Photo-catalysis using Carbon Nitrides: Esterification of Carboxylic Acids with Aryl Halides. *Angew. Chem. Int. Ed.* **58**, 9575-9580.
- 24 Zhang, G., Li, G., Lan, Z.-A., Lin, L., Savateev, A., Heil, T., Zafeiratos, S., Wang, X. & Antonietti, M. Optimizing Optical Absorption, Exciton Dissociation, and Charge Transfer of a Polymeric Carbon Nitride with Ultrahigh Solar Hydrogen Production Activity. *Angew. Chem. Int. Ed.* **56**, 13445-13449 (2017).
- 25 The strong resonance donating effect of fluorine appears sufficient to counteract the inductive withdrawing effect in dual photoredox/nickel catalyzed cross-couplings resulting in low reactivity (see Refs. 22-23).
- 26 Crabtree, R. H. Deactivation in Homogeneous Transition Metal Catalysis: Causes, Avoidance, and Cure. *Chem. Rev.* **115**, 127-150 (2015).
- 27 Molina de la Torre, J. A., Espinet, P. & Albéniz, A. C. Solvent-Induced Reduction of Palladium-Aryls, a Potential Interference in Pd Catalysis. *Organometallics* **32**, 5428-5434 (2013).
- 28 It has to be noted that a higher concentration does not increase the yield in case of $(\text{Ir}[\text{dF}(\text{CF}_3)\text{ppy}]_2(\text{dtbbpy}))\text{PF}_6$.
- 29 When no $\text{NiBr}_2 \cdot 3\text{H}_2\text{O}$ is added to the recovered CN-OA-m material containing deposited nickel, only trace amounts of the C-N coupling product were observed (see Supplementary Information).

Acknowledgments

We gratefully acknowledge the Max-Planck Society for generous financial support. S.G. and B.P. thank the International Max Planck Research School on Multiscale Bio-Systems for funding. B.P. und S.R. acknowledge financial support by a Liebig Fellowship of the German

Chemical Industry Fund (Fonds der Chemischen Industrie, FCI). B.P. thanks the Deutsche Forschungsgemeinschaft (DFG, German Research Foundation) under Germany's Excellence Strategy – EXC 2008/1 (UniSysCat) – 390540038 for financial support. We thank our colleagues Prof. Peter H. Seeberger, Dr. Jamal Malik, Dr. Kerry Gilmore, Dr. Tobias Heil, Dr. Daniel Cruz, Heike Runge, Rona Pitschke, Jessica Brandt and Katharina ten Brummelhuis (all MPIKG), for scientific, technical and analytical support.

manuscript.pdf (1.56 MiB)

[view on ChemRxiv](#) • [download file](#)

Supplementary Materials for

**Overcoming Limitations in Dual Photoredox/Nickel
catalyzed C–N Cross-Couplings due to Catalyst
Deactivation**

Sebastian Gisbertz,^{1,2} Susanne Reischauer^{1,2} & Bartholomäus Pieber^{1*}

*¹Department of Biomolecular Systems, Max-Planck-Institute of Colloids and Interfaces, Am
Mühlenberg 1, 14476 Potsdam, Germany*

*²Department of Chemistry and Biochemistry, Freie Universität Berlin, Am Mühlenberg 1,
14476 Potsdam, Germany*

**Corresponding author*

Email: bartholomaeus.pieber@mpikg.mpg.de

TABLE OF CONTENTS

1. General remarks	3
2. Literature analysis: aryl halides without electron withdrawing groups	5
3. Preparation of CN-OA-m.....	7
4. Setup for photochemical reactions	9
5. Reaction optimization	11
5.1 General experimental procedure for screening experiments.....	11
5.2 Screening of carbon nitride material	13
5.3 Solvent screening	14
5.4 Screening of Ni ^{II} sources.....	15
5.5 Base screening.....	16
5.6 Screening of conditions	18
5.7 Screening of aryl (pseudo)halides	20
5.8 Control studies.....	21
5.9 Time/Wavelength study	22
6. Recycling studies.....	25
7. Scale-up of amination.....	28
8. Studies on the reaction of 4-bromofluorobenzene with pyrrolidine.	30
8.1 Powder X-ray diffraction (XRD) and X-ray photoelectron spectroscopy (XPS)	34
8.2 Scanning transmission electron microscopy (STEM).....	37
8.2.1 CN-OA-m recovered from method A (blue LEDs) and method B (green LEDs)	37
8.2.2 Heterogeneous material generated during experiments using the UV method (photocatalyst-free and UV-light)	40
8.3 Scanning electron microscopy (SEM).....	41
8.4 Energy-dispersive X-ray spectroscopy (EDX) and inductively coupled plasma atomic emission spectroscopy (ICP-OES)	42
8.5 Fourier-transform infrared spectroscopy (FTIR) and Ultraviolet–visible spectroscopy (UV-VIS).....	43
9. Studies on the reaction of bromobenzene, 3-bromotoluene, 1-bromo-4- <i>tert</i> -butylbenzene, and 4-bromoanisole with pyrrolidine.	45
10. Studies on the reaction of methyl 4-chlorobenzoate	51
11. Scope and limitations	54
12. References	70
12. Copies of NMR spectra	74

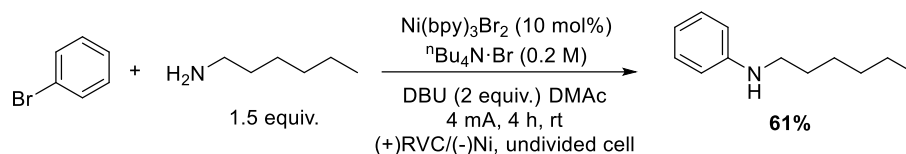
1. General remarks

Substrates, reagents, and solvents were purchased from commercial suppliers and used without further purification. Methyl 4-(trifluoromethylsulfonyloxy)benzoate,¹ methyl 4-(tosyloxy)benzoate², methyl 4-((methylsulfonyl)oxy)benzoate³ and *N*-tert-butylisopropylamine (BIPA)⁴ were prepared according to literature procedures. ¹H-, ¹³C- and ¹⁹F-NMR spectra were obtained using a Varian 400 spectrometer (400 MHz, Agilent), an Ascend™ 400 spectrometer (400 MHz, cryoprobe, Bruker) and a Varian 600 spectrometer (600 MHz, Agilent) at 298 K, and are reported in ppm relative to the residual solvent peaks. Peaks are reported as: s = singlet, d = doublet, t = triplet, q = quartet, m = multiplet or unresolved, with coupling constants in Hz. Analytical thin layer chromatography (TLC) was performed on pre-coated TLC-sheets, ALUGRAM Xtra SIL G/UV₂₅₄ sheets (Macherey-Nagel) and visualized with 254 nm light or staining solutions followed by heating. Purification of final compounds was carried out by flash chromatography on the Reveleris X2 Flash Chromatography System from GRACE using prepacked columns with 40 μm silica gel. Silica 60 M (0.04-0.063 mm) silica gel (Sigma Aldrich) was used for dry loading of the crude compounds on the flash chromatography system. Centrifugation was carried out using an Eppendorf 5430 centrifuge. High-resolution mass spectral data were obtained using a Waters XEVO G2-XS 4K spectrometer with the XEVO G2-XS QTOF capability kit. Emission spectra of LED lamps were recorded using 10 in. (24.5 cm) integrating sphere (Labsphere, Inc. Model LMS 1050) equipped with a diode array detector (International Light, Model RPS900). The UV/Vis spectrum of Ir(ppy)₂(dtbbpy)PF₆ was recorded using a UVmini-1240 spectrometer (Shimadzu). Inductively coupled plasma - optical emission spectrometry (ICP-OES) was carried out using a Horiba Ultra 2 instrument equipped with photomultiplier tube detection. FTIR spectra were recorded on a Thermo Scientific Nicolet iD5 spectrometer. Diffuse reflectance UV/Vis spectra of powders were recorded on a Shimadzu UV-2600 spectrometer equipped with an integrating sphere. For XRD measurements, a Bruker D8 Advanced X-ray diffractometer with Cu Kα radiation was used. Scanning electron microscopy (SEM) images were obtained on a LEO 1550-Gemini microscope. Energy-dispersive X-ray (EDX) investigations were conducted on a Link ISIS-300 system (Oxford Microanalysis Group) equipped with a Si(Li) detector and an energy resolution of 133 eV. X-ray photoelectron spectroscopic (XPS) measurements were carried out with a CISSY set-up, equipped with a SPECS XR 50 X-ray gun with Mg Kα excitation radiation (1254.6 eV) and combined with a lens analyzer module (CLAM) under ultra-high vacuum (UHV, 1.5x10⁻⁸ Pa). The calibration was performed using

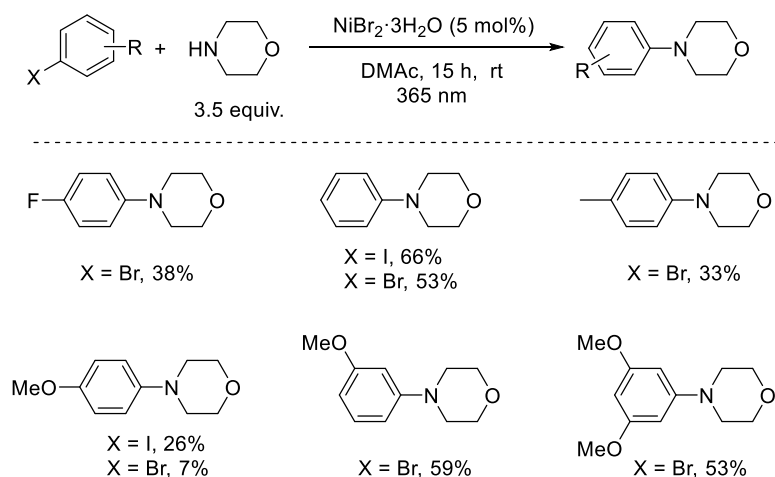
the Au 4f_{7/2} (84.0 eV) binding energy scale as reference. Quantitative analysis and deconvolution were achieved using “peakfit” and “Igor” software with Lorentzian-Gaussian functions and Shirley background deletion in photoemission spectra. The STEM images were acquired using a double-corrected Jeol ARM200F, equipped with a cold field emission gun. For the investigation, the acceleration voltage was set to 200kV, the emission was put to 5 μ A and a condenser aperture with a diameter of 20 μ m was used. With these settings, the microscope reaches a lattice resolution below 1Å. The STEM specimens were prepared by dissolving a powder sample of the material in ethanol, sonicating the solution for 15 minutes and finally dropping a few drops onto a copper TEM grid coated with holey carbon film. Once the solution had dried off, the specimens were investigated.

2. Literature analysis: aryl halides without electron withdrawing groups

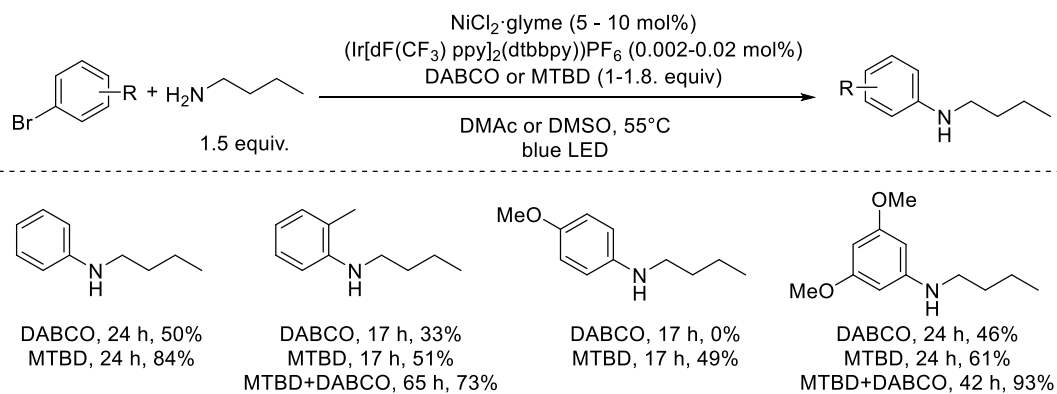
a) Electrochemically driven, Ni-catalyzed amination⁵



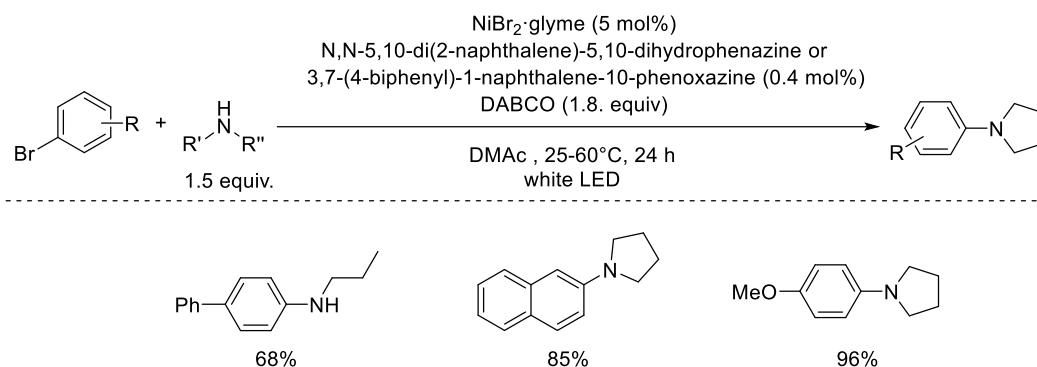
b) UV-light mediated, Ni-catalyzed amination⁶



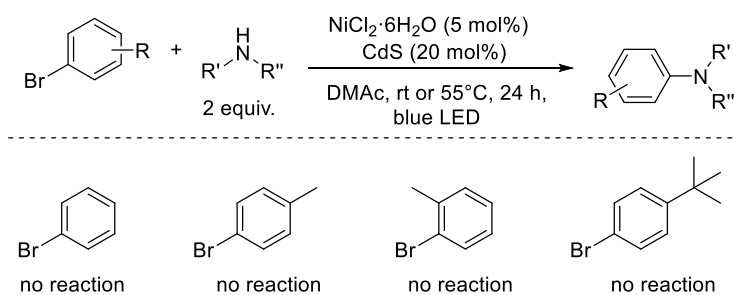
c) Dual nickel/photoredox catalyzed amination using (Ir[dF(CF₃)ppy]₂(dtbbpy))PF₆⁷



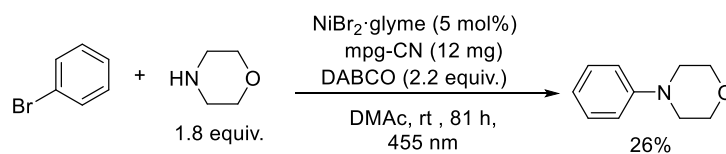
d) Dual nickel/photoredox catalyzed amination using organic dyes⁸



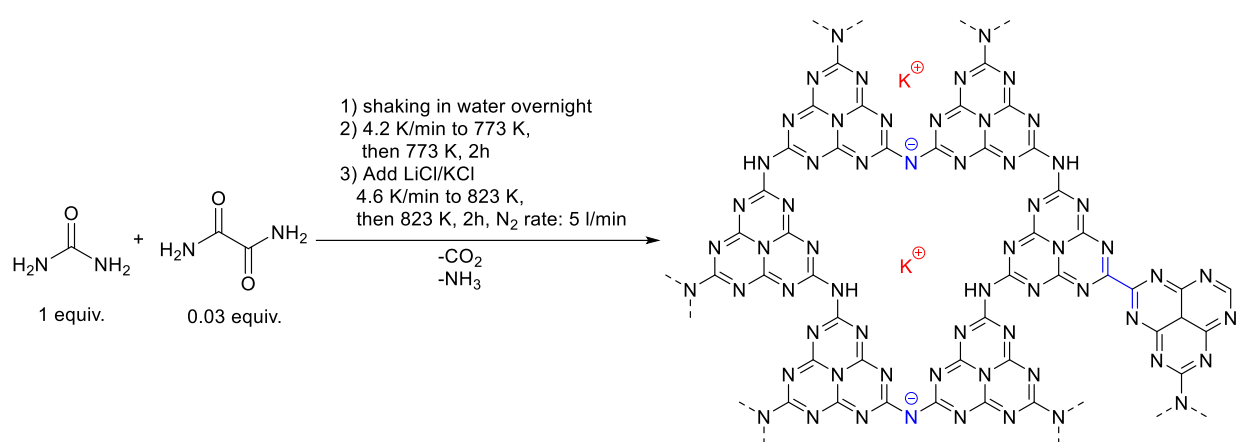
e) Dual nickel/photoredox catalyzed amination using CdS⁹



e) Dual nickel/photoredox catalyzed amination using mpg-CN¹⁰



3. Preparation of CN-OA-m



Scheme S1. Synthesis of CN-OA-m

The synthesis for CN-OA-m was carried out using a slightly adapted version of the literature procedure (Scheme S1)¹¹: For each batch of the photocatalyst, urea (10 g, 166.5 mmol) and oxamide (0.5 g, 5.7 mmol) were mixed in 10 ml of DI water to generate a homogeneous mixture. After drying at 373 K, the resulting solids were grinded, transferred into a crucible with a cover and heated up in an air-oven with a heating rate of 4.3 K/min to 773 K. After keeping the mixture for 2h at 773 K, the sample was allowed to cool to room temperature. Subsequently, KCl (3.3 g, 44.3 mmol) and LiCl (2.7 g, 63.7 mmol) were added and the solids were grinded to obtain a homogeneous mixture which was heated in an inert atmosphere (N₂ flow: 5 mL/min) to 823 K with a heating rate of 4.6 K/min. After keeping the mixture for 2 h at 823 K, the sample was allowed to cool to room temperature and the resulting solids were collected on a filter paper and washed with H₂O (3 x 100 mL). The resulting yellow material was dried at 373 K (average yield per batch: ~425 mg). All analytical data (FTIR, UV/Vis, XRD, SEM, etc.; see Section 7) are in full agreement with those published in the literature.¹¹

The cost of CN-OA-m was calculated to be 4.0 € g⁻¹ based on the prices of urea, oxamide, LiCl and KCl from Sigma-Aldrich (Merck).¹² As a comparison, the price of Ir[dF(CF₃)ppy]₂(dtbpy))PF₆ is 883 € g⁻¹.¹²

The UV/Vis spectrum of CN-OA-m shows a strong absorption up to ~460 nm and a comparably weaker absorption band up to ~700 nm (Figure S1, A) which are attributed to the π - π^* electron transition of the sp² hybridization of C and N in the heptazine framework and n- π^* electron transition involving the lone pairs of the edge nitrogen atoms in the heptazine units,

respectively.¹¹ The capability of harvesting low energy light is therefore superior compared to Ir and Ru photocatalysts (see Figure S1, B for the UV/Vis spectrum of Ir[dF(CF₃)ppy]₂(dtbbpy)PF₆ as a representative example) which have only a low absorption band between 400 and 500 nm in the visible region, which corresponds to the metal-to-ligand charge transfer transition.

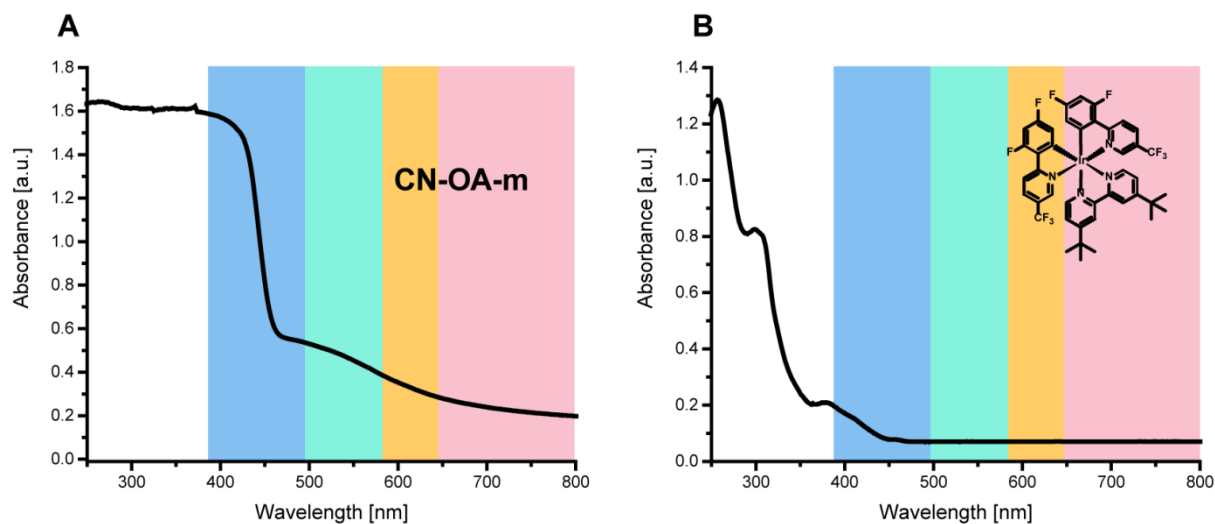


Figure S1. UV/VIS-absorption spectra of CN-OA-m (A) and Ir[dF(CF₃)ppy]₂(dtbbpy)PF₆ (B).

4. Setup for photochemical reactions

A flexible, red/green/blue LED strip¹³ (RGB, 5m, 24 W/strip; Tween Light, BAHAG AG, Germany) was wrapped around a 115 mm borosilicate crystallization dish (Figure S2, A). Blue, green, red or white (illumination of all three LED colors - red/green/blue) light was used at full power for all experiments (For emission spectra of a single diode, see Figure S3). The evaporating dish was filled with ethylene glycol and the temperature was set to 40°C to maintain a constant temperature. The sealed, cylindrical reaction vessels (16 x 100 mm) were placed at the same distance from the LED strip during all experiments (Figure S2, A). All reactions were performed with a stirring speed of 600 (1 mL) or 1400 rpm (3 or 6 mL). For large scale aminations a flexible, red/green/blue LED strip (RGB, 5m, 24 W/strip; Tween Light, BAHAG AG, Germany) was wrapped around a mm borosilicate beaker (Figure S2, B). The scale-up reaction was performed in a sealed, cylindrical reaction vessel (25 x 140 mm) with a stirring speed of 700 rpm and without additional heating (Figure S2, B).

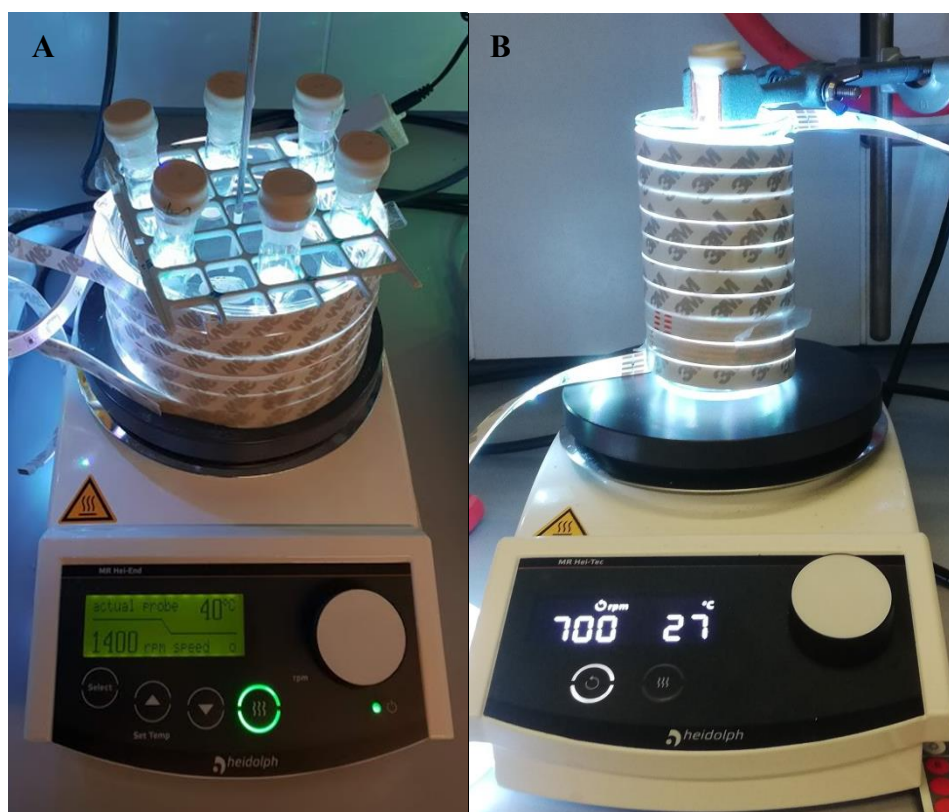


Figure S2. Experimental setup for general photochemical reactions (A) and for the scale-up reaction (B).

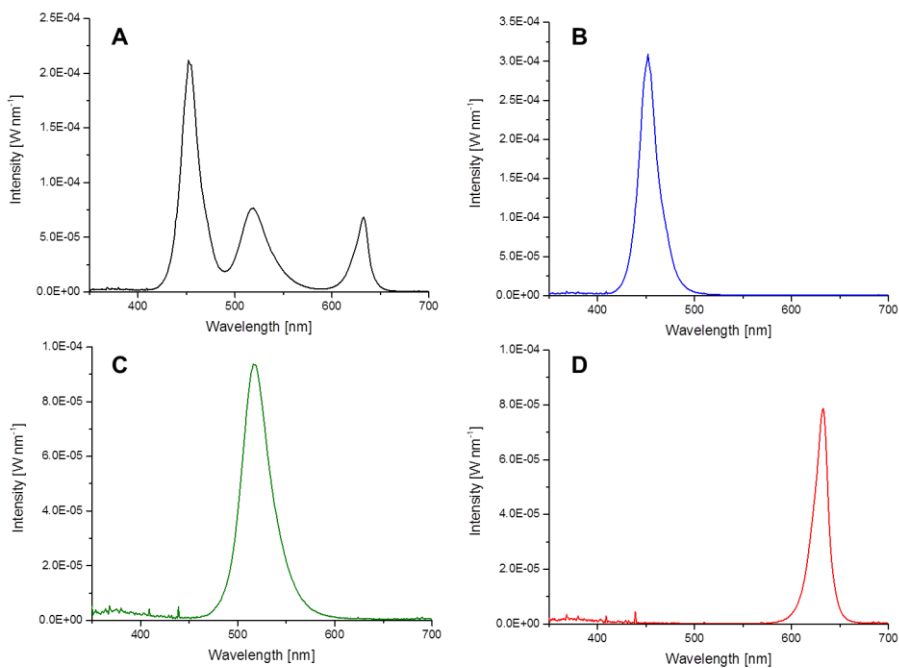


Figure S3. Emission spectra of the LED strips used for photochemical reactions. All experiments were carried out at maximum power. **A:** white light. **B:** blue light only. **C:** green light only. **D:** red light only.

A Kessil[®] PR 160-370nm lamp, a stir plate and a fan for cooling was used for UV-light experiments (Figure S4, A). All experiments were carried out with maximum lamp power. The sealed reaction vessels (16 x 100 mm) were placed at the same distance (4 cm) from the light source during all experiments. All reactions were performed with vigorous stirring.

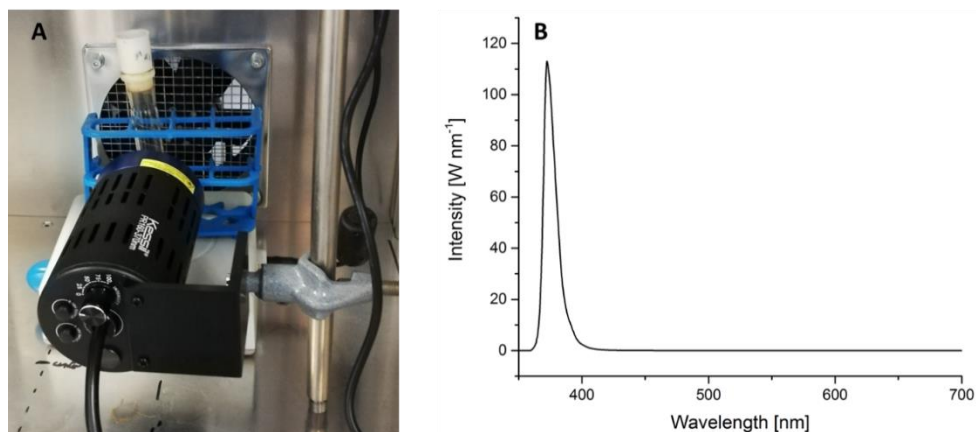


Figure S4. A: Picture of the Set-up for UV-light experiments **B:** Emission spectra of the Kessil[®] PR 160-370nm lamp used for photochemical reactions. All experiments were carried out at maximum power.

5. Reaction optimization

5.1 General experimental procedure for screening experiments

An oven dried vial (16 x 100 mm) equipped with a stir bar was charged with methyl 4-bromobenzoate (0.3 mmol, 64.5 mg, 1 equiv.), the base (0.9 mmol, 3.0 equiv.), the Ni^{II} catalyst (30 μmol, 10 mol%) and the carbon nitride material (10 mg). Subsequently, pyrrolidine (0.45 mmol, 37.0 μL, 1.5 equiv.) and the solvent (anhydrous, 3 mL) were added and the vial was sealed with a septum and Parafilm. The reaction mixture was sonicated for 5-10 min followed by stirring for 5 min until a fine dispersion of the solids was achieved and the mixture was then degassed by bubbling N₂ for 10 min. The mixture was irradiated in the photoreactor at 40 °C with rapid stirring (1400 rpm). After the respective reaction time, one equivalent of 1,3,5-trimethoxybenzene (0.3 mmol, 50.5 mg) was added. An aliquot of the reaction mixture (~300 μL) was filtered, diluted with DMSO-d₆ and subjected to ¹H-NMR analysis. (Alternatively, 1.5 mL CDCl₃ and 3 mL H₂O were added and the vial was sealed and vigorously shaken. After phase separation, the CDCl₃ layer was carefully removed using a syringe, filtered, and analyzed by ¹H-NMR.) For representative NMR spectra, see Figure S5.

5.2 Screening of carbon nitride material

Table S1. Screening of carbon nitride materials.^a

Entry	CN catalyst	Conversion [%] ^b	1 [%] ^c	2 [%] ^c	4 [%] ^c
1	CN-OA-m	73	65	2	5
2	CMB _{0.05} -CN	25	21	2	trace
3	mpg-CN	23	19	trace	trace
4	PHIK	18	14	trace	trace
5	CNS ₆₀₀	9	6	trace	trace

^aReaction conditions: methyl 4-bromobenzoate (0.3 mmol), pyrrolidine (0.45 mmol), NiCl₂·glyme (10 mol%), DABCO (0.9 mmol), carbon nitride (10 mg), DMAc (anhydrous, 3 mL), white LEDs at 40 °C for 16h. ^bConversion of methyl 4-bromobenzoate determined by ¹H-NMR using 1,3,5-trimethoxybenzene as internal standard. ^cNMR yields determined by ¹H-NMR using 1,3,5-trimethoxybenzene as internal standard.

Several carbon nitride materials were tested: Mesoporous graphitic carbon nitride (mpg-CN),¹⁴ a modified carbon nitride derived from a cyanuric acid/melamide/barbituric acid complex (CMB_{0.05}-CN),¹⁵ a sulfur-doped material (CNS₆₀₀),¹⁶ a strongly oxidizing potassium poly(heptazine imide) (K-PHI),¹⁷ and a carbon nitride derivative prepared *via* co-condensation of urea and oxamide followed by post-calcination in a molten salt (CN-OA-m),¹¹ all using white LED (RGB) irradiation at a constant temperature of 40 °C.

5.3 Solvent screening

Table S2. Solvent screening.^a

COC(=O)c1ccc(Br)cc1 + C1CCNC1
 $\xrightarrow[\text{white LED, } \sim 40^\circ\text{C}]{\text{CN-OA-m (3.33 mg/mL), NiCl}_2\cdot\text{glyme (10 mol\%), DABCO (3.0 equiv.), solvent (deg.), 16 h}}$
COC(=O)c1ccc(NC1CCNC1)cc1 + COC(=O)c1ccc(N)cc1 + COC(=O)c1ccc(Cl)cc1

0.1 M 1.5 equiv. 1 2 4

Entry	Solvent	Conversion [%] ^b	1 [%] ^c	2 [%] ^c	4 [%] ^c
1	DMAc	74	66	2	4
2	DMSO	28	24	trace	trace
3	DMF	n.d. ^d	18	trace	trace
4	MeCN	19	14	trace	trace
5	diglyme	15	11	trace	trace
6	toluene	6	6	trace	trace
7	DCM	11	trace	trace	trace

^aReaction conditions: methyl 4-bromobenzoate (0.3 mmol), pyrrolidine (0.45 mmol), NiCl₂·glyme (10 mol%), DABCO (0.9 mmol), CN-OA-m (10 mg), solvent (anhydrous, 3 mL), white LEDs at 40 °C for 16h. ^bConversion of methyl 4-bromobenzoate determined by ¹H-NMR using 1,3,5-trimethoxybenzene as internal standard. ^cNMR yields determined by ¹H-NMR using 1,3,5-trimethoxybenzene as internal standard. ^d not detected due to overlapping peaks.

5.4 Screening of Ni^{II} sources

Table S3. Screening Ni^{II} sources.^a

Reaction scheme: Methyl 4-bromobenzoate (0.1 M) + pyrrolidine (1.5 equiv.) $\xrightarrow[\text{DMAc (deg.), 16 h, white LED, -40}^\circ\text{C}]{\text{CN-OA-m (3.33 mg/mL), Ni}^{II}\text{ salt (10 mol\%), DABCO (3.0 equiv.)}}$ Product 1 (N-pyrrolidinyl methyl 4-oxobenzoate) + Product 2 (methyl 4-oxobenzoate) + Product 4 (methyl 4-chlorobenzoate).

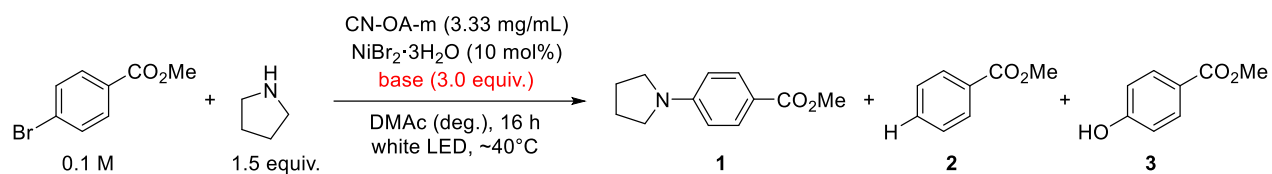
Entry	Ni ^{II} catalyst	Conversion [%] ^b	1 [%] ^c	2 [%] ^c	4 [%] ^c	Price [€ mol ⁻¹] ^d
1	NiI ₂	90	86	2	n.d.	2063
2	NiBr ₂ ·glyme	87	80	3	n.d.	10431
3	NiCl ₂	85	76	4	5	110
4	NiBr ₂	74	72	trace	n.d.	411
5	NiBr ₂ ·3H ₂ O	71	68	3	n.d.	116
6	NiCl ₂ ·glyme	74	66	trace	9	4161
7	Ni(ClO ₄) ₂ ·6H ₂ O	62	59	trace	n.d.	171
8	Ni(NO ₃) ₂ ·6H ₂ O	52	52	trace	n.d.	49
9	Ni(OTf) ₂	55	51	3	n.d.	12917
10	NiCl ₂ ·6H ₂ O	45	35	4	2	71
11	Ni(BF ₄) ₂ ·6H ₂ O	24	23	2	n.d.	223
12	Ni(TMHD) ₂	10	5	2	n.d.	35294
13	Ni(OAc) ₂ ·4H ₂ O	9	5	4	n.d.	28
14	Ni(SO ₄) ₂ ·6H ₂ O	9	4	2	n.d.	41
15	Ni(acac) ₂	3	n.d.	trace	n.d.	620

^aReaction conditions: methyl 4-bromobenzoate (0.3 mmol), pyrrolidine (0.45 mmol), Ni^{II} catalyst (10 mol%), DABCO (0.9 mmol), CN-OA-m (10 mg), DMAc (anhydrous, 3 mL), white LEDs at 40 °C for 16h. ^bConversion of methyl 4-bromobenzoate determined by ¹H-NMR using 1,3,5-trimethoxybenzene as internal standard. ^cNMR yields determined by ¹H-NMR using 1,3,5-trimethoxybenzene as internal standard. ^dPrices according to Sigma Aldrich (Merck)^x.

NiBr₂·3H₂O gave the best combination of price, selectivity (chloride formation in case of NiCl₂), activity and handling (NiI₂ and NiBr₂ are highly hygroscopic).

5.5 Base screening

Table S4. Base screening.^a



Entry	Base	Conversion [%] ^b	1 [%] ^c	2 [%] ^c	3 [%] ^c
1	TMP ^d	quant.	91	3	2
2	BIPA ^e	90	89	trace	n.d. ^f
3	DABCO ^g	71	68	3	trace
4	K ₂ HPO ₄	68	63	4	trace
5	dimethylaniline	59	62	n.d.	n.d.
6	CaCO ₃	65	61	trace	trace
7	2,6-lutidine	62	60	3	n.d.
8	without base	65	58	4	trace
9	tetramethylguanidine	53	43	n.d.	n.d.
10	DIPEA ^h	49	42	6	n.d.
11	Et ₃ N	42	35	5	trace
12	DMAPI ⁱ	43	31	6	trace
13	K ₃ PO ₄	33	21	trace	trace
14	DBU ^j	27	19	trace	trace
15	Na ₂ CO ₃	17	14	trace	trace
16	NaHCO ₃	14	8	4	trace
17	NaOtBu	29	5	trace	trace
18	KOH	quant.	4	n.d.	n.d.
19	NaOH	quant.	n.d.	n.d.	n.d.
20	K ₂ CO ₃	8	n.d.	trace	n.d.
21	NaH ₂ PO ₄	10	n.d.	n.d.	n.d.

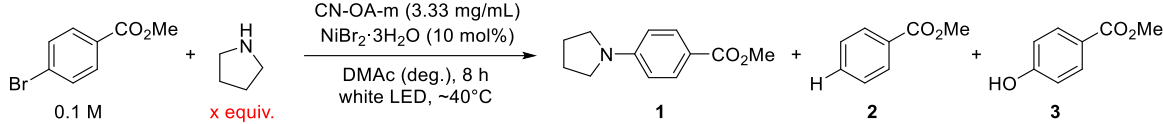
Entry	Base	Conversion [%] ^b	1 [%] ^c	2 [%] ^c	3 [%] ^c
22	LiOH	43	n.d.	n.d.	n.d.
23	Cs ₂ CO ₃	11	n.d.	5	trace
24	CsF	7	n.d.	trace	n.d.
25	CsOAc	2	n.d.	n.d.	n.d.
26	HMDS ^k	quant.	n.d.	n.d.	n.d.

^aReaction conditions: methyl 4-bromobenzoate (0.3 mmol), pyrrolidine (0.45 mmol), NiBr₂·3H₂O (10 mol%), base (0.9 mmol), CN-OA-m (10 mg), DMAc (anhydrous, 3 mL), white LEDs at 40 °C for 16h. ^bConversion of methyl 4-bromobenzoate determined by ¹H-NMR using 1,3,5-trimethoxybenzene as internal standard. ^cNMR yields determined by ¹H-NMR using 1,3,5-trimethoxybenzene as internal standard. ^d2,2,6,6-tetramethylpiperidin ^e*N*-*tert*-butylisopropylamine. ^fnot detected. ^g1,4-diazabicyclo[2.2.2]octane. ^h*N,N*-diisopropylethylamine. ⁱ4-(dimethylamino)pyridine. ^j1,8-diazabicyclo[5.4.0]undec-7-ene. ^kGexamethyldisilazane

N-*tert*-butylisopropylamine (BIPA) and 2,2,6,6-tetramethylpiperidine (TMP) gave best results. No C-N coupling between the aryl halide and these secondary, sterically hindered amines was observed. The absence of a base resulted in 58% yield indicating that the amine substrate can play several roles simultaneously (substrate, ligand, base). All other tested bases did not significantly increase the yield compared to the base-free method.

5.6 Screening of conditions

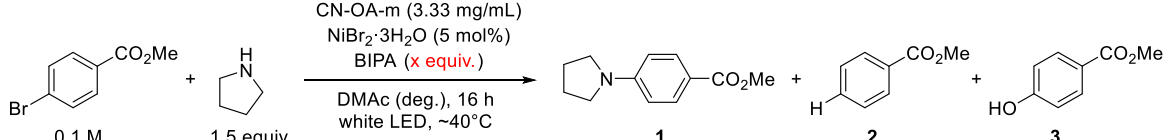
Table S5. Screening of amine equivalents for the base-free method.



Entry	Pyrrolidine [equiv.]	Conversion [%] ^b	1 [%] ^c	2 [%] ^c	3 [%] ^c
1	1	33	24	4	1
2	1.5	53	43	6	1
3	2.0	67	59	7	1
4	2.5	91	83	6	2
5	3.0	quant.	94	5	2
6	3.5	quant.	92	6	3

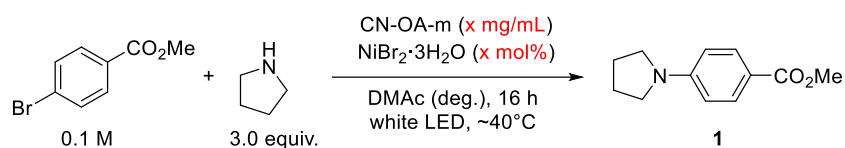
^aReaction conditions: methyl 4-bromobenzoate (0.3 mmol), pyrrolidine (x equiv.), NiBr₂·3H₂O (10 mol%), CN-OA-m (10 mg), DMAc (anhydrous, 3 mL), white LEDs at 40 °C for 8 h. ^bConversion of methyl 4-bromobenzoate determined by ¹H-NMR using 1,3,5-trimethoxybenzene as internal standard. ^cNMR yields determined by ¹H-NMR using 1,3,5-trimethoxybenzene as internal standard.

Table S6. Screening of base (BIPA) equivalents for reactions with 1.5 equiv. pyrrolidine.^a



Entry	BIPA [equiv.]	Conversion [%] ^b	1 [%] ^c	2 [%] ^c	3 [%] ^c
1	-	65	58	5	n.d. ^d
2	0.5	68	58	5	3
3	1	87	81	4	2
4	1.5	91	82	5	n.d.
5	2.0	92	84	5	n.d.

^aReaction conditions: methyl 4-bromobenzoate (0.3 mmol), pyrrolidine (0.45 mmol), NiBr₂·3H₂O (5 mol%), CN-OA-m (10 mg), BIPA (0-2 equiv.), DMAc (anhydrous, 3 mL), white LEDs at 40 °C for 16 h. ^bConversion of methyl 4-bromobenzoate determined by ¹H-NMR using 1,3,5-trimethoxybenzene as internal standard. ^cNMR yields determined by ¹H-NMR using 1,3,5-trimethoxybenzene as internal standard. ^dnot detected.

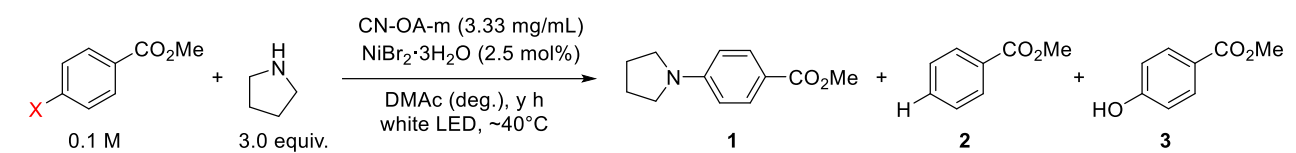
Table S7. Effect of the amount of NiBr₂·3H₂O and CN-OA-m on the yield of **1**.^a

Entry	NiBr ₂ ·3H ₂ O [mol%]	CN-OA-m [g/mL]	Conversion [%] ^b	1 [%] ^c
1	10	3.33	quant.	95
2	5	3.33	quant.	98
3	5	1.66	quant.	97
4	2.5	1.66	quant.	98
5	1	1.66	47	47
6	2.5	0.88	56	56

^aReaction conditions: methyl 4-bromobenzoate (0.3 mmol), pyrrolidine (0.9 mmol), NiBr₂·3H₂O (y mol%), base (0.9 mmol), CN-OA-m (x mg), DMAc (anhydrous, 3 mL), white LEDs at 40 °C for 16h. ^bConversion of methyl 4-bromobenzoate determined by ¹H-NMR using 1,3,5-trimethoxybenzene as internal standard. ^cNMR yields determined by ¹H-NMR using 1,3,5-trimethoxybenzene as internal standard.

5.7 Screening of aryl (pseudo)halides

Table S8. Screening of aryl (pseudo)halides.^a



Entry	X	Time [h]	Conversion [%] ^b	1 [%] ^c	2 [%] ^c	3 [%] ^c
1	I	8	quant.	99	1	n.d.
2	Br	8	quant.	98	2	1
3	Cl	168	76	72	4	n.d.
4	OTf	72	75	67	5	2
5	OTs	16	2	n.d.	n.d.	n.d.
6	OMs	16	5	n.d.	n.d.	4

^aReaction conditions: aryl (pseudo)halide (0.3 mmol), pyrrolidine (0.9 mmol), NiBr₂·3H₂O (2.5 mol%), CN-OA-m (10 mg), DMAc (anhydrous, 3 mL), white LEDs at 40 °C for x h. ^bConversion of methyl 4-bromobenzoate determined by ¹H-NMR using 1,3,5-trimethoxybenzene as internal standard. ^cNMR yields determined by ¹H-NMR using 1,3,5-trimethoxybenzene as internal standard. ^dnot detected.

5.8 Control studies

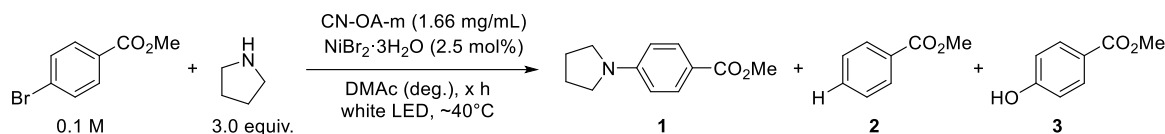
Table S9. Control studies.^a

Entry	Deviation from standard conditions	Conversion [%] ^b	1 [%] ^c	2 [%] ^c	3 [%] ^c
1	None	quant.	98	2	n.d. ^d
2	dtbbpy ^e (2.5 mol%) as ligand	48	45	2	n.d.
3	No CN-OA-m	5	n.d.	2	1
4	No NiBr ₂ ·3H ₂ O	5	n.d.	n.d.	n.d.
5	No light	<1	n.d.	n.d.	n.d.
6	No degassing	10	10	n.d.	n.d.

^aReaction conditions: methyl 4-bromobenzoate (1.2 mmol), pyrrolidine (3.6 mmol), NiBr₂·3H₂O (2.5 mol%), CN-OA-m (20 mg), DMAc (anhydrous, 6 mL), white LEDs at 40 °C for 8 h. ^bConversion of methyl 4-bromobenzoate determined by ¹H-NMR using 1,3,5-trimethoxybenzene as internal standard. ^cNMR yields determined by ¹H-NMR using 1,3,5-trimethoxybenzene as internal standard. ^dnot detected. ^e4,4'-Di-tert-butyl-2,2'-bipyridyl.

5.9 Time/Wavelength study

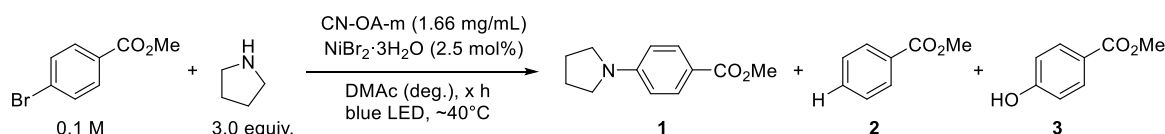
Table S10. Time study using white light.



Entry	Time [h]	Conversion [%] ^b	1 [%] ^c	2 [%] ^c	3 [%] ^c
1	1	25	24	n.d. ^d	n.d.
2	2	39	38	n.d.	n.d.
3	3	48	48	trace	n.d.
4	4	77	76	1	n.d.
5	5	87	83	2	n.d.
6	6	91	91	2	n.d.
7	7	97	94	3	n.d.
8	8	quant.	96	2	1

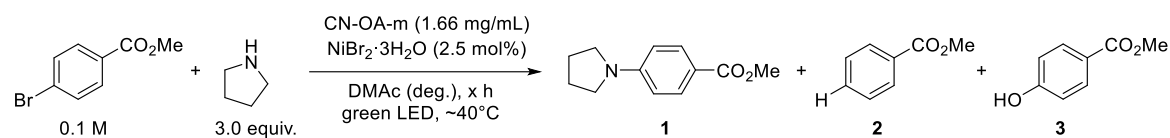
^aReaction conditions: methyl 4-bromobenzoate (0.6 mmol), pyrrolidine (1.8 mmol), NiBr₂·3H₂O (2.5 mol%), CN-OA-m (10 mg), DMAc (anhydrous, 6 mL), white LEDs at 40 °C for x h. ^bConversion of methyl 4-bromobenzoate determined by ¹H-NMR using 1,3,5-trimethoxybenzene as internal standard. ^cNMR yields determined by ¹H-NMR using 1,3,5-trimethoxybenzene as internal standard. ^dnot detected.

Table S11. Time study using blue light.



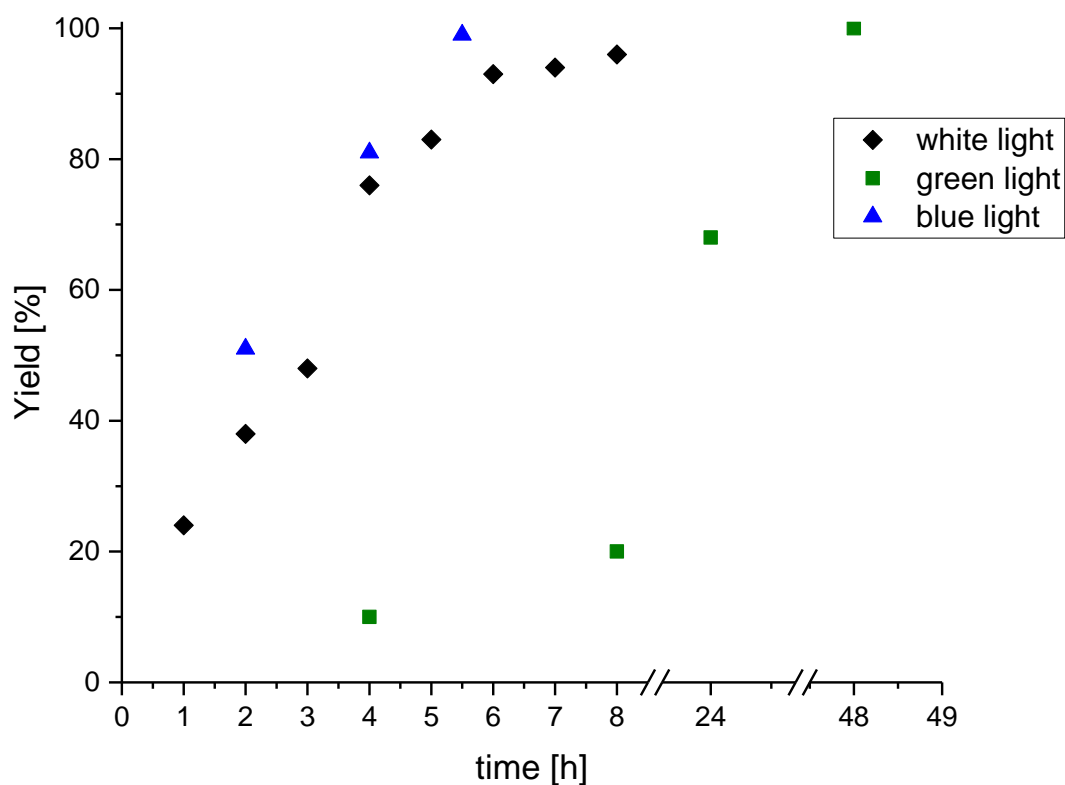
Entry	Time [h]	Conversion [%] ^b	1 [%] ^c	2 [%] ^c	3 [%] ^c
1	2	51	51	n.d. ^d	n.d.
2	4	77	80	trace	n.d.
3	5.5	quant.	>99	trace	n.d.

^aReaction conditions: methyl 4-bromobenzoate (0.6 mmol), pyrrolidine (1.8 mmol), NiBr₂·3H₂O (2.5 mol%), CN-OA-m (10 mg), DMAc (anhydrous, 6 mL), blue LEDs at 40 °C for x h. ^bConversion of methyl 4-bromobenzoate determined by ¹H-NMR using 1,3,5-trimethoxybenzene as internal standard. ^cNMR yields determined by ¹H-NMR using 1,3,5-trimethoxybenzene as internal standard. ^dnot detected.

Table S12. Time study using green light.

Entry	Time [h]	Conversion [%] ^b	1 [%] ^c	2 [%] ^c	3 [%] ^c
1	4	10	10	n.d. ^d	n.d.
2	8	21	20	n.d.	n.d.
3	24	69	68	n.d.	n.d.
4	48	quant.	>99	n.d.	n.d.

^aReaction conditions: methyl 4-bromobenzoate (0.6 mmol), pyrrolidine (1.8 mmol), NiBr₂·3H₂O (2.5 mol%), CN-OA-m (10 mg), DMAc (anhydrous, 6 mL), green LEDs at 40 °C for x h. ^bConversion of methyl 4-bromobenzoate determined by ¹H-NMR using 1,3,5-trimethoxybenzene as internal standard. ^cNMR yields determined by ¹H-NMR using 1,3,5-trimethoxybenzene as internal standard. ^dnot detected.

**Figure S6.** Time study using blue, green and white light for model reaction.

For ICP-OES experiments, the reaction mixture was centrifuged at 3000 rpm for 20 min and the liquid phase was carefully separated and analyzed by $^1\text{H-NMR}$. The carbon nitride was washed with DMAc (anhydrous, 6 mL, followed by centrifugation at 3000 rpm for 20 min and separation of the liquid phase), water (6 mL, followed by centrifugation at 3000 rpm for 20 min and separation of the liquid phase) and lyophilized (overnight) before analysis.

Table S13: ICP-OES measurements of the nickel content on the new and recovered CN-OA-m after 8 h white light and 48 h green light standard reaction.

Sample	Ni [mg/g CN]	% adsorbed Ni
CN-OA-m new	0.117	/
CN-OA-m white light standard reaction 1	14.2	16.1
CN-OA-m green light standard reaction	13.8	15.7



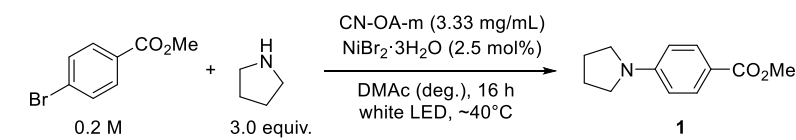
Figure S7. Fresh CN-OA-m (A), CN-OA-m after 8 h white light irradiation for standard reaction (B) and CN-OA-m after 48 h green light irradiation for standard reaction (C).

Note: Although 1.66 mg mL^{-1} of CN-OA-m is suitable for the C-N cross-coupling, a higher loading (3.33 mg mL^{-1}) was used for further experiments in order to obtain enough material for material characterization (ICP-OES, EDX, SEM, TEM, etc).

6. Recycling studies

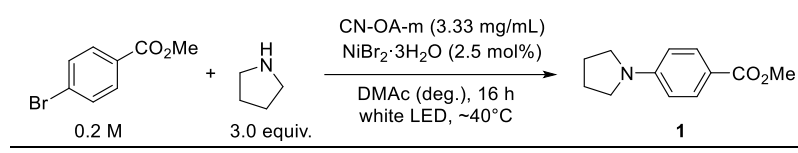
An oven dried vial (13 x 80 mm) equipped with a stir bar was charged with CN-OA-m (20 mg), 4-bromomethylbenzoate (258.0 mg, 1.2 mmol, 1.0 equiv.) and NiBr₂·3H₂O (8.2 mg, 30 μmol, 2.5 mol%). Subsequently, pyrrolidine (256.0 mg, 295.6 μl, 3.6 mmol, 3.0 equiv.) and DMAc (anhydrous, 6 mL) were added and the vial was sealed with a septum and Parafilm. The reaction mixture was sonicated for 5-10 min followed by stirring for 5 min until fine dispersion of the solids was achieved and the mixture was then degassed by bubbling N₂ for 10 min. The mixture was irradiated in the photoreactor (white light or green light) at 40 °C with rapid stirring (1400 rpm). After the respective reaction time, one equivalent of 1,3,5-trimethoxybenzene (202.0 mg, 1.2 mmol) was added and the mixture was stirred for 5 min. The reaction mixture was centrifuged at 3000 rpm for 20 min and the liquid phase was carefully separated and analyzed by ¹H-NMR. The carbon nitride was washed with DMAc (anhydrous, 6 mL, followed by centrifugation at 3000 rpm for 20 min and separation of the liquid phase), lyophilized (overnight) and reused in the next reaction.

Table S14. Reusability of CN-OA-m using white light.^a

	
Cycle	1 [%] ^b
1	99
2	98
3	43
4	27
5	33

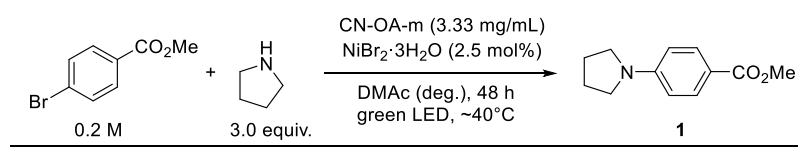
^aReaction conditions: methyl 4-bromobenzoate (1.2 mmol), pyrrolidine (3.6 mmol), NiBr₂·3H₂O (2.5 mol%), CN-OA-m (20 mg - reused), DMAc (anhydrous, 6 mL), white LEDs at 40 °C for 16h. ^bNMR yields determined by ¹H-NMR using 1,3,5-trimethoxybenzene as internal standard.

Table S15. Reusability of CN-OA-m without additional NiBr₂·3H₂O using white light.^a

	
Cycle	1 [%] ^b
1	99
2 ^c	1

^aReaction conditions: methyl 4-bromobenzoate (1.2 mmol), pyrrolidine (3.6 mmol), NiBr₂·3H₂O (2.5 mol%), CN-OA-m (20 mg - reused), DMAc (anhydrous, 6 mL), white LEDs at 40 °C for 16h. ^bNMR yields determined by ¹H-NMR using 1,3,5-trimethoxybenzene as internal standard. ^cNo NiBr₂·3H₂O added.

Table S16. Reusability of CN-OA-m using green light.^a

	
Cycle	1 [%] ^b
1	99
2	99
3	98
4	98
5	94

^aReaction conditions: methyl 4-bromobenzoate (1.2 mmol), pyrrolidine (3.6 mmol), NiBr₂·3H₂O (2.5 mol%), CN-OA-m (20 mg - reused), DMAc (anhydrous, 6 mL), green LEDs at 40 °C for 48h. ^bNMR yields determined by ¹H-NMR using 1,3,5-trimethoxybenzene as internal standard.

Table S17: ICP-OES measurements of the nickel content on recovered CN-OA-m after white light and green light recyclability tests.

Sample	Ni [mg/g CN]	% adsorbed Ni
CN-OA-m white light recyclability tests	60.5	13.7
CN-OA-m green light recyclability tests	38.8	8.8



Figure S8. Fresh CN-OA-m (A), CN-OA-m after recyclability tests with white light irradiation (B) and CN-OA-m after recyclability tests with green light irradiation (C).

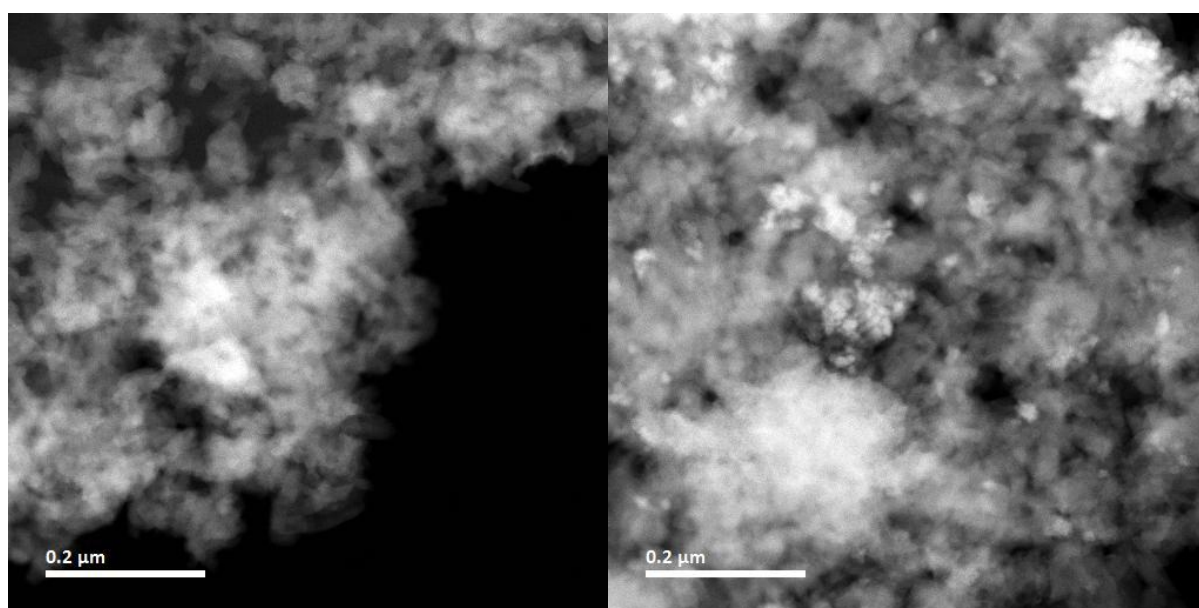


Figure S9. HAADF-STEM brightfield images show almost no nickel particle agglomerates (bright spots) on CN-OA-m after recyclability tests with green light irradiation (left) and a significant amount of agglomerates after recyclability tests with white light irradiation (right).

7. Scale-up of amination

An oven dried vial (25 x 140 mm) (Figure S10, A) equipped with a stir bar was charged with NiBr₂·3H₂O (54.5 mg, 0.2 mmol, 2.5 mol%), methyl 4-bromobenzoate (1.720 g, 8.0 mmol, 1 equiv.) and CN-OA-m (133.3 mg). Subsequently, pyrrolidine (1.706 g, 1.97 ml, 24.0 mmol, 3 equiv.) and DMAc (anhydrous, 6 mL) were added and the vial was sealed with a septum and parafilm. The reaction mixture was sonicated for 10 min and the mixture was then degassed by bubbling N₂ for 30 min and stirring the reaction mixture. The mixture was irradiated in a beaker wrapped with a LED-band (Figure S2, B) at ~40°C with rapid stirring (700 rpm). The completion of the reaction (14 h) was confirmed by taking an aliquot and measuring ¹H-NMR of the crude mixture in DMSO-d₆. The catalyst was removed by centrifugation (3000 rpm, 20 min) and the liquid phase was diluted with H₂O (200 mL) and extracted with ethyl acetate (3 x 200 mL). The combined organic phases were washed with H₂O (200 mL), a sat. NaHCO₃ solution (200 ml), and brine (200 mL), dried over Na₂SO₄ and concentrated. The crude product was purified by flash column chromatography (SiO₂, Hexane/EtOAc; gradient 0-5% ethyl acetate in hexane; 2. Isocratic 5% ethyl acetate in hexane)) on a Grace™ Reveleris™ system using a 24 g cartridge to afford (1-(4-methylbenzoate)pyrrolidine) (**1**) in 93 % (1.5338 g, 7.47 mmol) as a white solid (Figure S11).

¹H NMR (400 MHz, Chloroform-*d*) δ 7.88 (d, *J* = 8.7 Hz, 2H), 6.46 (d, *J* = 8.7 Hz, 2H), 3.83 (s, 3H), 3.40 – 3.09 (m, 4H), 2.05 – 1.86 (m, 4H). ¹³C NMR (101 MHz, Chloroform-*d*) δ = 167.57, 150.79, 131.31, 116.16, 110.62, 51.37, 47.47, 25.41. HRMS (ESI-TOF) *m/z* calcd. for C₁₂H₁₆NO₂ [(M+H)⁺]: 206.1176; found: 206.116.

These data are in full agreement with those previously published in the literature.¹⁸

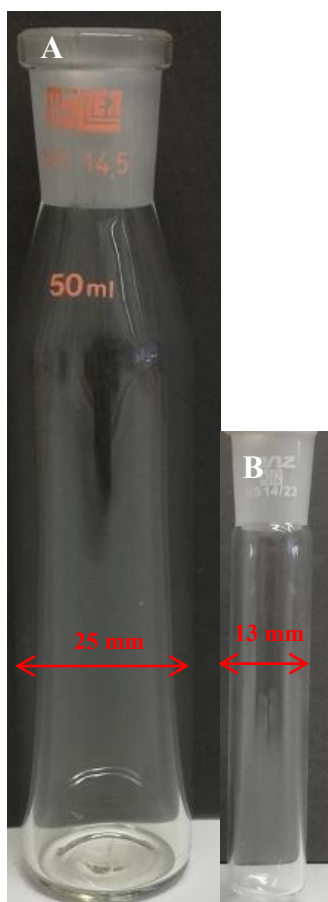


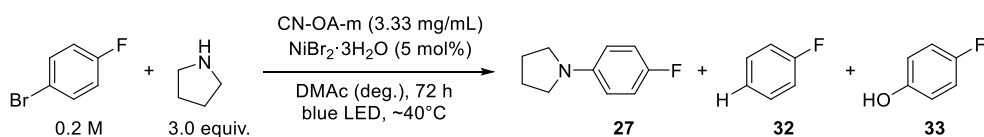
Figure S10. Vessel dimensions of vial for scale-up reaction (A) and vial for “standard scale” reactions (B).



Figure S11. Isolated product (1-(4-methylbenzoate)pyrrolidine) (**1**) from 8 mmol scale.

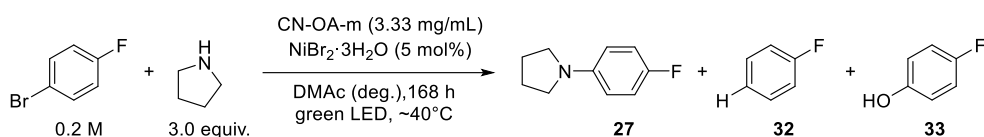
8. Studies on the reaction of 4-bromofluorobenzene with pyrrolidine.

Procedure A: Dual CN-OA-m/Ni catalysis with irradiation at 450 nm



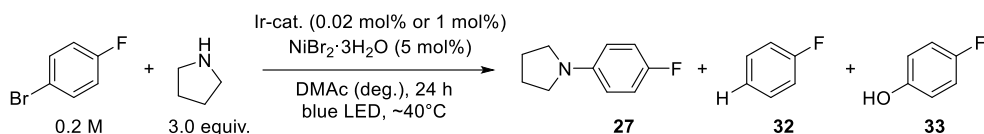
An oven dried vial (19 x 80 mm) equipped with a stir bar was charged with the CN-OA-m (20 mg), 4-bromofluorobenzene (210.0 mg, 131.8 μ l, 1.2 mmol, 1.0 equiv.) and NiBr₂·3H₂O (16.4 mg, 60 μ mol, 5.0 mol%). Subsequently, pyrrolidine (256.0 mg, 295.6 μ l, 3.6 mmol, 3.0 equiv.) and DMAc (anhydrous, 6 mL) were added and the vial was sealed with a septum and Parafilm. The reaction mixture was sonicated for 5-10 min followed by stirring for 5 min until fine dispersion of the solids was achieved and the mixture was then degassed by bubbling N₂ for 10 min. The mixture was irradiated in the photoreactor (blue light function of RGB LED strip) at 40 °C with rapid stirring (1400 rpm). After 72 h, one equivalent of 1,3,5-trimethoxybenzene (1.2 mmol) was added and the mixture was stirred for 5 min. An aliquot of the reaction mixture (~300 μ L) was filtered, diluted with DMSO-d₆ and subjected to ¹H-NMR analysis.

Procedure B: Dual CN-OA-m/Ni catalysis with irradiation at 520 nm



An oven dried vial (19 x 80 mm) equipped with a stir bar was charged with the CN-OA-m (20 mg), 4-bromofluorobenzene (210.0 mg, 131.8 μ l, 1.2 mmol, 1.0 equiv.) and (16.4 mg, 60 μ mol, 5.0 mol%). Subsequently, pyrrolidine (256.0 mg, 295.6 μ l, 3.6 mmol, 3.0 equiv.) and DMAc (anhydrous, 6 mL) were added and the vial was sealed with a septum and Parafilm. The reaction mixture was sonicated for 5-10 min followed by stirring for 5 min until fine dispersion of the solids was achieved and the mixture was then degassed by bubbling N₂ for 10 min. The mixture was irradiated in the photoreactor (green light function of RGB LED strip) at 40 °C with rapid stirring (1400 rpm). After 168 h, one equivalent of 1,3,5-trimethoxybenzene (1.2 mmol) was added and the mixture was stirred for 5 min. An aliquot of the reaction mixture (~300 μ L) was filtered, diluted with DMSO-d₆ and subjected to ¹H-NMR analysis.

Procedure Ir: Dual Ir/Ni catalysis with irradiation at 420 nm



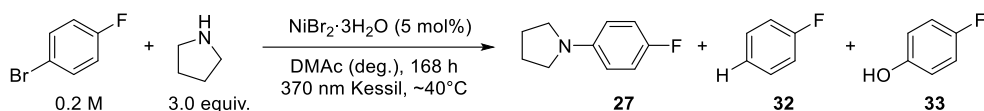
Ir1: An oven dried vial (19 x 80 mm) equipped with a stir bar was charged with 4-bromofluorobenzene (210.0 mg, 131.8 μ l, 1.2 mmol, 1.0 equiv.) and NiBr₂·3H₂O (16.4 mg, 60 μ mol, 5.0 mol%) and a solution of Ir[dF(CF₃)ppy]₂(dtbbpy)PF₆ (0.27 mg, 0.02 mol%) in DMAc (48 μ l). Subsequently, pyrrolidine (256.0 mg, 295.6 μ l, 3.6 mmol, 3.0 equiv.) and DMAc (anhydrous, 6 mL) were added and the vial was sealed with a septum and Parafilm.

Ir2: An oven dried vial (19 x 80 mm) equipped with a stir bar was charged with 4-bromofluorobenzene (52.5 mg, 33.0 μ l, 0.3 mmol, 1.0 equiv.), NiBr₂·3H₂O (4.1 mg, 15 μ mol, 5.0 mol%) and a solution of Ir [dF(CF₃)ppy]₂(dtbbpy)PF₆ (3.37 mg, 1 mol%) in DMAc (600 μ l). Subsequently, pyrrolidine (64.0 mg, 73.9 μ l, 0.9 mmol, 3.0 equiv.) and DMAc (anhydrous, 2.4 mL) were added and the vial was sealed with a septum and Parafilm.

The reaction mixture was sonicated for 5-10 min followed by stirring for 5 min and the mixture was then degassed by bubbling N₂ for 10 min. The mixture was irradiated in the photoreactor (blue light function of LED-band) at 40 °C with rapid stirring (1400 rpm). After 24 h, one equivalent of 1,3,5-trimethoxybenzene (Ir1: 202.0 mg, 1.2 mmol/ Ir2: 50.5 mg, 0.3 mmol) was added and the mixture was stirred for 5 min. An aliquot of the reaction mixture (~300 μ L) was filtered, diluted with DMSO-d₆ and subjected to ¹H-NMR analysis.

Note: In case of procedure C2, the formation of small amounts of black particles was observed after the reaction.

Procedure UV: Ni catalysis with irradiation at 370 nm

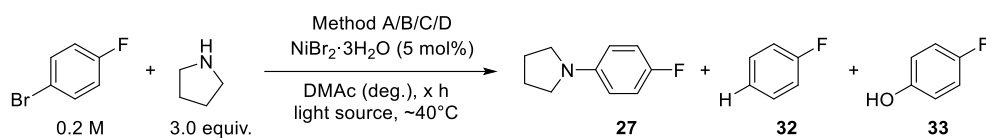


An oven dried vial (19 x 80 mm) equipped with a stir bar was charged 4-bromofluorobenzene (210.0 mg, 131.8 μl , 1.2 mmol, 1.0 equiv.) and $\text{NiBr}_2 \cdot 3\text{H}_2\text{O}$ (16.4 mg, 60 μmol , 5.0 mol%). Subsequently, pyrrolidine (256.0 mg, 295.6 μl , 3.6 mmol, 3.0 equiv.) and DMAc (anhydrous, 6 mL) were added and the vial was sealed with a septum and Parafilm. The reaction mixture was sonicated for 5-10 min followed by stirring for 5 min and the mixture was then degassed by bubbling N_2 for 10 min. The mixture was irradiated with UV light using the Kessil[®] PR 160-370 nm lamp with rapid stirring (~ 800 rpm) and cooling by a fan. After 3 h (UV1), 15 h (UV2), 72 h (UV3) and 168 h (UV4) one equivalent of 1,3,5-trimethoxybenzene (202.0 mg, 1.2 mmol) was added and the mixture was stirred for 5 min. An aliquot of the reaction mixture (~ 300 μL) was filtered, diluted with DMSO-d_6 and subjected to $^1\text{H-NMR}$ analysis.

Note: The color of the reaction solution changed from yellowish to black and a significant amount of black particles was formed.

The reaction mixtures of procedure A, B, and D were centrifuged at 3000 rpm for 20 min. The carbon nitride from the blue (procedure A) and green light experiment (procedure B) and the black particles formed during the UV-light experiment (procedure D) were washed with DMAc (anhydrous 6 mL, followed by centrifugation at 3000 rpm for 20 min and separation of the liquid phase) and acetone (6 mL, followed by centrifugation at 3000 rpm for 20 min and separation of the liquid phase), lyophilized (overnight) and subjected to FTIR, UV-Vis, XRD, UV-Vis, ICP-OES, EDX, XPS as well as SEM and TEM analysis. For comparison, an unused sample of CN-OA-m from the same batch was also analyzed.

Table S18. Coupling of 4-bromofluorobenzene and pyrrolidine using different light sources and catalysts.



Entry	Procedure	Conversion [%] ^a	27 [%] ^b	32 [%] ^b	33 [%] ^b
1	A	93	70	6	9
2	A	92	69	7	8
3	A	91	68	6	9
4	A	92	63	7	6
5	A	87	60	7	9
6	A	18	6	2	n.d. ^c
7	A	22	5	n.d.	3
8	B	quant.	91	5	2
9	B	quant.	89	1	10
10	B	quant.	89	9	1
11	B	99	86	9	2
12	B	quant.	88	1	10
13	B	97	86	2	9
14	B	quant.	84	9	n.d.
15	Ir1	quant.	77	7	4
16	Ir2	79	33	20	13
17	UV1	18	7	3	n.d.
18	UV2	39	17	9	4
19	UV3	94	26	32	16
20	UV4	quant.	10	23	9

^aConversion of 4-bromofluorobenzene determined by ¹H-NMR using 1,3,5-trimethoxybenzene as internal standard. ^bNMR yields determined by ¹H-NMR using 1,3,5-trimethoxybenzene as internal standard. ^cnot detected.

8.1 Powder X-ray diffraction (XRD) and X-ray photoelectron spectroscopy (XPS)

The powder X-ray diffraction spectra (PXRD) of the black material generated during the UV-light experiment (Table S18, Entry 17) showed diffraction peaks at 44° , 51° and 76° that could be assigned to the (1 1 1), (2 0 0), (2 2 0) planes of nickel(0) (Figure S12). Spectra of the recovered CN-OA-m (Table 17, Entry 7 & 8) materials show a characteristic peak at 27.4° , which corresponds to the in-planar structural packing and inter-planar stacking peaks of the aromatic systems of CN-OA-m. Nickel(0) (diffraction peaks at 44° , 51° and 76°) was detected in the material recovered from experiment using blue LEDs (Method A), and, although in significantly lower quantity, in the material recovered from the experiment using green LEDs (Method B).

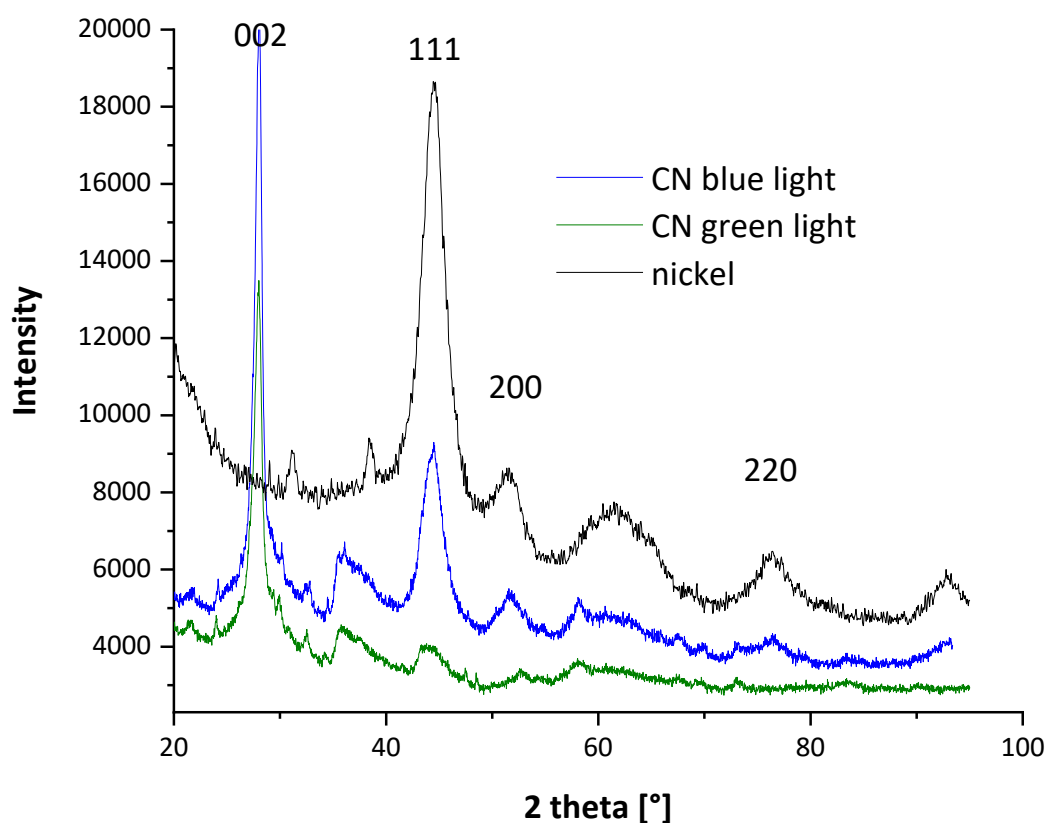
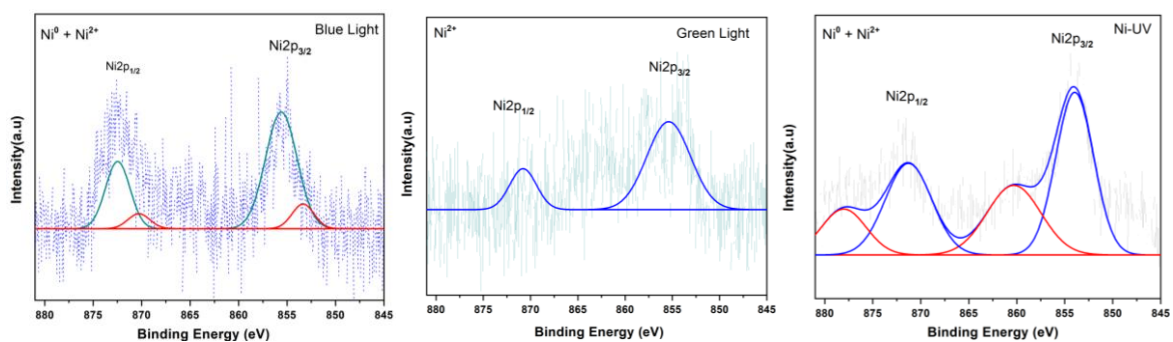


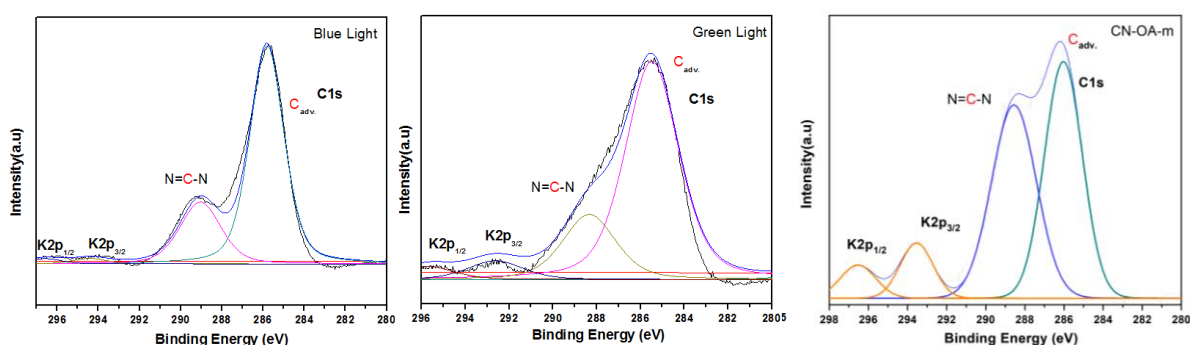
Figure S12. XRD measurements of the material generated by UV-light (black line), CN-OA-m after method A with blue light irradiation (blue line) and CN-OA-m after method B with green light irradiation (green line).

XPS scans of the solid material generated during UV light experiments and CN-OA-m recovered from the experiments using blue (Method A) and green LED (Method B) irradiation confirmed the presence of nickel in both samples (Figure S13). High-resolution XPS analysis spectra for core levels of Ni2p confirm the presence of Ni²⁺ and Ni⁰ at 854.6 (\pm 0.02) eV and 852.3 (\pm 0.02) eV, for CN-OA-m recovered from method A (blue light) and the material generated during UV light irradiation (Figure S13, A). Only Ni²⁺ (854.6 (\pm 0.02) eV) species were detected in the CN-OA-m sample recovered from the experiment using method B (green light). The high-resolution XPS spectra of the C 1s core level spectra shows typical C-C and N-C=N bonding signals for all CN-OA-m samples (Figure S13, B). The N 1s spectra contain two main peaks that are typical for carbon nitrides and can be assigned to i) sp² bonded nitrogen in tri-s-triazine groups (C-N=C), and ii) sp³ amino groups (C-NH) for all CN-OA-m samples. The calculated elemental composition indicates a two times higher concentration of nickel on CN-OA-m recovered from method A (blue light) compared to CN-OA-m recovered from method B (green light) (Table S19).

A



B



C

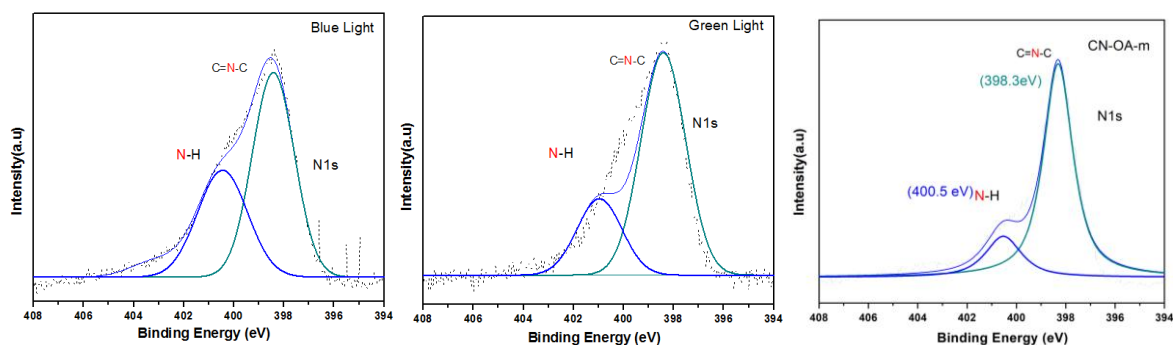


Figure S13. A) High-resolution XPS analysis spectra for core levels of Ni $2p_{3/2}$: CN-OA-m recovered from experiments using method A (blue light) and method B (green light), and the heterogeneous material generated during UV-light experiments (Ni-UV). **B)** High-resolution XPS analysis spectra for core levels of C $1s$: CN-OA-m recovered from experiments using method A (blue light) and method B (green light), and unused CN-OA-m. **C)** High-resolution XPS analysis spectra for core levels of N $1s$: CN-OA-m recovered from experiments using method A (blue light) and method B (green light), and unused CN-OA-m. has been deconvoluted using *Lorentzian-Gaussian* peak fitting functions with Shirley background deletion.

Table S19. XPS Elemental composition of CN-OA-m and CN-OA-m recovered from experiments using method A and B.

Sample	% w/w N	% w/w C	% w/w K	% w/w Ni
CN-OA-m	57.257	41.191	1.552	---
CN-OA-m blue light ^a	61.094	37.718	0.365	0.822
CN-OA-m green light ^b	59.021	39.983	0.709	0.377

^aSample recovered from experiment described in Table S18, Entry 7. ^bSample recovered from experiment described in Table S18, Entry 8.

8.2 Scanning transmission electron microscopy (STEM)

8.2.1 CN-OA-m recovered from method A (blue LEDs) and method B (green LEDs)

Scanning transmission electron microscopy (STEM) was used to visualize nickel particles on the surface of the recovered CN-OA-m. High-angle annular dark-field (HAADF) images show round- to oval-shaped particles with sizes ranging 10-20 nm. The polycrystalline particle consist of smaller ones (1-5 nm), which agglomerated on the surface (Figure S14 and S15). The images show the porous structure of CN-OA-m containing particles that show a diffraction pattern indicating Ni-species deposition. The exact lattice of a selected nickel particle is shown in higher resolution. The STEM images of CN-OA-m recovered from experiments using method B (green LED) (Figure S15) show a significantly lower amount of (agglomerated) nickel particles compared to using method A (blue LED, Figure S14). This confirms the results obtained using XRD (Figure S12), XPS (Figure S13), EDX (Table S20) and ICP-OES (Table S21) analysis.

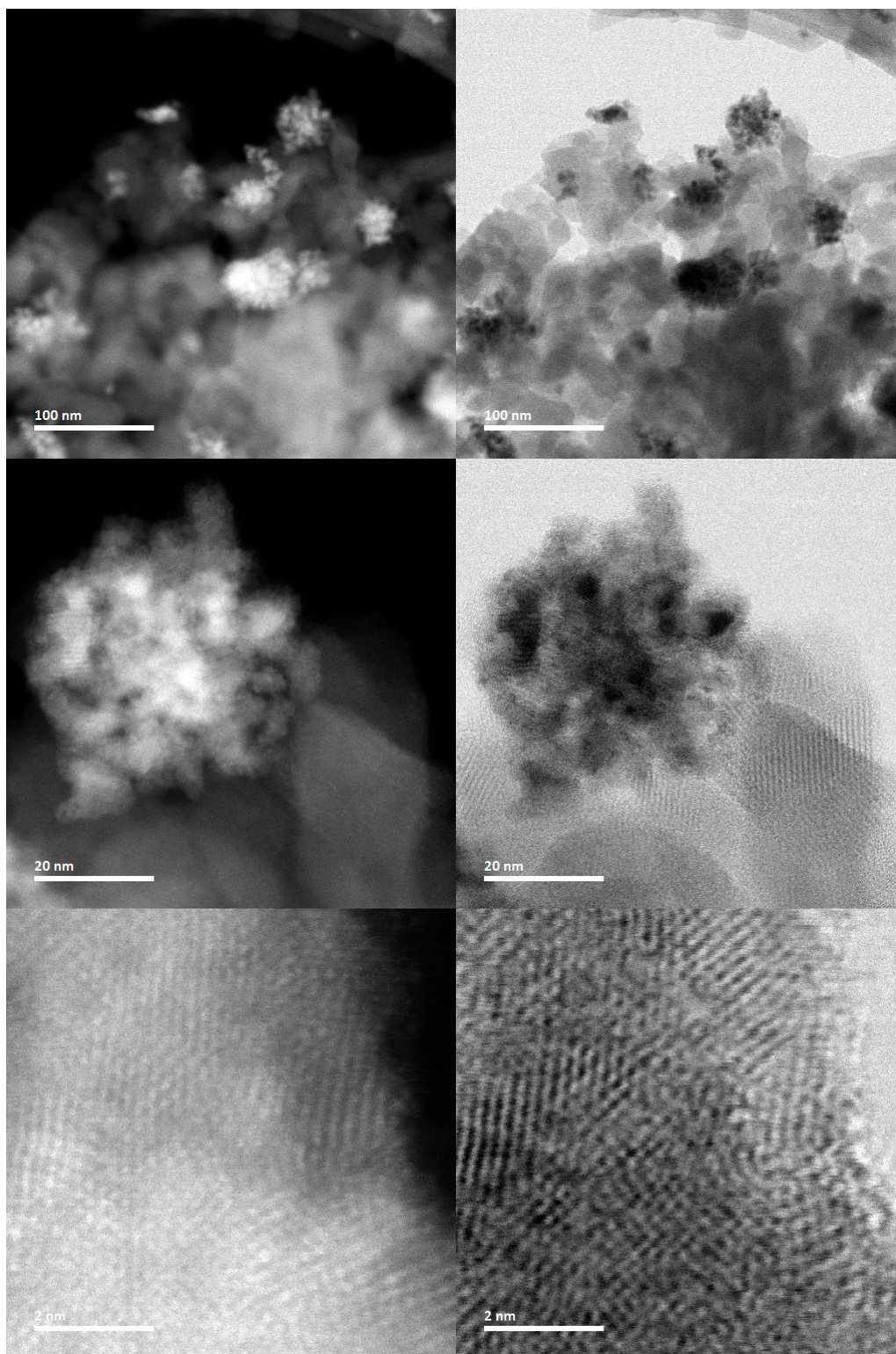


Figure S14. HAADF-STEM brightfield (left)/darkfield (right) images showing nickel particles (bright spots in brightfield and dark spots in darkfield) on CN-OA-m recovered from the experiment using method A (blue LED).

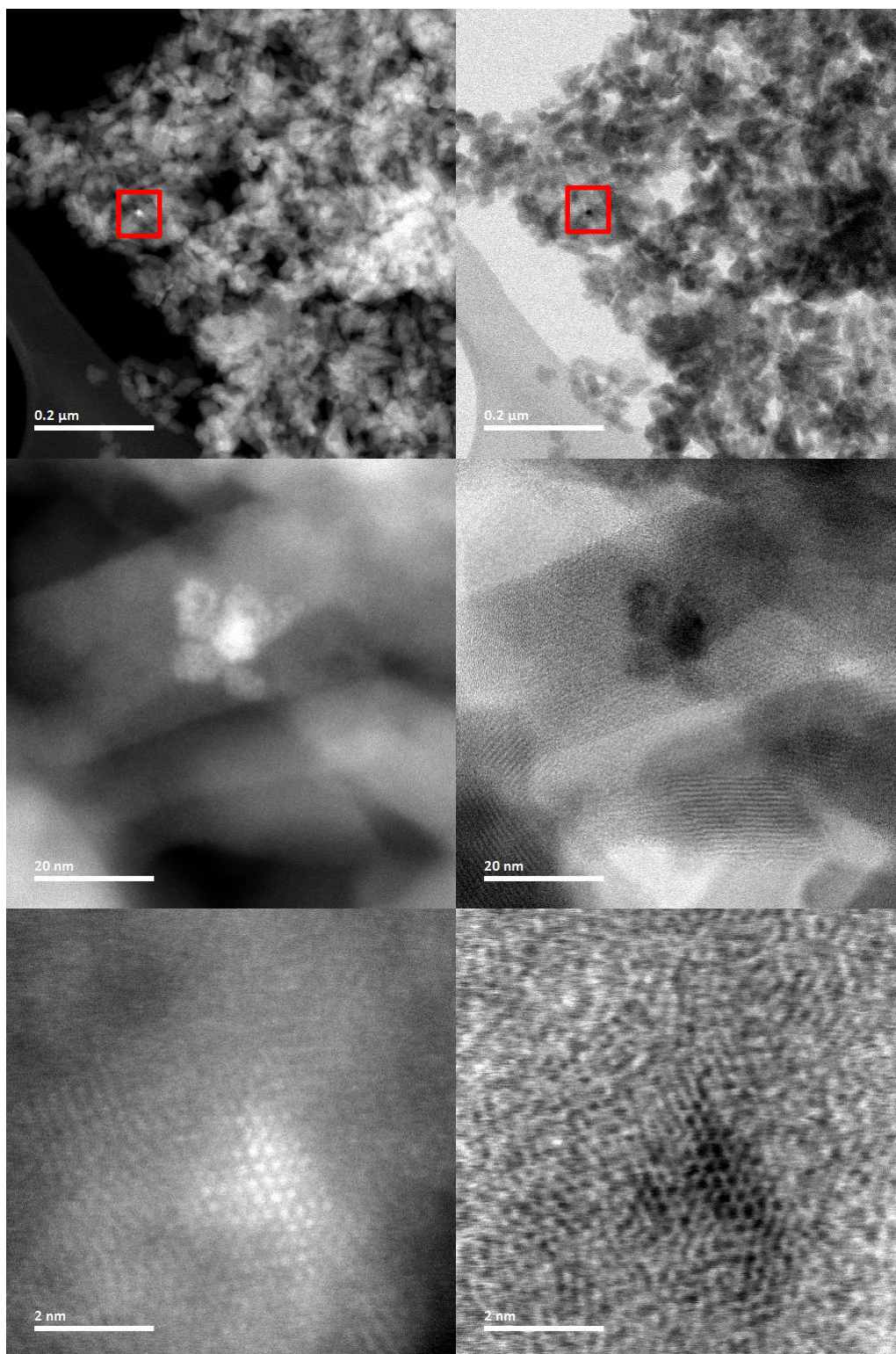


Figure S15. HAADF-STEM brightfield (left)/darkfield (right) showing a nickel particle (bright spot in brightfield and dark spot in darkfield) on CN-OA-m recovered from the experiment using method B (green LED).

8.2.2 Heterogeneous material generated during experiments using the UV method (photocatalyst-free and UV-light)

The STEM image shows the solid material formed using method C (UV-light). Although the particle mainly consists of nickel, lighter elements can be additionally identified. EDX analysis (Table S20) shows the presence of carbon, indicating that agglomerated nickel species incorporate organic materials. This is in agreement with the low mass-balance observed during these reactions (e.g. Table S18, Entry 20), suggesting substrate/product degradation presumably by the high energy light source.

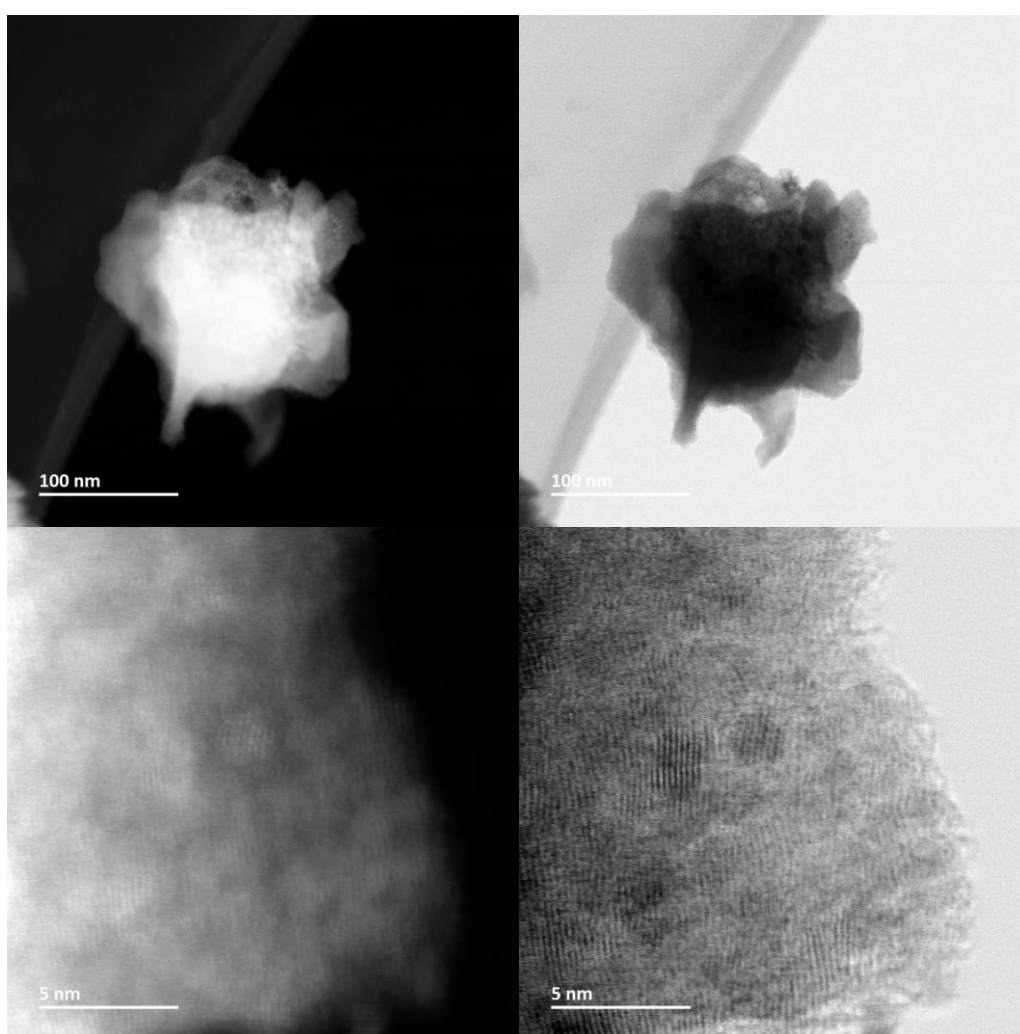


Figure S16. HAADF-STEM brightfield (left)/darkfield (right) images of nickel particles (bright spots in brightfield and dark spots in darkfield) after UV-light method (photocatalyst-free).

8.3 Scanning electron microscopy (SEM)

SEM images of the new and recovered CN-OA-m samples showed a porous texture that was not altered during the catalytic transformation (Figure S17).

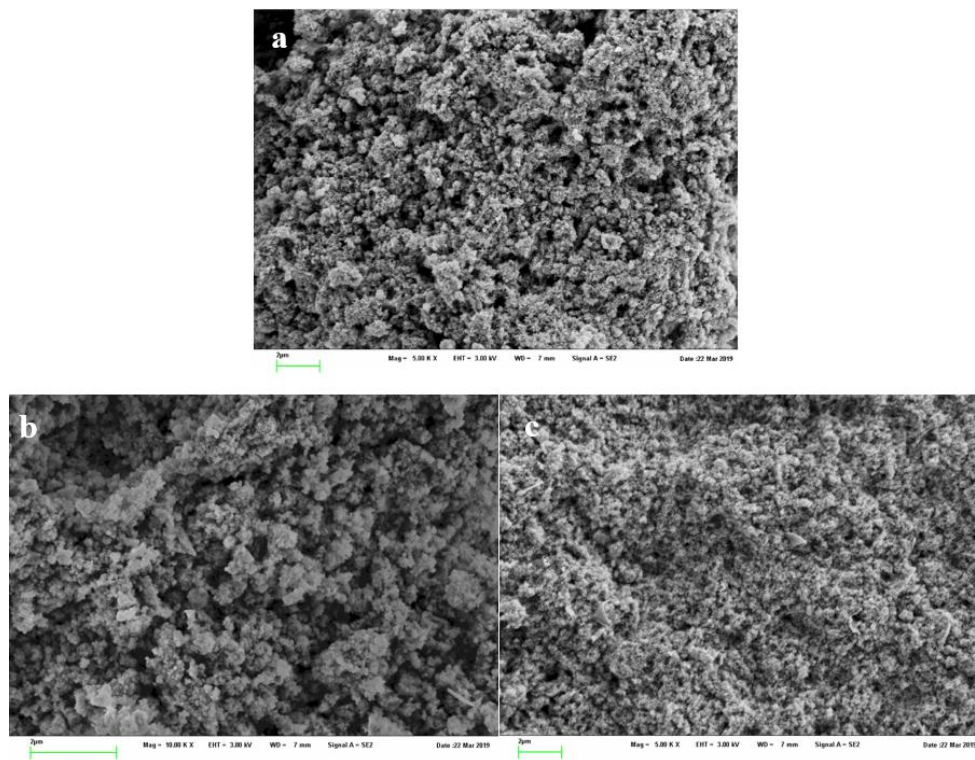


Figure S17- SEM images of CN-OA-m new (A), CN-OA-m recovered from the cross-coupling using blue light (Table S18, Entry 7) (B), and CN-OA-m recovered from the cross-coupling using green light (Table S18, Entry 8) (C).

8.4 Energy-dispersive X-ray spectroscopy (EDX) and inductively coupled plasma atomic emission spectroscopy (ICP-OES)

Elemental analysis via EDX (Table S20) and ICP-OES (Table S21) analysis of the recovered CN-OA-m samples shows a 3 times higher Ni concentration for the blue light experiment. The material from the blue light experiment contains ~12-14 w/w % Ni suggesting that ~70% of the homogeneous nickel catalyst were deposited on the CN-OA-m during the model reaction. The material from the green light experiment contains ~3-4 w/w % Ni suggesting that ~70% of the homogeneous nickel catalyst were deposited on the CN-OA-m during the model reaction.

Table S20: EDX elemental composition acquired from new and recovered CN-OA-m.

Sample	% w/w N	% w/w C	% w/w O	% w/w K	% w/w Ni
CN-OA-m	42.56	37.59	3.65	1.06	0.05
CN-OA-m from Method A (blue light) ^a	36.25	30.27	7.16	8.60	13.90
CN-OA-m from Method B (green light) ^b	47.19	29.46	7.79	8.86	3.38
Solid from UV-experiment ^c	22.8	21.00	18.92	-	26.71

^aSample recovered from experiment described in Table S18, Entry 7. ^bSample recovered from experiment described in Table S18, Entry 8. ^cSample recovered from experiment described in Table S18, Entry 17.

Table S21: ICP-OES measurements of the nickel content on the new and recovered CN-OA-m.

Sample	Ni [mg/g CN]	% absorbed Ni
CN-OA-m new	0.69	0.39
CN-OA-m from Method A (blue light) ^a	126	71.2
CN-OA-m from Method B (green light) ^b	35.5	20.1

^aSample recovered from experiment described in Table S18, Entry 7.

^bSample recovered from experiment described in Table S18, Entry 8.

8.5 Fourier-transform infrared spectroscopy (FTIR) and Ultraviolet-visible spectroscopy (UV-VIS)

FTIR spectra of the new and recovered CN-OA-m samples were identical (Figure S18).

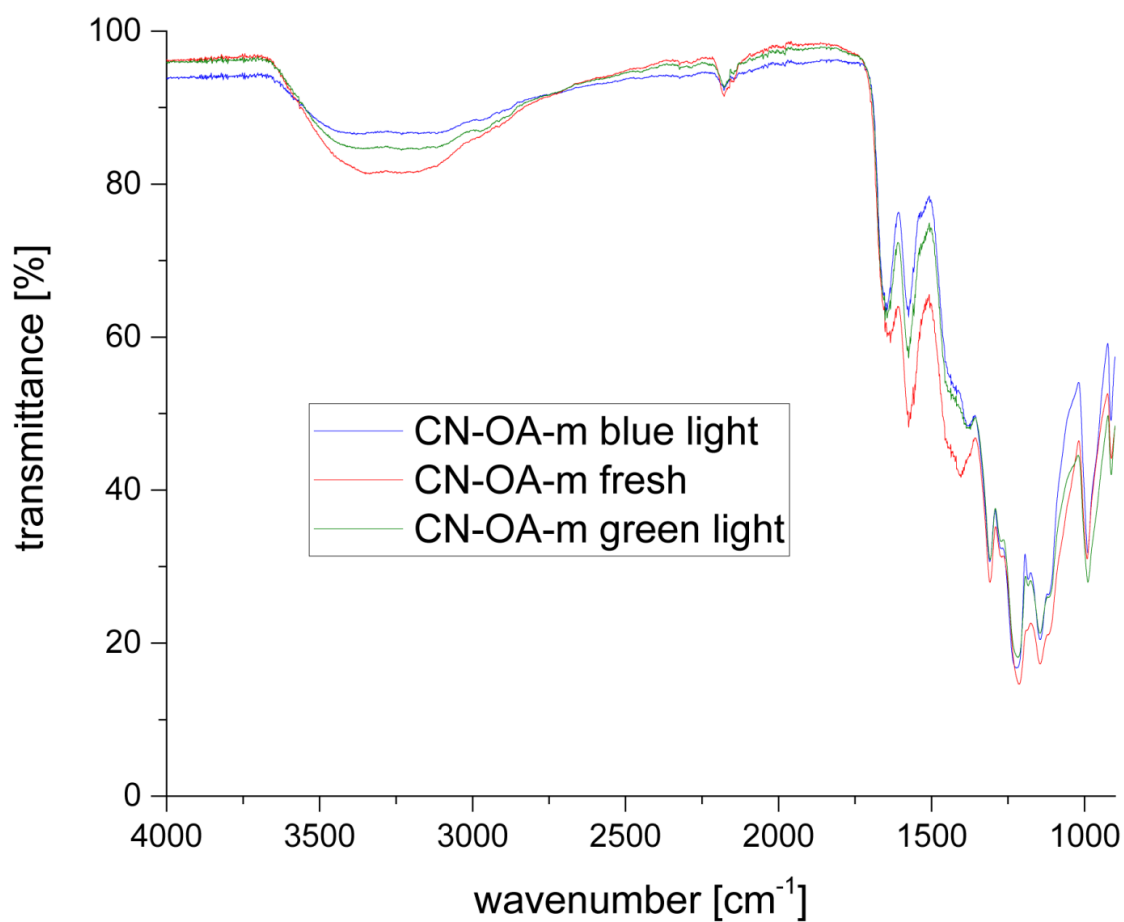


Figure S18. FTIR spectra of CN-OA-m new (red), CN-OA-m recovered from the cross-coupling using blue light (blue), and CN-OA-m recovered from the cross-coupling using green light (green).

The UV-Vis spectra of the CN-OA-m recovered from the cross-coupling using green light and CN-OA-m recovered from the cross-coupling using blue showed an increased absorption in the visible region (>460 nm) compared to a unused CN-OA-m sample.

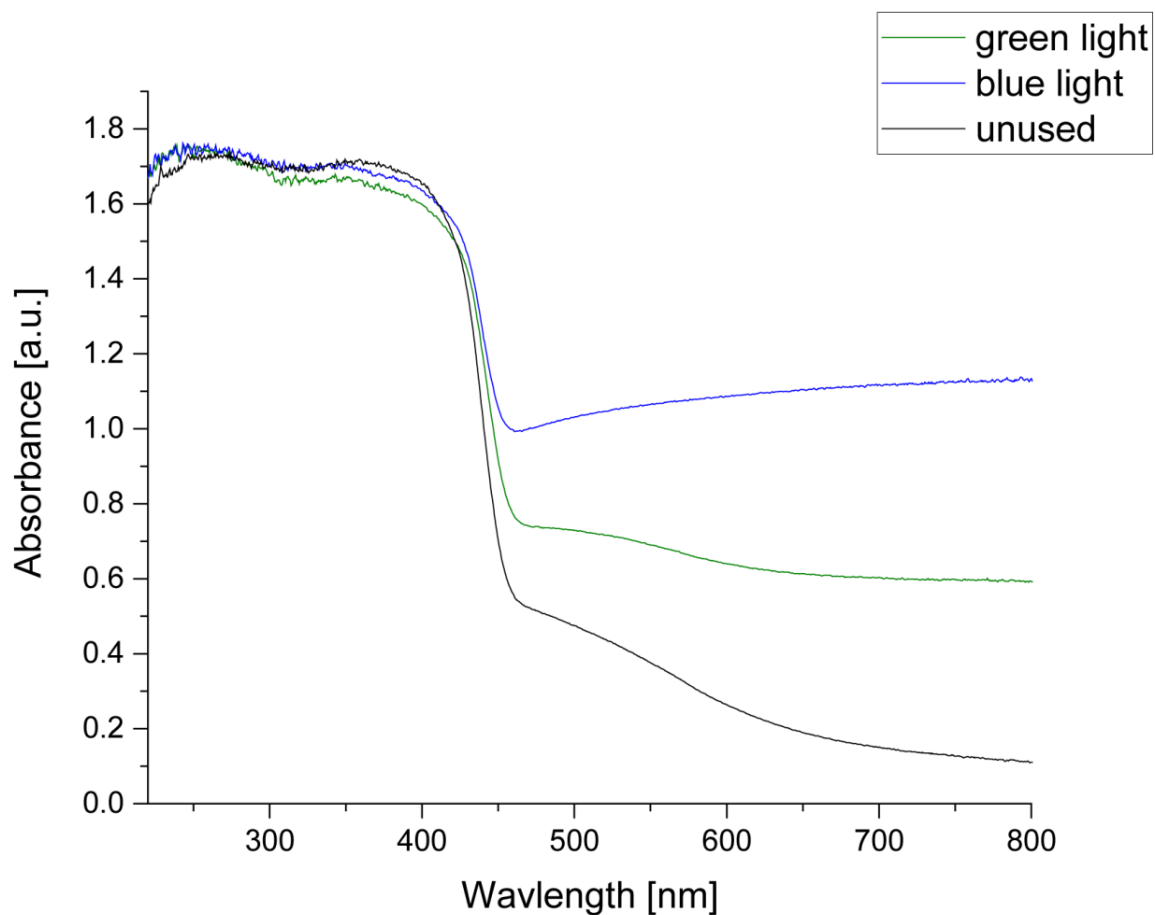
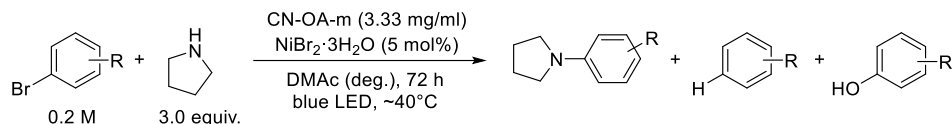


Figure S19. UV/Vis absorption spectra of CN-OA-m new (grey), CN-OA-m recovered from the cross-coupling using blue light (blue), and CN-OA-m recovered from the cross-coupling using green light (green).

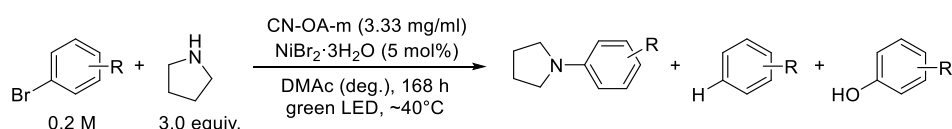
9. Studies on the reaction of bromobenzene, 3-bromotoluene, 1-bromo-4-*tert*-butylbenzene, and 4-bromoanisole with pyrrolidine.

Procedure A: Dual CN-OA-m/Ni catalysis with irradiation at 450 nm



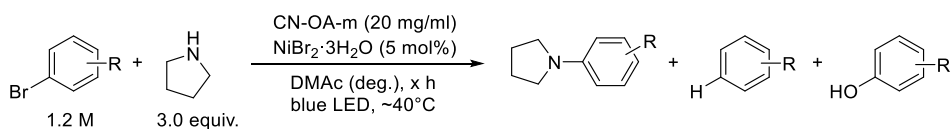
An oven dried vial (19 x 80 mm) equipped with a stir bar was charged with the CN-OA-m (20 mg), aryl bromide (1.2 mmol, 1.0 equiv.) and NiBr₂·3H₂O (16.4 mg, 60 μmol, 5.0 mol%). Subsequently, pyrrolidine (256.0 mg, 295.6 μl, 3.6 mmol, 3.0 equiv.) and DMAc (anhydrous, 6 mL) were added and the vial was sealed with a septum and Parafilm. The reaction mixture was sonicated for 5-10 min followed by stirring for 5 min until fine dispersion of the solids was achieved and the mixture was then degassed by bubbling N₂ for 10 min. The mixture was irradiated in the photoreactor (blue light function of RGB LED strip) at 40 °C with rapid stirring (1400 rpm). After 72 h, one equivalent of 1,3,5-trimethoxybenzene (1.2 mmol) was added and the mixture was stirred for 5 min. An aliquot of the reaction mixture (~300 μL) was filtered, diluted with DMSO-d₆ and subjected to ¹H-NMR analysis.

Procedure B: Dual CN-OA-m/Ni catalysis with irradiation at 520 nm

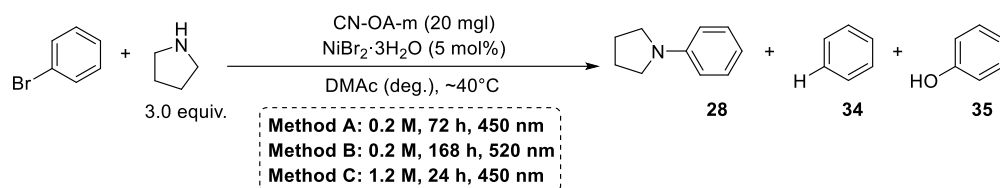


An oven dried vial (19 x 80 mm) equipped with a stir bar was charged with the CN-OA-m (20 mg), aryl bromide (1.2 mmol, 1.0 equiv.) and NiBr₂·3H₂O (16.4 mg, 60 μmol, 5.0 mol%). Subsequently, pyrrolidine (256.0 mg, 295.6 μl, 3.6 mmol, 3.0 equiv.) and DMAc (anhydrous, 6 mL) were added and the vial was sealed with a septum and Parafilm. The reaction mixture was sonicated for 5-10 min followed by stirring for 5 min until fine dispersion of the solids was achieved and the mixture was then degassed by bubbling N₂ for 10 min. The mixture was irradiated in the photoreactor (green light function of RGB LED strip) at 40 °C with rapid stirring (1400 rpm). After 168 h, one equivalent of 1,3,5-trimethoxybenzene (1.2 mmol) was added and the mixture was stirred for 5 min. An aliquot of the reaction mixture (~300 μL) was filtered, diluted with DMSO-d₆ and subjected to ¹H-NMR analysis.

Procedure C: Dual CN-OA-m/Ni catalysis with irradiation at 450 nm and higher concentration (1.2 M)



An oven dried vial (19 x 80 mm) equipped with a stir bar was charged with the CN-OA-m (20 mg), aryl bromide (1.2 mmol, 1.0 equiv.) and NiBr₂·3H₂O (16.4 mg, 60 μmol, 5.0 mol%). Subsequently, pyrrolidine (256.0 mg, 295.6 μl, 3.6 mmol, 3.0 equiv.) and DMAc (anhydrous, 1 mL) were added and the vial was sealed with a septum and Parafilm. The reaction mixture was sonicated for 5-10 min followed by stirring for 5 min until fine dispersion of the solids was achieved and the mixture was then degassed by bubbling N₂ for 10 min. The mixture was irradiated in the photoreactor (blue light function of RGB LED strip) at 40 °C with moderate stirring (600 rpm). After respective reaction time, one equivalent of 1,3,5-trimethoxybenzene (202.0 mg, 1.2 mmol) was added and the mixture was stirred for 5 min. An aliquot of the reaction mixture (~300 μL) was filtered, diluted with DMSO-d₆ and subjected to ¹H-NMR analysis.

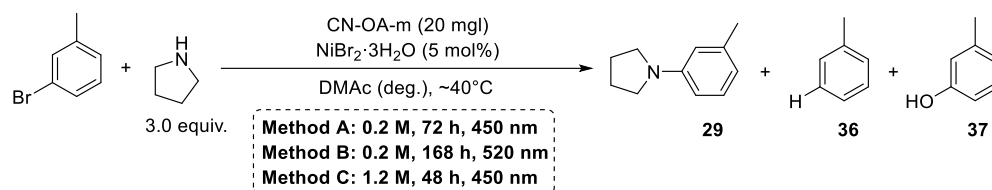
Table S22. Coupling of bromobenzene and pyrrolidine using methods A-C.

Entry	Procedure	Conversion [%] ^a	28 [%] ^b	34 [%] ^b	35 [%] ^b
1	A	quant.	74	8	11
2	A	quant.	68	11	10
3	A	quant.	67	11	12
4	A	quant.	66	10	11
5	A	67	44	7	6
6	A	56	32	5	4
7	B	quant.	94	4	3
8	B	quant.	93	4	3
9	B	quant.	91	5	5
10	B	quant.	90	4	4
11	B	quant.	88	4	5
12	B	quant.	87	4	5
13	C	quant.	86	8	4
14	C	quant.	85	7	3
15	C	99	85	8	3
16	C	quant.	85	9	3
17	C	quant.	84	8	3
18	C	quant.	84	9	3
19	C ^d	quant.	85	5	2
20	C ^d	quant.	82	5	1

^aConversion of bromobenzene determined by ¹H-NMR using 1,3,5-trimethoxybenzene as internal standard.

^bNMR yields determined by ¹H-NMR using 1,3,5-trimethoxybenzene as internal standard. ^cnot detected.

^dCarried out using 520 nm LEDs and 168 h reaction time.

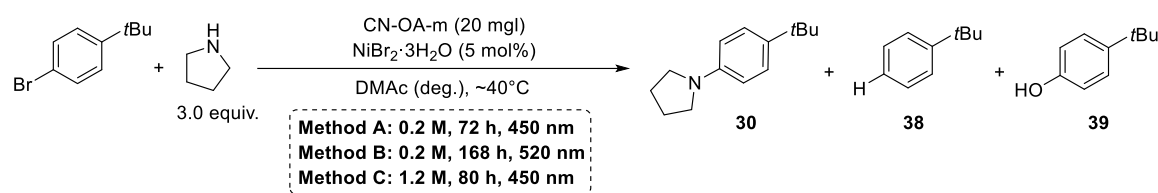
Table S23. Coupling of 3-bromotoluene and pyrrolidine using methods A-C.

Entry	Procedure	Conversion [%] ^a	29 [%] ^b	36 [%] ^b	37 [%] ^b
1	A	quant.	74	17	6
2	A	quant.	72	17	6
3	A	quant.	72	18	4
4	A	quant.	61	18	12
5	A	64	31	12	9
6	A	52	20	13	8
7	B	quant.	93	5	4
8	B	quant.	86	10	4
9	B	quant.	85	10	5
10	B	quant.	84	10	5
11	B	quant.	84	10	7
12	B	quant.	83	10	6
13	C	quant.	85	14	2
14	C	quant.	84	14	3
15	C	quant.	83	14	3
16	C	quant.	83	14	3
17	C	quant.	82	15	3
18	C	quant.	81	16	3
19	C ^d	quant.	80	6	0

^aConversion of 3-bromotoluene determined by ¹H-NMR using 1,3,5-trimethoxybenzene as internal standard.

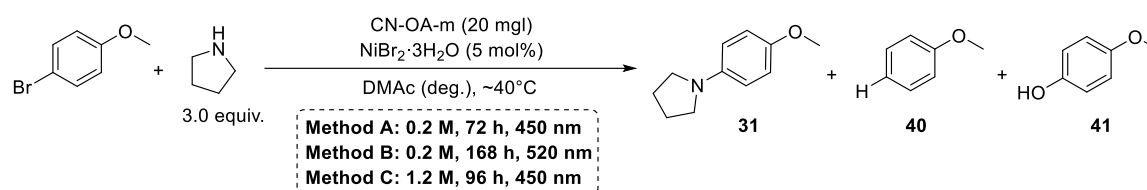
^bNMR yields determined by ¹H-NMR using 1,3,5-trimethoxybenzene as internal standard. ^cnot detected.

^dCarried out using 520 nm LEDs and 168 h reaction time.

Table S24. Coupling of 4-bromotertbutylbenzene and pyrrolidine using methods A-C.

Entry	Procedure	Conversion [%] ^a	30 [%] ^b	38 [%] ^b	39 [%] ^b
1	A	98	70	13	9
2	A	99	69	17	7
3	A	quant.	67	14	8
4	A	88	57	16	9
5	A	82	53	15	9
6	A	90	52	13	7
7	B	quant.	92	5	3
8	B	96	90	4	2
9	B	94	87	3	3
10	B	91	85	3	2
11	B	57	50	4	2
12	B	30	28	1	2
13	C	quant.	82	9	2
14	C	quant.	80	9	1
15	C	quant.	80	9	2
16	C	quant.	80	9	2
17	C	quant.	80	9	3
18	C	quant.	80	10	3
19	C ^d	91	82	4	0

^aConversion of 4-bromotertbutylbenzene determined by ¹H-NMR using 1,3,5-trimethoxybenzene as internal standard. ^bNMR yields determined by ¹H-NMR using 1,3,5-trimethoxybenzene as internal standard. ^cnot detected. ^dCarried out using 520 nm LEDs and 72 h reaction time.

Table S25. Coupling of 4-bromoanisole and pyrrolidine using methods A-C.

Entry	Procedure	Conversion [%] ^a	31 [%] ^b	40 [%] ^b	41 [%] ^b
1	A	86	80	6	n.d. ^c
2	A	91	78	12	2
3	A	90	72	10	5
4	A	66	53	8	2
5	A	43	32	4	2
6	A	13	4	n.d.	2
7	B	82	77	7	0
8	B	83	77	6	0
9	B	76	68	6	0
10	B	68	60	4	4
11	B	68	60	4	3
12	B	58	52	4	2
13	C	quant.	81	8	5
14	C	quant.	80	11	5
15	C	quant.	80	11	5
16	C	quant.	80	8	4
17	C	quant.	79	11	4
18	C	quant.	77	9	6
19	C ^d	quant.	84	8	1
20	C ^d	quant.	83	8	0

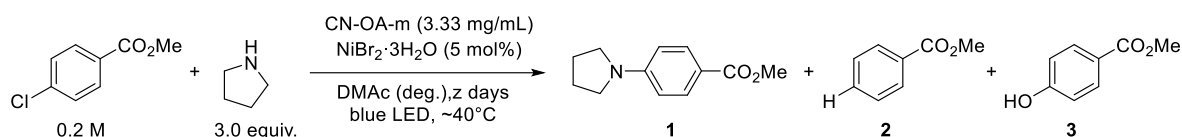
^aConversion of 4-bromoanisole determined by ¹H-NMR using 1,3,5-trimethoxybenzene as internal standard.

^bNMR yields determined by ¹H-NMR using 1,3,5-trimethoxybenzene as internal standard. ^cnot detected.

^dCarried out using 520 nm LEDs and 168 h reaction time.

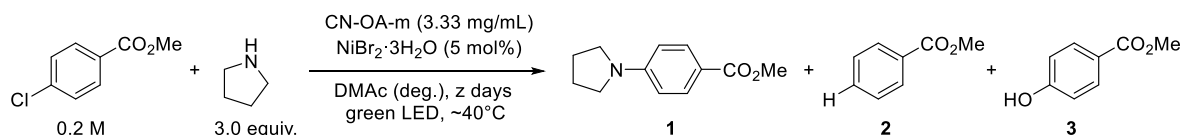
10. Studies on the reaction of methyl 4-chlorobenzoate

Procedure A: Dual CN-OA-m/Ni catalysis with irradiation at 450 nm



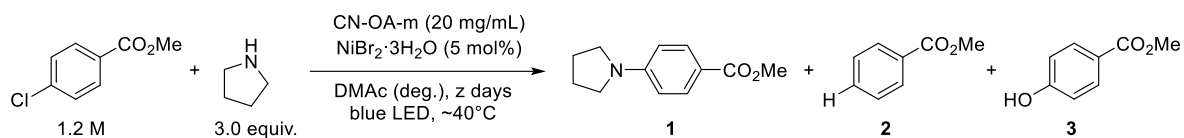
An oven dried vial (19 x 80 mm) equipped with a stir bar was charged with the CN-OA-m (20 mg), methyl 4-chloromethylbenzoate (204.7 mg, 1.2 mmol, 1.0 equiv.) and NiBr₂·3H₂O (16.4 mg, 60 μmol, 5.0 mol%). Subsequently, pyrrolidine (64.0 mg, 295.6 μl, 3.6 mmol, 3.0 equiv.) and DMAc (anhydrous, 6 mL) were added and the vial was sealed with a septum and Parafilm. The reaction mixture was sonicated for 5-10 min followed by stirring for 5 min until fine dispersion of the solids was achieved and the mixture was then degassed by bubbling N₂ for 10 min. The mixture was irradiated in the photoreactor (blue light of LED-band) at 40 °C with rapid stirring (1400 rpm). After respective reaction time, one equivalent of 1,3,5-trimethoxybenzene (202.0 mg, 1.2 mmol) was added and the mixture was stirred for 5 min. An aliquot of the reaction mixture (~300 μL) was filtered, diluted with DMSO-d₆ and subjected to ¹H-NMR analysis.

Procedure B: Dual CN-OA-m/Ni catalysis with irradiation at 520 nm

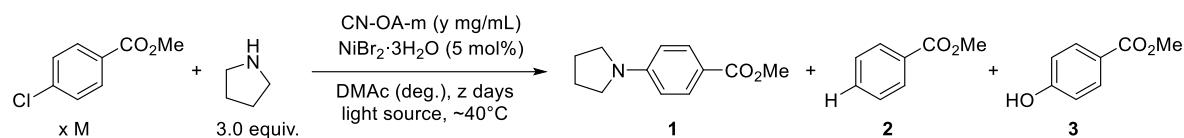


An oven dried vial (19 x 80 mm) equipped with a stir bar was charged with the CN-OA-m (20 mg), methyl 4-chloromethylbenzoate (204.7 mg, 1.2 mmol, 1.0 equiv.) and NiBr₂·3H₂O (16.4 mg, 60 μmol, 5.0 mol%). Subsequently, pyrrolidine (64.0 mg, 295.6 μl, 3.6 mmol, 3.0 equiv.) and DMAc (anhydrous, 6 mL) were added and the vial was sealed with a septum and Parafilm. The reaction mixture was sonicated for 5-10 min followed by stirring for 5 min until fine dispersion of the solids was achieved and the mixture was then degassed by bubbling N₂ for 10 min. The mixture was irradiated in the photoreactor (blue light of LED-band) at 40 °C with rapid stirring (1400 rpm). After respective reaction time, one equivalent of 1,3,5-trimethoxybenzene (202.0 mg, 1.2 mmol) was added and the mixture was stirred for 5 min. An aliquot of the reaction mixture (~300 μL) was filtered, diluted with DMSO-d₆ and subjected to ¹H-NMR analysis.

Procedure C: Dual CN-OA-m/Ni catalysis with irradiation at 450 nm and higher concentration (1.2 M)



An oven dried vial (19 x 80 mm) equipped with a stir bar was charged with the CN-OA-m (20 mg), methyl 4-chloromethylbenzoate (204.7 mg, 1.2 mmol, 1.0 equiv.) and NiBr₂·3H₂O (16.4 mg, 60 μmol, 5.0 mol%). Subsequently, pyrrolidine (64.0 mg, 295.6 μl, 3.6 mmol, 3.0 equiv.) and DMAc (anhydrous, 1 mL) were added and the vial was sealed with a septum and Parafilm. The reaction mixture was sonicated for 5-10 min followed by stirring for 5 min until fine dispersion of the solids was achieved and the mixture was then degassed by bubbling N₂ for 10 min. The mixture was irradiated in the photoreactor (blue light or green function of LED-band) at 40 °C with moderate stirring (600 rpm). After respective reaction time, one equivalent of 1,3,5-trimethoxybenzene (202.0 mg, 1.2 mmol) was added and the mixture was stirred for 5 min. An aliquot of the reaction mixture (~300 μL) was filtered, diluted with DMSO-d₆ and subjected to ¹H-NMR analysis.

Table S26. Coupling of methyl 4-chlorobenzoate and pyrrolidine using methods A-C.

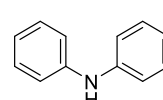
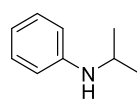
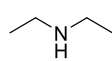
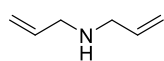
Entry	Method	Time [days]	Conversion [%] ^a	1 [%] ^b	2 [%] ^b	3 [%] ^b
1	A	3	47	37	2	n.d. ^c
2	A	7	78	65	7	3
3	A	14	91	65	16	7
4	B	3	59	41	1	12
5	B	7	76	72	4	n.d.
6	B	14	89	83	n.d.	9
7	C	1	79	75	3	1
8	C	2	97	92	3	2
9	C	3	97	89	4	2
10	C	4	99	89	3	2

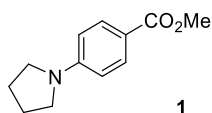
^aConversion of methyl 4-chlorobenzoate determined by ¹H-NMR using 1,3,5-trimethoxybenzene as internal standard. ^bNMR yields determined by ¹H-NMR using 1,3,5-trimethoxybenzene as internal standard. ^cnot detected

11. Scope and limitations

General experimental procedure. An oven dried vial (13 x 95 mm) equipped with a stir bar was charged with $\text{NiBr}_2 \cdot 3\text{H}_2\text{O}$ (8.2 mg, 30 μmol , 2.5 mol%), aryl bromide (1.2 mmol, 1 equiv.) and CN-OA-m (20 mg). Subsequently, the amine (3.6 mmol, 3 equiv.) and DMAc (anhydrous, 6 mL) were added and the vial was sealed with a septum and parafilm. The reaction mixture was sonicated for 5-10 min and the mixture was then degassed by bubbling N_2 for 10 min. The mixture was irradiated in the batch reactor (described above) at 40°C with rapid stirring (1400 rpm). After the respective reaction time, one equivalent of 1,3,5-trimethoxybenzene (202.0 mg, 1.2 mmol, internal standard) was added. An aliquot (~300 μL) of the reaction mixture was diluted with DMSO-d_6 and subjected to $^1\text{H-NMR}$ analysis. After full consumption of the arene starting material, the liquid phase was diluted with H_2O (40 mL) and extracted with ethyl acetate (3 x 30 mL). The combined organic phases were washed with H_2O (40 mL), NaHCO_3 solution (40 mL) and brine (40 mL), dried over Na_2SO_4 and concentrated. The crude product was purified by flash column chromatography (SiO_2 , Hexane/EtOAc, dichloromethane/EtOAc or dichloromethane/MeOH) on a Grace™ Reveleris™ system using a 12 g cartridge to afford the desired product. The final product was characterized by $^1\text{H-NMR}$, $^{13}\text{C-NMR}$, $^{19}\text{F-NMR}$ and HRMS (ESI-TOF).

Unsuccessful amines

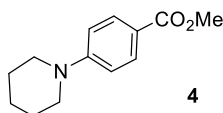




1-(4-methylbenzoate)pyrrolidine. From pyrrolidine (256.0 mg, 295.6 μ l, 3.6 mmol, 3.0 equiv.) and 4-bromomethylbenzoate (258.0 mg, 1.2 mmol, 1.0 equiv.). Reaction time: 8 h. Purification with flash chromatography (1. gradient 0-5% ethyl acetate in hexane; 2. Isocratic 5% ethyl acetate in hexane) afforded the title compound (231.1 mg, 1.13 mmol, 94%) as a white solid.

^1H NMR (400 MHz, Chloroform-*d*) δ 7.88 (d, J = 8.7 Hz, 2H), 6.46 (d, J = 8.7 Hz, 2H), 3.83 (s, 3H), 3.40 – 3.09 (m, 4H), 2.05 – 1.86 (m, 4H). ^{13}C NMR (101 MHz, Chloroform-*d*) δ = 167.58, 150.79, 131.32, 116.17, 110.62, 51.37, 47.47, 25.41. HRMS (ESI-TOF) m/z calcd. for $\text{C}_{12}\text{H}_{16}\text{NO}_2$ [(M+H) $^+$]: 206.1176; found: 206.1158.

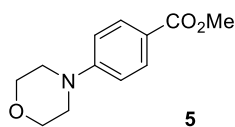
These data are in full agreement with those previously published in the literature.¹⁸



Methyl 4-(piperidin-1-yl)benzoate. From piperidine (306.5 mg, 356.4 μ l, 3.6 mmol, 3.0 equiv.) and 4-bromomethylbenzoate (258.0 mg, 1.2 mmol, 1.0 equiv.). Reaction time: 72 h. Double amount of $\text{NiBr}_2 \cdot 3\text{H}_2\text{O}$ (16.4 mg, 60 μ mol, 5.0 mol%) was used. Purification with flash chromatography (1. gradient 0-5% ethyl acetate in hexane; 2. Isocratic 5% ethyl acetate in hexane) afforded the title compound (225.8 mg, 1.03 mmol, 86%) as a white solid.

^1H NMR (600 MHz, Chloroform-*d*) δ 7.87 (d, J = 9.1 Hz, 2H), 6.82 (d, J = 9.0 Hz, 2H), 3.83 (s, 3H), 3.28 (m, 4H), 1.67 – 1.56 (m, 6H). ^{13}C NMR (151 MHz, Chloroform-*d*) δ 167.18, 154.46, 131.19, 118.61, 113.52, 51.49, 48.73, 25.35, 24.32. HRMS (ESI-TOF) m/z calcd. for $\text{C}_{13}\text{H}_{18}\text{NO}_2$ [(M+H) $^+$]: 220.1332 ; found: 220.1340.

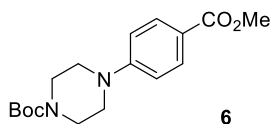
These data are in full agreement with those previously published in the literature.¹⁹



Methyl 4-morpholinobenzoate. From morpholine (313.6 mg, 313.6 μ l, 3.6 mmol, 3.0 equiv.) and 4-bromomethylbenzoate (258.0 mg, 1.2 mmol, 1.0 equiv.). Reaction time: 16 h. Purification with flash chromatography (gradient 0-2% ethyl acetate in DCM; 2. Isocratic 2% ethyl acetate in DCM) afforded the title compound (255.5 mg, 1.15 mmol, 96%) as a white solid.

^1H NMR (400 MHz, Chloroform-*d*) δ 7.93 (d, J = 9.0 Hz, 2H), 6.86 (d, J = 9.0 Hz, 2H), 3.92 – 3.72 (m, 7H), 3.26 (d, J = 5.1 Hz, 4H). ^{13}C NMR (101 MHz, Chloroform-*d*) δ 167.04, 154.15, 131.21, 120.34 113.50, 66.59, 51.71, 47.72. HRMS (ESI-TOF) m/z calcd. for $\text{C}_{12}\text{H}_{16}\text{NO}_3$ [(M+H) $^+$]: 222.1125; found: 222.1139.

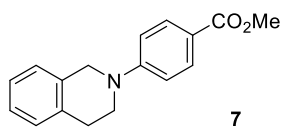
These data are in full agreement with those previously published in the literature.²⁰



***tert*-Butyl 4-(4-(methoxycarbonyl)phenyl)piperazine-1-carboxylate.** From *tert*-butyl piperazine-1-carboxylate (335.3 mg, 1.8 mmol, 3.0 equiv.) and 4-bromomethylbenzoate (129.0 mg, 0.6 mmol, 1.0 equiv.) using 5 mol% $\text{NiBr}_2 \cdot 3\text{H}_2\text{O}$ (8.2 mg, 60 μ mol) and pyrrolidine (4.3 mg, 4.9 μ l, 0.06 mmol, 10 mol%) as additive. Reaction time: 24 h. Purification with flash chromatography (1. gradient 0-3% ethyl acetate in DCM; 2. Isocratic 3% ethyl acetate in DCM) afforded the title compound (146.2 mg, 0.45 mmol, 76%) as a white solid. The pyrrolidine-coupled side-product was formed in 10% yield, as determined by analysis of the crude mixture by ^1H NMR spectroscopy.

^1H NMR (400 MHz, Chloroform-*d*) δ 7.92 (d, J = 8.9 Hz, 2H), 6.85 (d, J = 8.9 Hz, 2H), 3.86 (s, 3H), 3.57 (m, 4H), 3.29 (m, 4H), 1.48 (s, 9H). ^{13}C NMR (101 MHz, Chloroform-*d*) δ 167.48, 155.09, 154.41, 131.69, 120.63, 114.42, 80.56, 52.15, 47.98, 43.46, 28.92, 28.78. HRMS (ESI-TOF) m/z calcd. for $\text{C}_{17}\text{H}_{25}\text{N}_2\text{O}_4$ [(M+H) $^+$]: 321.1809; found: 321.1818

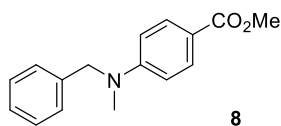
These data are in full agreement with those previously published in the literature.¹⁹



Methyl 4-(3,4-dihydroisoquinolin-2(1H)-yl)benzoate. From 1,2,3,4-tetrahydroisoquinoline (479.5 mg, 456.7 μ l, 3.6 mmol, 3.0 equiv.) and 4-bromomethylbenzoate (258.0 mg, 1.2 mmol, 1.0 equiv.). Reaction time: 16 h. Purification with flash chromatography (1. gradient 0-5% ethyl acetate in hexane; 2. Isocratic 5% ethyl acetate in hexane) afforded the title compound (281.6 mg, 1.06 mmol, 88%) as a white solid.

^1H NMR (600 MHz, Chloroform-*d*) δ 7.97 (d, J = 9.0 Hz, 2H), 7.23 – 7.13 (m, 4H), 6.86 (d, J = 9.0 Hz, 2H), 4.49 (s, 2H), 3.88 (s, 3H), 3.62 (t, J = 5.9 Hz, 2H), 2.97 (t, J = 5.8 Hz, 2H). ^{13}C NMR (151 MHz, Chloroform-*d*) δ 167.29, 153.00, 135.02, 133.80, 131.36, 128.22, 126.73, 126.51, 126.37, 118.29, 112.10, 51.56, 49.01, 44.78, 29.04. HRMS (ESI-TOF) m/z calcd. for $\text{C}_{17}\text{H}_{18}\text{NO}_2$ [(M+H) $^+$]: 268.1332; found: 268.1344

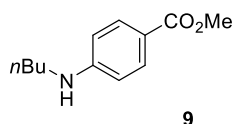
These data are in full agreement with those previously published in the literature.²¹



Methyl 4-(benzyl(methyl)amino)benzoate. From *N*-methylbenzylamine (438.6 mg, 467.1 μ l, 3.6 mmol, 3.0 equiv.) and 4-bromomethylbenzoate (258.0 mg, 1.2 mmol, 1.0 equiv.). Reaction time: 72 h. Purification with flash chromatography (1.gradient 0-4% ethyl acetate in hexane; 2. Isocratic 4% ethyl acetate in hexane) afforded the title compound (245.4 mg, 0.96 mmol, 80%) as a white solid.

^1H NMR (400 MHz, Chloroform-*d*) δ 7.92 (d, J = 9.1 Hz, 2H), 7.34 (t, J = 7.2 Hz, 2H), 7.28 (d, J = 7.2 Hz, 1H), 7.20 (d, J = 7.1 Hz, 2H), 6.71 (d, J = 9.1 Hz, 2H), 4.62 (s, 2H), 3.86 (s, 3H), 3.12 (s, 3H). ^{13}C NMR (101 MHz, Chloroform-*d*) δ 167.39, 152.75, 137.79, 131.43, 128.78, 127.20, 126.46, 117.37, 110.88, 55.92, 51.52, 38.69. HRMS (ESI-TOF) m/z calcd. for $\text{C}_{16}\text{H}_{18}\text{NO}_2$ [(M+H) $^+$]: 256.1332; found: 256.1344

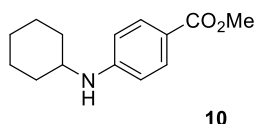
These data are in full agreement with those previously published in the literature.²²



Methyl 4-(butylamino)benzoate. From *n*-butylamine (263.3 mg, 355.8 μ l, 3.6 mmol, 3.0 equiv.) and 4-bromomethylbenzoate (258.0 mg, 1.2 mmol, 1.0 equiv.) using 5 mol% NiBr₂·3H₂O (16.4 mg, 60 μ mol,). Reaction time: 72 h. Purification with flash chromatography (1. gradient 0-8% ethyl acetate in hexane; 2. Isocratic 8% ethyl acetate in hexane) afforded the title compound (223.2 mg, 1.08 mmol, 90%) as a white solid.

¹H NMR (400 MHz, Chloroform-*d*) δ 7.85 (d, *J* = 8.6 Hz, 2H), 6.52 (d, *J* = 8.6 Hz, 2H), 4.21 (brs, 1H), 3.83 (s, 3H), 3.16 – 3.07 (m, 2H), 1.63 – 1.52 (m, 2H), 1.41 (h, *J* = 7.3, 6.9 Hz, 2H), 0.94 (td, *J* = 7.3, 1.0 Hz, 3H). ¹³C NMR (101 MHz, Chloroform-*d*) δ 167.40, 152.24, 131.52, 117.77, 111.26, 51.46, 43.01, 31.35, 20.21, 13.84. HRMS (ESI-TOF) *m/z* calcd. for C₁₂H₁₈NO₂ [(M+H)⁺]: 208.1332; found: 208.1342.

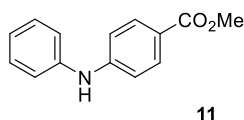
These data are in full agreement with those previously published in the literature.²³



Methyl 4-(cyclohexylamino)benzoate. From cyclohexylamine (357.0 mg, 415.4 μ l, 3.6 mmol, 3.0 equiv.) and 4-bromomethylbenzoate (258.0 mg, 1.2 mmol, 1.0 equiv.) using 5 mol% NiBr₂·3H₂O (16.4 mg, 60 μ mol,). Reaction time: 72 h. Purification with flash chromatography (1. gradient 0-5% ethyl acetate in hexane; 2. Isocratic 5% ethyl acetate in hexane) afforded the title compound (203.2 mg, 0.87 mmol, 73%) as a white solid.

¹H NMR (400 MHz, Chloroform-*d*) δ 7.82 (d, *J* = 8.8 Hz, 2H), 6.51 (d, *J* = 8.9 Hz, 2H), 4.01 (brs, 1H), 3.83 (s, 3H), 3.30 (m, 1H), 2.06 – 2.00 (m, 2H), 1.81 – 1.73 (m, 2H), 1.69 – 1.61 (m, 1H), 1.42 – 1.32 (m, 2H), 1.28 – 1.13 (m, 3H). ¹³C NMR (101 MHz, Chloroform-*d*) δ 167.36, 151.10, 131.60, 117.56, 111.59, 51.47, 51.24, 33.10, 25.73, 24.87. HRMS (ESI-TOF) *m/z* calcd. for C₁₄H₂₀NO₂ [(M+H)⁺]: 234.1489; found: 234.1500.

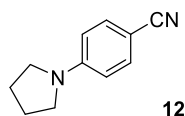
These data are in full agreement with those previously published in the literature.²⁴



Methyl 4-(butylamino)benzoate. From aniline (335.5 mg, 329.2 μ l, 3.6 mmol, 3.0 equiv.) and 4-bromomethylbenzoate (258.0 mg, 1.2 mmol, 1.0 equiv.) using 5 mol% NiBr₂·3H₂O (8.2 mg, 60 μ mol) and pyrrolidine (4.3 mg, 4.9 μ l, 0.06 mmol, 10 mol) as well as *N*-tert-butylisopropylamine (BIPA) (414.8 mg, 570.6 μ l, 3.6 mmol, 3.0 equiv.) as additives Reaction time: 72 h. Purification with flash chromatography (1. gradient 0-10% ethyl acetate in hexane; 2. Isocratic 10% ethyl acetate in hexane) afforded the title compound (246.7 mg, 1.09 mmol, 90%) as a white solid. The pyrrolidine-coupled side-product was formed in 2% yield, as determined by analysis of the crude mixture by ¹H NMR spectroscopy.

¹H NMR (400 MHz, Chloroform-*d*) δ 7.93 (d, *J* = 8.1 Hz, 2H), 7.34 (m, 2H), 7.18 (d, *J* = 7.7 Hz, 2H), 7.07 (t, *J* = 7.4 Hz, 1H), 6.99 (d, *J* = 8.6 Hz, 2H), 6.19 (brs, 1H), 3.88 (s, 3H). ¹³C NMR (101 MHz, Chloroform-*d*) δ 167.08, 148.16, 140.88, 131.50, 129.51, 123.07, 120.94, 120.42, 114.56, 51.77. HRMS (ESI-TOF) *m/z* calcd. for C₁₄H₁₄NO₂ [(M+H)⁺]: 228.1019; found: 228.1033.

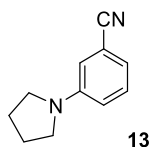
These data are in full agreement with those previously published in the literature.²⁵



1-(4-benzonitrile)pyrrolidine. From pyrrolidine (256.0 mg, 295.6 μ l, 3.6 mmol, 3.0 equiv.) and 4-bromobenzonitrile (218.4 mg, 1.2 mmol, 1.0 equiv.). Reaction time: 24 h. Purification with flash chromatography (1. gradient 0-5% ethyl acetate in hexane; 2. Isocratic 5% ethyl acetate in hexane) afforded the title compound (189.6mg, 1.11 mmol, 92%) as a white solid.

¹H NMR (400 MHz, Chloroform-*d*) δ 7.42 (d, *J* = 8.8 Hz, 2H), 6.48 (d, *J* = 8.9 Hz, 2H), 3.32 – 3.28 (m, 4H), 2.09 – 1.94 (m, 4H). ¹³C NMR (101 MHz, Chloroform-*d*) δ = 150.00, 133.43, 121.11, 111.47, 96.38, 47.51, 25.44. HRMS (ESI-TOF) *m/z* calcd. for C₁₁H₁₃N₂ [(M+H)⁺]: 173.1074; found: 173.1081.

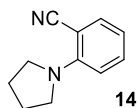
These data are in full agreement with those previously published in the literature.²⁶



1-(3-benzonitrile)pyrrolidine. From pyrrolidine (256.0 mg, 295.6 μ l, 3.6 mmol, 3.0 equiv.) and 3-bromobenzonitrile (218.4 mg, 1.2 mmol, 1.0 equiv.). Reaction time: 24 h. No internal standard (1,3,5-trimethoxybenzene was used) due to poor separation from the product during flash chromatography. Purification with flash chromatography (1. gradient 0-5% ethyl acetate in hexane; 2. Isocratic 5% ethyl acetate in hexane) afforded the title compound (180.4 mg, 1.05 mmol, 87%) as a white solid.

^1H NMR (400 MHz, Chloroform-*d*) δ 7.30 – 7.23 (m, 1H), 6.90 (m, 1H), 6.77 – 6.69 (m, 2H), 3.34 – 3.23 (m, 4H), 2.13 – 1.99 (m, 4H). ^{13}C NMR (101 MHz, Chloroform-*d*) δ 147.62, 129.73, 119.95, 118.50, 115.78, 114.24, 112.63, 47.55, 25.46. HRMS (ESI-TOF) m/z calcd. for $\text{C}_{11}\text{H}_{13}\text{N}_2$ [(M+H) $^+$]: 173.1074; found: 173.1080

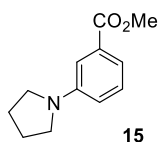
These data are in full agreement with those previously published in the literature.²⁷



1-(2-benzonitrile)pyrrolidine. From pyrrolidine (256.0 mg, 295.6 μ l, 3.6 mmol, 3.0 equiv.) and 2-bromobenzonitrile (218.4 mg, 1.2 mmol, 1.0 equiv.) using 5 mol% $\text{NiBr}_2 \cdot 3\text{H}_2\text{O}$ (8.2 mg, 60 μ mol). Reaction time: 72 h. No internal standard (1,3,5-trimethoxybenzene was used) due to poor separation from the product during flash chromatography. Purification with flash chromatography (eluent: 1. gradient 0-5% ethyl acetate in hexane; 2. Isocratic 5% ethyl acetate in hexane) afforded the title compound (190.5 mg, 1.11 mmol, 92%) as a colorless oil.

^1H NMR (400 MHz, Chloroform-*d*) δ 7.42 (m, 1H), 7.31 (m, 1H), 6.67 – 6.59 (m, 2H), 3.63 – 3.53 (m, 4H), 2.03 – 1.94 (m, 4H). ^{13}C NMR (101 MHz, Chloroform-*d*) δ 150.04, 135.72, 133.40, 121.51, 115.86, 114.24, 94.27, 49.81, 25.76. HRMS (ESI-TOF) m/z calcd. for $\text{C}_{11}\text{H}_{13}\text{N}_2$ [(M+H) $^+$]: 173.1074; found: 173.1081

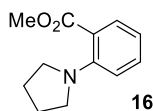
These data are in full agreement with those previously published in the literature.¹



1-(3-methylbenzoate)pyrrolidine. From pyrrolidine (256.0 mg, 295.6 μ l, 3.6 mmol, 3.0 equiv.) and 3-bromomethylbenzoate (258.0 mg, 1.2 mmol, 1.0 equiv.). Reaction time: 24 h. No internal standard (1,3,5-trimethoxybenzene was used) due to poor separation from the product during flash chromatography. Purification with flash chromatography (1. gradient 0-5% ethyl acetate in hexane; 2. Isocratic 5% ethyl acetate in hexane) afforded the title compound (218.4 mg, 1.06 mmol, 89%) as a colorless oil.

^1H NMR (400 MHz, Chloroform-*d*) δ 7.32 (d, J = 7.6 Hz, 1H), 7.25 (t, J = 7.8 Hz, 1H), 7.22 – 7.91 (s, 1H), 6.71 (m, 1H), 3.89 (s, 3H), 3.29 (t, J = 6.6 Hz, 4H), 2.00 (t, J = 6.6 Hz, 4H). ^{13}C NMR (101 MHz, Chloroform-*d*) δ 167.89, 147.78, 130.73, 129.02, 116.39, 115.93, 112.38, 52.00, 47.70, 25.48. HRMS (ESI-TOF) m/z calcd. for $\text{C}_{12}\text{H}_{16}\text{NO}_2$ [(M+H) $^+$]: 206.17556; found: 206.1185.

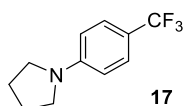
These data are in full agreement with those previously published in the literature.²⁰



1-(2-methylbenzoate)pyrrolidine. From pyrrolidine (256.0 mg, 295.6 μ l, 3.6 mmol, 3.0 equiv.) and 2-bromomethylbenzoate (258.0 mg, 1.2 mmol, 1.0 equiv.) using 5 mol% $\text{NiBr}_2 \cdot 3\text{H}_2\text{O}$ (8.2 mg, 60 μ mol). Reaction time: 72 h. No internal standard (1,3,5-trimethoxybenzene was used) due to poor separation from the product during flash chromatography. Purification with flash chromatography (1. gradient 0-5% ethyl acetate in hexane; 2. Isocratic 5% ethyl acetate in hexane) afforded the title compound (87.2 mg, 0.42 mmol, 35%) as a colourless oil.

^1H NMR (400 MHz, Chloroform-*d*) δ 7.57 (m, 1H), 7.31 (t, J = 8.7 Hz, 1H), 6.79 (m, 1H), 6.71 (t, J = 7.4 Hz, 1H), 3.88 (s, 3H), 3.28 – 3.19 (m, 4H), 1.99 – 1.88 (m, 4H). ^{13}C NMR (101 MHz, Chloroform-*d*) δ 169.57, 147.93, 131.79, 131.08, 117.09, 115.63, 113.95, 52.00, 50.87, 25.88. HRMS (ESI-TOF) m/z calcd. for $\text{C}_{12}\text{H}_{16}\text{NO}_2$ [(M+H) $^+$]: 206.17556; found: 206.1185.

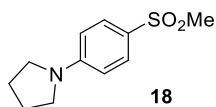
These data are in full agreement with those previously published in the literature.²⁸



1-(4-(trifluoromethyl)phenyl)pyrrolidine. From pyrrolidine (256.0 mg, 295.6 μ l, 3.6 mmol, 3.0 equiv.) and 4-bromobenzotrifluoride (270.0 mg, 168.0 μ l, 1.2 mmol, 1.0 equiv.). Reaction time: 8 h. Purification with flash chromatography (1. gradient 0-3% ethyl acetate in hexane; 2. Isocratic 3% ethyl acetate in hexane) afforded the title compound (238.2 mg, 1.11 mmol, 92%) as a white solid.

^1H NMR (400 MHz, Chloroform-*d*) δ 7.48 (d, J = 8.7 Hz, 2H), 6.58 (d, J = 8.7 Hz, 2H), 3.37 – 3.27 (m, 4H), 2.10 – 2.00 (m, 4H). ^{13}C NMR (101 MHz, Chloroform-*d*) δ 149.76, 126.38 (q, J = 3.7 Hz), 125.42 (q, J = 269.9 Hz), 116.56 (q, J = 32.5 Hz), 110.84, 47.53, 25.48. ^{19}F NMR (376 MHz, Chloroform-*d*) δ -60.58(s, 3F). HRMS (ESI-TOF) m/z calcd. for $\text{C}_{11}\text{H}_{13}\text{F}_3\text{N}$ [(M+H) $^+$]: 216.0922 ; found: 216.1008.

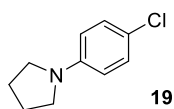
These data are in full agreement with those previously published in the literature.²⁹



1-(4-(methylsulfonyl)phenyl)pyrrolidine. From pyrrolidine (256.0 mg, 295.6 μ l, 3.6 mmol, 3.0 equiv.) and 4-bromophenyl methylsulfone (282.1 mg, 1.2 mmol, 1.0 equiv.). Reaction time: 24 h. Purification with flash chromatography (1. gradient 0-2% ethyl acetate in DCM; 2. Isocratic 2% ethyl acetate in DCM) afforded the title compound (251.0 mg, 1.11 mmol, 93%) as a white solid.

^1H NMR (600 MHz, Chloroform-*d*) δ 7.65 (d, J = 8.9 Hz, 2H), 6.51 (d, J = 9.0 Hz, 2H), 3.30 – 3.24 (m, 4H), 2.94 (s, 3H), 2.05 – 1.93 (m, 4H). ^{13}C NMR (151 MHz, Chloroform-*d*) δ 150.89, 129.02, 125.04, 110.98, 47.61, 45.13, 25.39. HRMS (ESI-TOF) m/z calcd. for $\text{C}_{11}\text{H}_{16}\text{NO}_2\text{S}$ [(M+H) $^+$]: 226.0897; found: 226.0907.

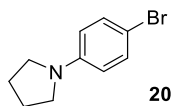
These data are in full agreement with those previously published in the literature.³⁰



1-(4-chlorophenyl)pyrrolidine. From pyrrolidine (256.0 mg, 295.6 μ l, 3.6 mmol, 3.0 equiv.) and 4-bromochlorobenzene (229.7 mg, 1.2 mmol, 1.0 equiv.). Reaction time: 24 h. Purification with flash chromatography (1. gradient 0-2% ethyl acetate in hexane; 2. Isocratic 2% ethyl acetate in hexane) afforded the title compound (196.8 mg, 1.08 mmol, 90%) as a white solid.

^1H NMR (600 MHz, Chloroform-*d*) δ 7.17 (d, J = 8.9 Hz, 2H), 6.48 (d, J = 8.9 Hz, 2H), 3.28 – 3.18 (m, 4H), 2.06 – 1.97 (m, 4H). ^{13}C NMR (151 MHz, Chloroform-*d*) δ 146.49, 128.81, 120.04, 112.61, 47.73, 25.48. HRMS (ESI-TOF) m/z calcd. for $\text{C}_{10}\text{H}_{13}\text{ClN}$ [(M+H) $^+$]: 182.0731; found: 182.0738.

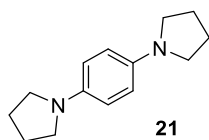
These data are in full agreement with those previously published in the literature.¹⁸



1-(4-bromophenyl)pyrrolidine. From pyrrolidine (256.0 mg, 295.6 μ l, 3.6 mmol, 3.0 equiv.) and 1,4-dibromobenzene (283.1 mg, 1.2 mmol, 1.0 equiv.). Reaction time: 24 h. Purification with flash chromatography (1. gradient 0-2% ethyl acetate in hexane; 2. Isocratic 2% ethyl acetate in hexane) afforded the title compound (218.4 mg, 0.97 mmol, 80%) as a white solid.

^1H NMR (400 MHz, Chloroform-*d*) δ 7.28 (d, J = 8.9 Hz, 2H), 6.42 (d, J = 8.9 Hz, 2H), 3.29 – 3.16 (m, 4H), 2.05 – 1.96 (m, 4H). ^{13}C NMR (101 MHz, Chloroform-*d*) δ 146.82, 131.68, 113.19, 107.08, 47.68, 25.50. HRMS (ESI-TOF) m/z calcd. for $\text{C}_{10}\text{H}_{13}\text{BrN}$ [(M+H) $^+$]: 226.0226; found: 226.0231.

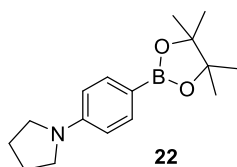
These data are in full agreement with those previously published in the literature.³¹



1-di(4-pyrrolidin-1-yl)benzene. From pyrrolidine (853.3 mg, 985.3 μ l, 12.0 mmol, 10 equiv.) and 1,4-dibromobenzene (283.1 mg, 1.2 mmol, 1.0 equiv.). Reaction time: 144 h. Purification with flash chromatography (1. gradient 0-5% ethyl acetate in hexane; 2. Isocratic 5% ethyl acetate in hexane) afforded the title compound (157.3 mg, 0.73 mmol, 61%) as a white solid. For analysis via NMR spectroscopy, the final product was treated with deuterated trifluoroacetic acid in D_2O .

1H NMR (400 MHz, deuterium oxide) δ 7.17 (s, 4H), 3.20 (m, 8H), 1.68 (m, 8H). ^{13}C NMR (101 MHz, deuterium oxide) δ 143.24, 126.02, 61.01, 25.62. HRMS (ESI-TOF) m/z calcd. for $C_{14}H_{21}N_2$ [(M+H) $^+$]: 217.1700; found: 217.1709

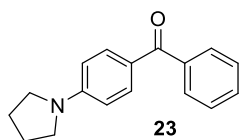
These data are in full agreement with those previously published in the literature.³²



1-(4-(4,4,5,5-tetramethyl-1,3,2-dioxaborolan-2-yl)phenyl)pyrrolidine. From pyrrolidine (256.0 mg, 295.6 μ l, 3.6 mmol, 3.0 equiv.) and 4-bromomethyl-phenylboronic acid pinacol ester (339.6 mg, 1.2 mmol, 1.0 equiv.). Reaction time: 48 h. No internal standard (1,3,5-trimethoxybenzene was used) due to poor separation from the product during flash chromatography. Purification with flash chromatography (1. gradient 0-10% ethyl acetate in hexane; 2. Isocratic 2% ethyl acetate in hexane) afforded the title compound (284.3 mg, 1.04 mmol, 87%) as a white solid.

1H NMR (400 MHz, Chloroform-*d*) δ 7.70 (d, J = 8.6 Hz, 2H), 6.55 (d, J = 8.6 Hz, 2H), 3.39 – 3.17 (m, 4H), 2.13 – 1.92 (m, 4H), 1.35 (s, 12H). ^{13}C NMR (101 MHz, Chloroform-*d*) δ 150.00, 136.24, 113.94, 110.93, 83.06, 47.40, 25.46, 24.88. HRMS (ESI-TOF) m/z calcd. for $C_{16}H_{25}BNO_2$ [(M+H) $^+$]: 274.1973; found: 274.1987.

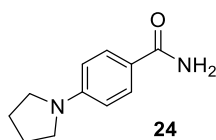
These data are in full agreement with those previously published in the literature.³³



phenyl(4-(pyrrolidin-1-yl)phenyl)methanone. From pyrrolidine (256.0 mg, 295.6 μ l, 3.6 mmol, 3.0 equiv.) and 4-bromobenzophenone (313.3 mg, 1.2 mmol, 1.0 equiv.). Reaction time: 48 h. Purification with flash chromatography (1. gradient 0-5% ethyl acetate in hexane; 2. Isocratic 5% ethyl acetate in hexane) afforded the title compound (281.9 mg, 1.12 mmol, 93%) as a white solid.

^1H NMR (600 MHz, Chloroform-*d*) δ 7.78 (d, J = 8.9 Hz, 2H), 7.72 – 7.66 (m, 2H), 7.49 (t, J = 7.4 Hz, 1H), 7.45 – 7.37 (m, 2H), 6.51 (d, J = 8.9 Hz, 2H), 3.38 – 3.27 (m, 4H), 2.02 – 1.95 (m, 4H). ^{13}C NMR (151 MHz, Chloroform-*d*) δ 195.01, 150.88, 139.51, 132.90, 130.95, 129.37, 127.97, 124.20, 110.63, 47.58, 25.42. HRMS (ESI-TOF) m/z calcd. for $\text{C}_{17}\text{H}_{17}\text{NO}$ [(M+H) $^+$]: 252.1383; found: 252.1394.

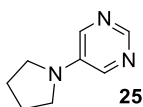
These data are in full agreement with those previously published in the literature.³⁴



1-(4-benzamide)pyrrolidine. From pyrrolidine (256.0 mg, 295.6 μ l, 3.6 mmol, 3.0 equiv.) and 4-bromobenzamide (240.0 mg, 1.2 mmol, 1.0 equiv.). Reaction time: 72 h. Purification with flash chromatography (1. gradient 0-5% methanol in DCM; 2. Isocratic 5% methanol in DCM) afforded the title compound (175.0 mg, 0.92 mmol, 77%) as a white solid.

^1H NMR (400 MHz, DMSO-*d*₆) δ 7.69 (d, J = 8.8 Hz, 2H), 7.58 – 7.52 (brs, 1H), 6.86 – 6.80 (brs, 1H), 6.47 (d, J = 8.8 Hz, 2H), 3.23 (s, 4H), 1.92 (s, 4H). ^{13}C NMR (101 MHz, DMSO-*d*₆) δ 168.05, 149.49, 129.08, 120.24, 110.47, 47.22, 25.01. HRMS (ESI-TOF) m/z calcd. for $\text{C}_{11}\text{H}_{15}\text{N}_2\text{O}$ [(M+H) $^+$]: 191.1179; found: 191.1188.

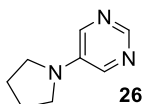
These data are in full agreement with those previously published in the literature.³⁵



5-(4-pyrrolidin-1-yl)pyrimidine. From pyrrolidine (256.0 mg, 295.6 μ l, 3.6 mmol, 3.0 equiv.) and 5-bromopyrimidine (190.8 mg, 1.2 mmol, 1.0 equiv.) using 5 mol% NiBr₂·3H₂O (16.4 mg, 60 μ mol). Reaction time: 72 h. Purification with flash chromatography (1. gradient 0-50% ethyl acetate in hexane with 1% Et₃N; 2. Isocratic 50% ethyl acetate in hexane with 1% Et₃N) afforded the title compound (141.3 mg, 0.95 mmol, 79%) as a colorless solid.

¹H NMR (400 MHz, Chloroform-*d*) δ 8.47 (s, 1H), 7.97 (s, 2H), 3.32 – 3.16 (m, 4H), 2.06 – 1.90 (m, 4H). ¹³C NMR (101 MHz, Chloroform-*d*) δ 146.60, 141.09, 139.35, 46.84, 25.27. HRMS (ESI-TOF) *m/z* calcd. for C₈H₁₂N₃ [(M+H)⁺]: 150.1026 ; found: 150.1033.

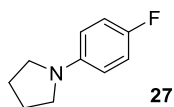
These data are in full agreement with those previously published in the literature.³⁶



3-(pyrrolidin-1-yl)pyridine. From pyrrolidine (256.0 mg, 295.6 μ l, 3.6 mmol, 3.0 equiv.) and 3-bromopyridine (189.6 mg, 115.6 μ l, 1.2 mmol, 1.0 equiv.) using 5 mol% NiBr₂·3H₂O (16.4 mg, 60 μ mol). Reaction time: 72 h. Purification with flash chromatography (1. gradient 0-40% ethyl acetate in hexane with 1% Et₃N; 2. Isocratic 40% ethyl acetate in hexane with 1% Et₃N) afforded the title compound (135.2 mg, 0.91 mmol, 76%) as a colorless oil.

¹H NMR (400 MHz, Chloroform-*d*) δ 7.96 – 7.81 (m, 2H), 7.03 (m, 1H), 6.72 (m, 1H), 3.21 (m, 4H), 2.00 – 1.87 (m, 4H). ¹³C NMR (101 MHz, Chloroform-*d*) δ 143.68, 136.74, 134.23, 123.49, 117.60, 47.19, 25.32. HRMS (ESI-TOF) *m/z* calcd. for C₉H₁₃N₂ [(M+H)⁺]: 149.1074 ; found: 149.1081

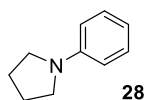
These data are in full agreement with those previously published in the literature.³⁷



1-(4-fluorophenyl)pyrrolidine. From pyrrolidine (256.0 mg, 295.6 μ l, 3.6 mmol, 3.0 equiv.) and 4-bromofluorobenzene (210.0 mg, 131.8 μ l, 1.2 mmol, 1.0 equiv.) using 5 mol% NiBr₂·3H₂O (16.4 mg, 60 μ mol). Reaction time: 72 h. Purification with flash chromatography (1. gradient 0-3% ethyl acetate in hexane; 2. Isocratic 3% ethyl acetate in hexane) afforded the title compound (128.8 mg, 0.78 mmol, 65 %) as a white solid.

¹H NMR (400 MHz, Chloroform-*d*) δ 6.99 – 6.89 (m, 2H), 6.52 – 6.44 (m, 2H), 3.30 – 3.19 (m, 4H), 2.05 – 1.96 (m, 4H). ¹³C NMR (101 MHz, Chloroform-*d*) δ 154.81 (d, *J* = 233.3 Hz), 144.78, 115.48 (d, *J* = 22.0 Hz), 112.05 (d, *J* = 7.1 Hz), 48.10, 25.50. ¹⁹F NMR (564 MHz, Chloroform-*d*) δ -131.00 (s, 1F). HRMS (ESI-TOF) *m/z* calcd. for C₁₀H₁₃FN [(M+H)⁺]: 166.1027 ; found: 166.1033.

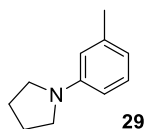
These data are in full agreement with those previously published in the literature.³¹



1-phenylpyrrolidine. From pyrrolidine (256.0 mg, 295.6 μ l, 3.6 mmol, 3.0 equiv.) and bromobenzene (188.4 mg, 125.6 μ l, 1.2 mmol, 1.0 equiv.) using 5 mol% NiBr₂·3H₂O (16.4 mg, 60 μ mol). Reaction time: 72 h. Purification with flash chromatography (1. gradient 0-2% ethyl acetate in hexane; 2. Isocratic 2% ethyl acetate in hexane) afforded the title compound (136.9 mg, 0.93 mmol, 77%) as a colourless oil.

¹H NMR (400 MHz, Chloroform-*d*) δ 7.35 (m, 2H), 6.78 (t, *J* = 7.3 Hz, 1H), 6.69 (d, *J* = 8.0 Hz, 2H), 3.43 – 3.30 (m, 4H), 2.13 – 2.05 (m, 4H). ¹³C NMR (101 MHz, Chloroform-*d*) δ 148.04, 129.25, 115.49, 111.77, 47.71, 25.61. HRMS (ESI-TOF) *m/z* calcd. for C₁₀H₁₄N [(M+H)⁺]: 148.1121; found: 148.1122.

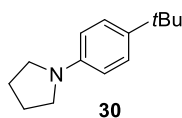
These data are in full agreement with those previously published in the literature.¹⁸



1-(m-tolyl)pyrrolidine. From pyrrolidine (256.0 mg, 295.6 μ l, 3.6 mmol, 3.0 equiv.) and 3-bromotoluene (188.4 mg, 145.6 μ l, 1.2 mmol, 1.0 equiv.) using 5 mol% NiBr₂·3H₂O (16.4 mg, 60 μ mol). Reaction time: 72 h. Purification with flash chromatography (1. gradient 0-2% ethyl acetate in hexane; 2. Isocratic 2% ethyl acetate in hexane) afforded the title compound (134.0 mg, 0.93 mmol, 69%) as a colorless oil.

¹H NMR (400 MHz, Chloroform-*d*) δ 7.24-7.16 (t, *J* = 8.8 Hz, 1H), 6.58 (d, *J* = 7.4 Hz, 1H), 6.51 – 6.44 (m, 2H), 3.35 (m, 4H), 2.41 (s, 3H), 2.11 – 2.00 (m, 4H). ¹³C NMR (101 MHz, Chloroform-*d*) δ 148.13, 138.86, 129.09, 116.44, 112.45, 108.99, 47.68, 25.56, 21.98. HRMS (ESI-TOF) *m/z* calcd. for C₁₁H₁₆N [(M+H)⁺]: 162.1278; found: 162.1282.

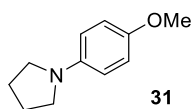
These data are in full agreement with those previously published in the literature.²⁹



1-(4-(tert-butyl)phenyl)pyrrolidine. From pyrrolidine (256.0 mg, 295.6 μ l, 3.6 mmol, 3.0 equiv.) and 4-bromotertbutylbenzene (255.7 mg, 208.8 μ l, 1.2 mmol, 1.0 equiv.) using 5 mol% NiBr₂·3H₂O (16.4 mg, 60 μ mol). Reaction time: 72 h. Purification with flash chromatography (1. gradient 0-3% ethyl acetate in hexane; 2. Isocratic 3% ethyl acetate in hexane) afforded the title compound (203.2 mg, 1.00 mmol, 83%) as a white solid.

¹H NMR (400 MHz, Chloroform-*d*) δ 7.37 (d, *J* = 7.0 Hz, 2H), 6.64 (d, *J* = 7.0 Hz, 2H), 3.42 – 3.30 (m, 4H), 2.11 – 2.02 (m, 4H), 1.40 (s, 9H). ¹³C NMR (101 MHz, Chloroform-*d*) δ 145.94, 138.03, 125.99, 111.43, 47.79, 33.82, 31.70, 25.56. HRMS (ESI-TOF) *m/z* calcd. for C₁₄H₂₂N [(M+H)⁺]: 204.1747; found: 204.1759.

These data are in full agreement with those previously published in the literature.¹⁸



1-(4-methoxyphenyl)pyrrolidine. From pyrrolidine (256.0 mg, 295.6 μ l, 3.6 mmol, 3.0 equiv.) and 4-bromoanisole (224.4 mg, 150.2 μ l, 1.2 mmol, 1.0 equiv.) using 5 mol% NiBr₂·3H₂O (16.4 mg, 60 μ mol). Reaction time: 72 h. No internal standard (1,3,5-trimethoxybenzene was used) due to poor separation from the product during flash chromatography. Purification with flash chromatography (1. gradient 0-5% ethyl acetate in hexane; 2. Isocratic 5% ethyl acetate in hexane) afforded the title compound (154.7 mg, 0.87 mmol, 73%) as a white solid.

¹H NMR (400 MHz, Chloroform-*d*) δ 6.88 (d, *J* = 8.1 Hz, 2H), 6.57 (d, *J* = 8.1 Hz, 2H), 3.78 (s, 3H), 3.32 – 3.18 (m, 4H), 2.07 – 1.94 (m, 4H). ¹³C NMR (101 MHz, Chloroform-*d*) δ 150.75, 143.25, 115.01, 112.59, 56.01, 48.24, 25.41. HRMS (ESI-TOF) *m/z* calcd. for C₁₁H₁₆NO [(M+H)⁺]: 178.1227; found: 178.1236

These data are in full agreement with those previously published in the literature.¹⁸

12. References

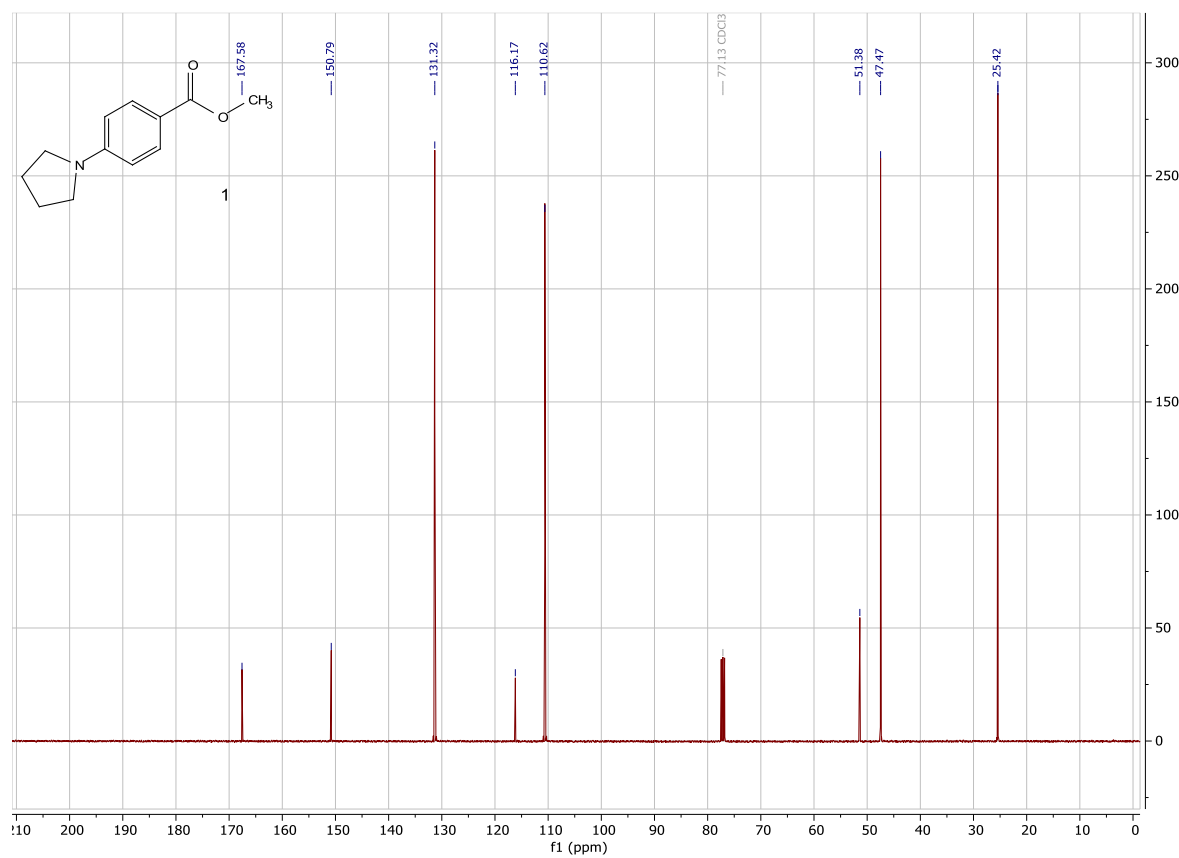
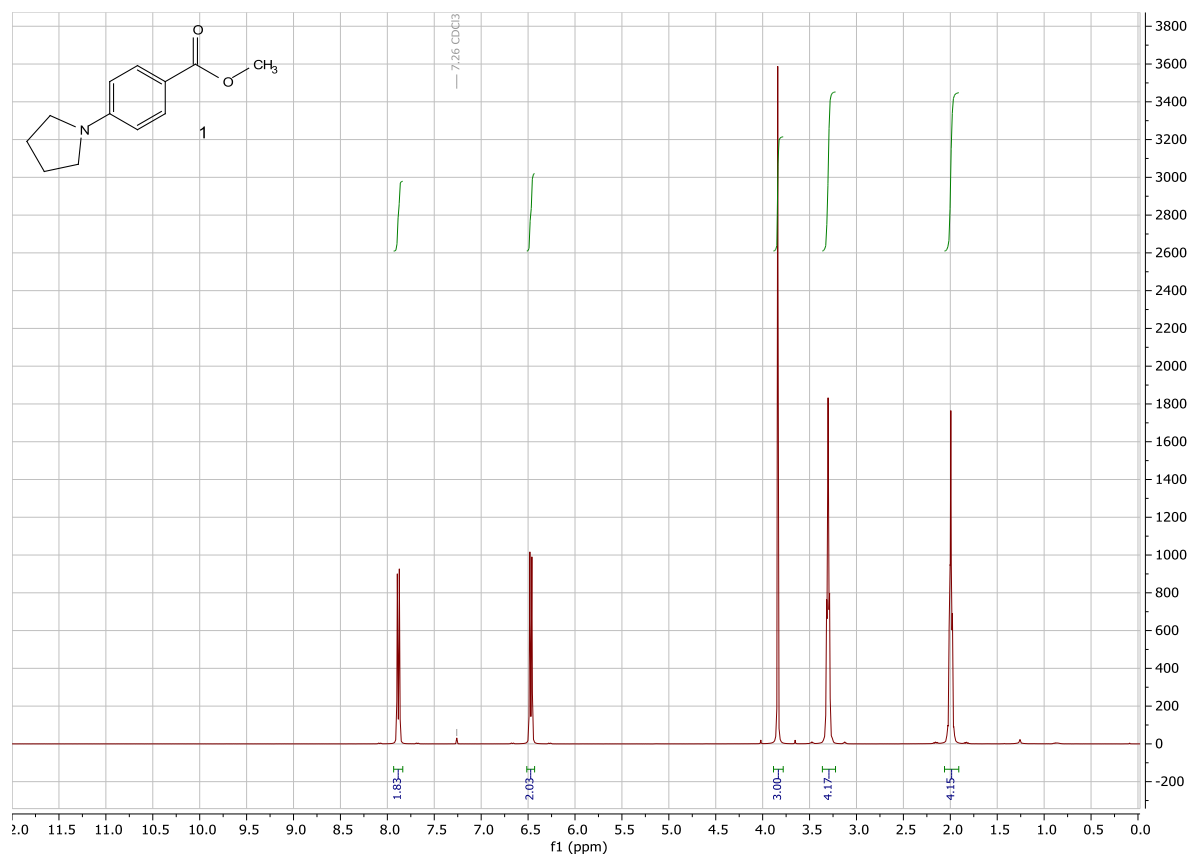
- 1 Yu, P. & Morandi, B. Nickel-Catalyzed Cyanation of Aryl Chlorides and Triflates Using Butyronitrile: Merging Retro-hydrocyanation with Cross-Coupling. *Angew. Chem. Int. Ed.* **56**, 15693-15697 (2017).
- 2 Wang, J., Zhao, J. & Gong, H. Nickel-catalyzed methylation of aryl halides/tosylates with methyl tosylate. *Chem. Commun.* **53**, 10180-10183 (2017).
- 3 Mori, A., Mizusaki, T., Ikawa, T., Maegawa, T., Monguchi, Y. & Sajiki, H. Mechanistic Study of a Pd/C-Catalyzed Reduction of Aryl Sulfonates Using the Mg–MeOH–NH₄OAc System. *Chem. Eur. J.* **13**, 1432-1441 (2007).
- 4 Brown, H. C., Kanth, J. V. B., Dalvi, P. V. & Zaidlewicz, M. Molecular Addition Compounds. 15. Synthesis, Hydroboration, and Reduction Studies of New, Highly Reactive tert-Butyldialkylamine–Borane Adducts. *J. Org. Chem.* **64**, 6263-6274 (1999).
- 5 Kawamata, Y., Vantourout, J. C., Hickey, D. P., Bai, P., Chen, L., Hou, Q., Qiao, W., Barman, K., Edwards, M. A., Garrido-Castro, A. F., deGruyter, J. N., Nakamura, H., Knouse, K., Qin, C., Clay, K. J., Bao, D., Li, C., Starr, J. T., Garcia-Irizarry, C., Sach, N., White, H. S., Neurock, M., Minter, S. D. & Baran, P. S. Electrochemically Driven, Ni-Catalyzed Aryl Amination: Scope, Mechanism, and Applications. *J. Am. Chem. Soc.* **141**, 6392-6402 (2019).
- 6 Lim, C.-H., Kudisch, M., Liu, B. & Miyake, G. M. C–N Cross-Coupling via Photoexcitation of Nickel–Amine Complexes. *J. Am. Chem. Soc.* **140**, 7667-7673 (2018).
- 7 Corcoran, E. B., Pirnot, M. T., Lin, S., Dreher, S. D., DiRocco, D. A., Davies, I. W., Buchwald, S. L. & MacMillan, D. W. C. Aryl amination using ligand-free Ni(II) salts and photoredox catalysis. *Science* **353**, 279-283 (2016).
- 8 Du, Y., Pearson, R. M., Lim, C.-H., Sartor, S. M., Ryan, M. D., Yang, H., Damrauer, N. H. & Miyake, G. M. Strongly Reducing, Visible-Light Organic Photoredox Catalysts as Sustainable Alternatives to Precious Metals. *Chem. Eur. J.* **23**, 10962-10968 (2017).
- 9 Liu, Y.-Y., Liang, D., Lu, L.-Q. & Xiao, W.-J. Practical heterogeneous photoredox/nickel dual catalysis for C–N and C–O coupling reactions. *Chem. Commun.* **55**, 4853-4856 (2019).

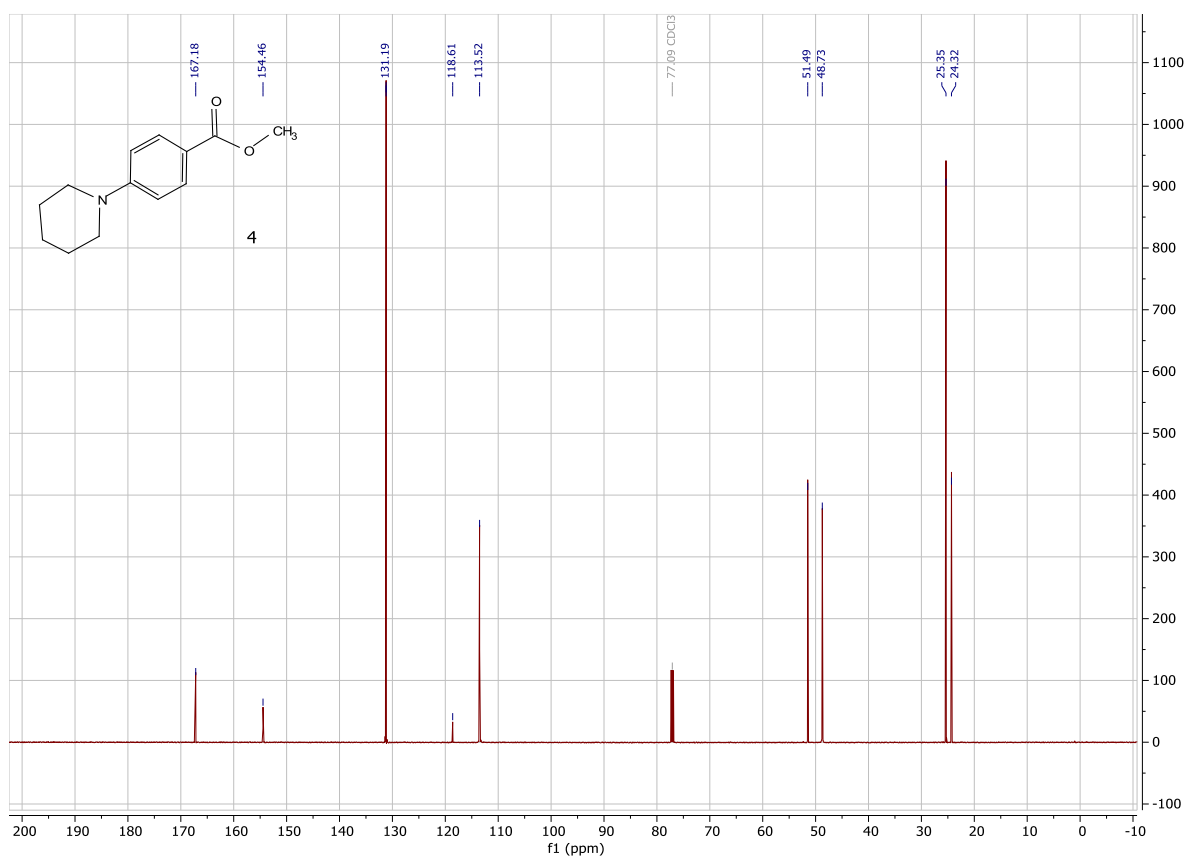
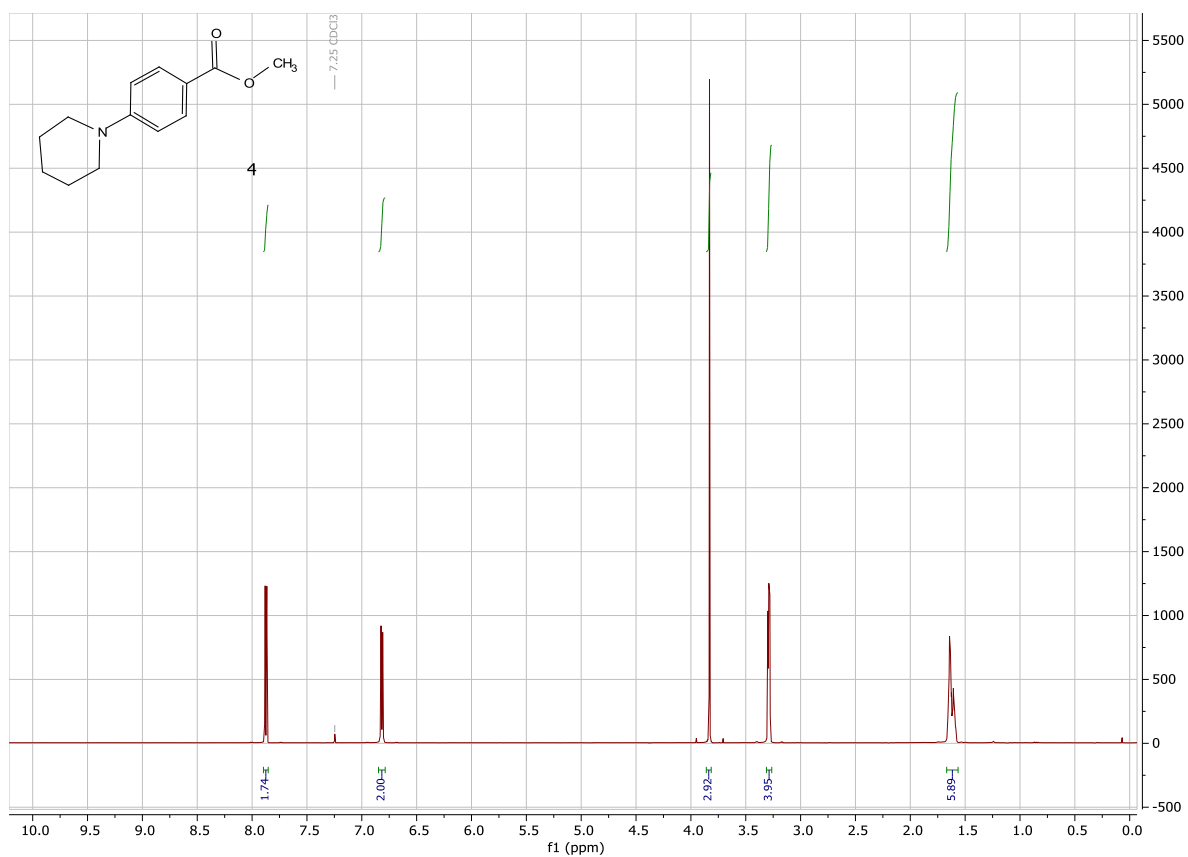
- 10 Ghosh, I., Khamrai, J., Savateev, A., Shlapakov, N., Antonietti, M. & König, B. Organic semiconductor photocatalyst can bifunctionalize arenes and heteroarenes. *Science* **365**, 360-366 (2019).
- 11 Zhang, G., Li, G., Lan, Z.-A., Lin, L., Savateev, A., Heil, T., Zafeiratos, S., Wang, X. & Antonietti, M. Optimizing Optical Absorption, Exciton Dissociation, and Charge Transfer of a Polymeric Carbon Nitride with Ultrahigh Solar Hydrogen Production Activity. *Angew. Chem. Int. Ed.* **56**, 13445-13449 (2017).
- 12 (<https://www.sigmaaldrich.com> (Germany; 2019 October 16).).
- 13 https://www.bauhaus.info/led-baender/tween-light-led-band/p/22517610?gclid=EAIaIQobChMIoLWto9zl3wIVTZSyCh3YDweqEAQYASABEgJmRfD_BwE&s_kwcid=AL!5677!3!190027496787!!!g!462716337331!&pla_prp aid=462716337331&ef_id=EAIaIQobChMIoLWto9zl3wIVTZSyCh3YDweqEAQYASABEgJmRfD_BwE:G:s&pla_adgrid=41635814775&pla_campid=225980581&pla_p rch=online&pla_prid=22517610&cid=PSEGoo225980581_41635814775&pla_adt=pl a (Germany; 2019 October 16).
- 14 Goettmann, F., Fischer, A., Antonietti, M. & Thomas, A. Chemical Synthesis of Mesoporous Carbon Nitrides Using Hard Templates and Their Use as a Metal-Free Catalyst for Friedel–Crafts Reaction of Benzene. *Angew. Chem. Int. Ed.* **45**, 4467-4471 (2006).
- 15 Shalom, M., Guttentag, M., Fettkenhauer, C., Inal, S., Neher, D., Llobet, A. & Antonietti, M. In Situ Formation of Heterojunctions in Modified Graphitic Carbon Nitride: Synthesis and Noble Metal Free Photocatalysis. *Chem. Mater.* **26**, 5812-5818 (2014).
- 16 Zhang, J., Sun, J., Maeda, K., Domen, K., Liu, P., Antonietti, M., Fu, X. & Wang, X. Sulfur-mediated synthesis of carbon nitride: Band-gap engineering and improved functions for photocatalysis. *Energy Environ. Sci.* **4**, 675-678 (2011).
- 17 Savateev, A., Pronkin, S., Epping, J. D., Willinger, M. G., Wolff, C., Neher, D., Antonietti, M. & Dontsova, D. Potassium Poly(heptazine imides) from Aminotetrazoles: Shifting Band Gaps of Carbon Nitride-like Materials for More Efficient Solar Hydrogen and Oxygen Evolution. *ChemCatChem* **9**, 167-174 (2017).
- 18 Hamid, M. H. S. A., Allen, C. L., Lamb, G. W., Maxwell, A. C., Maytum, H. C., Watson, A. J. A. & Williams, J. M. J. Ruthenium-Catalyzed N-Alkylation of Amines

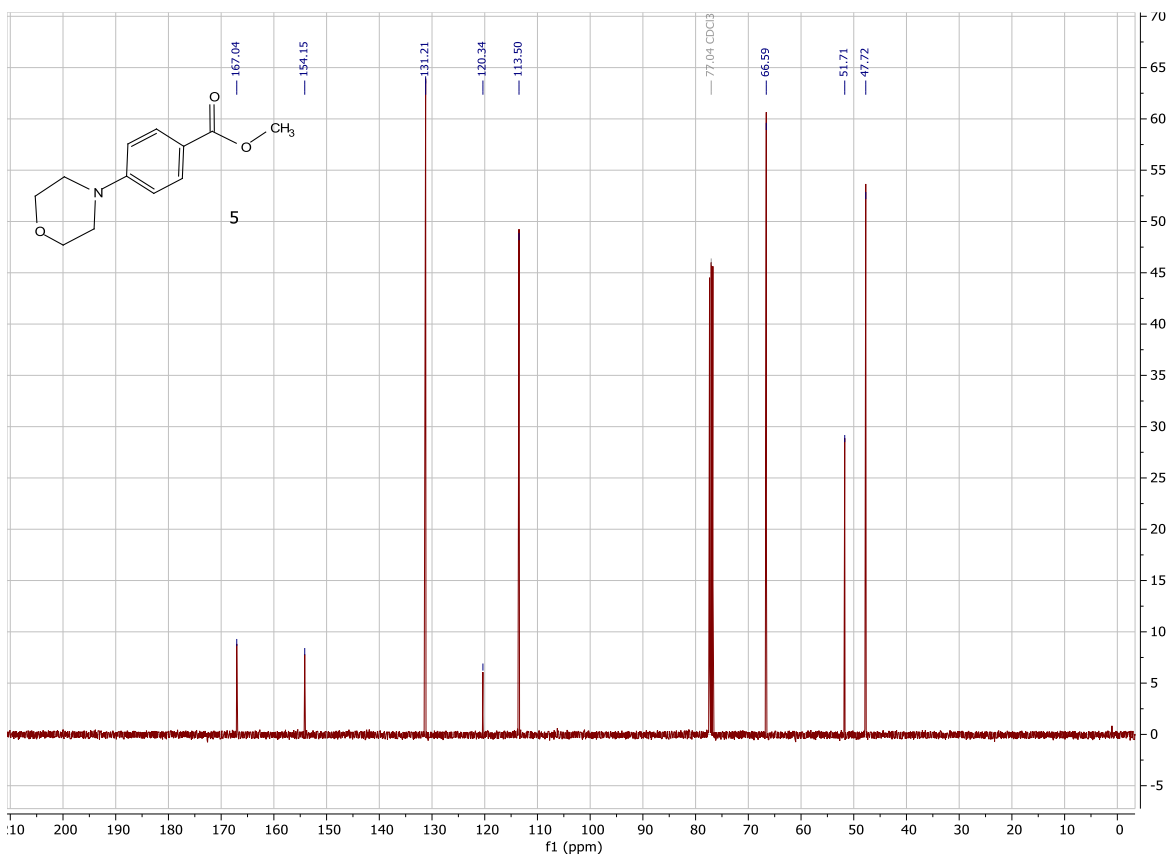
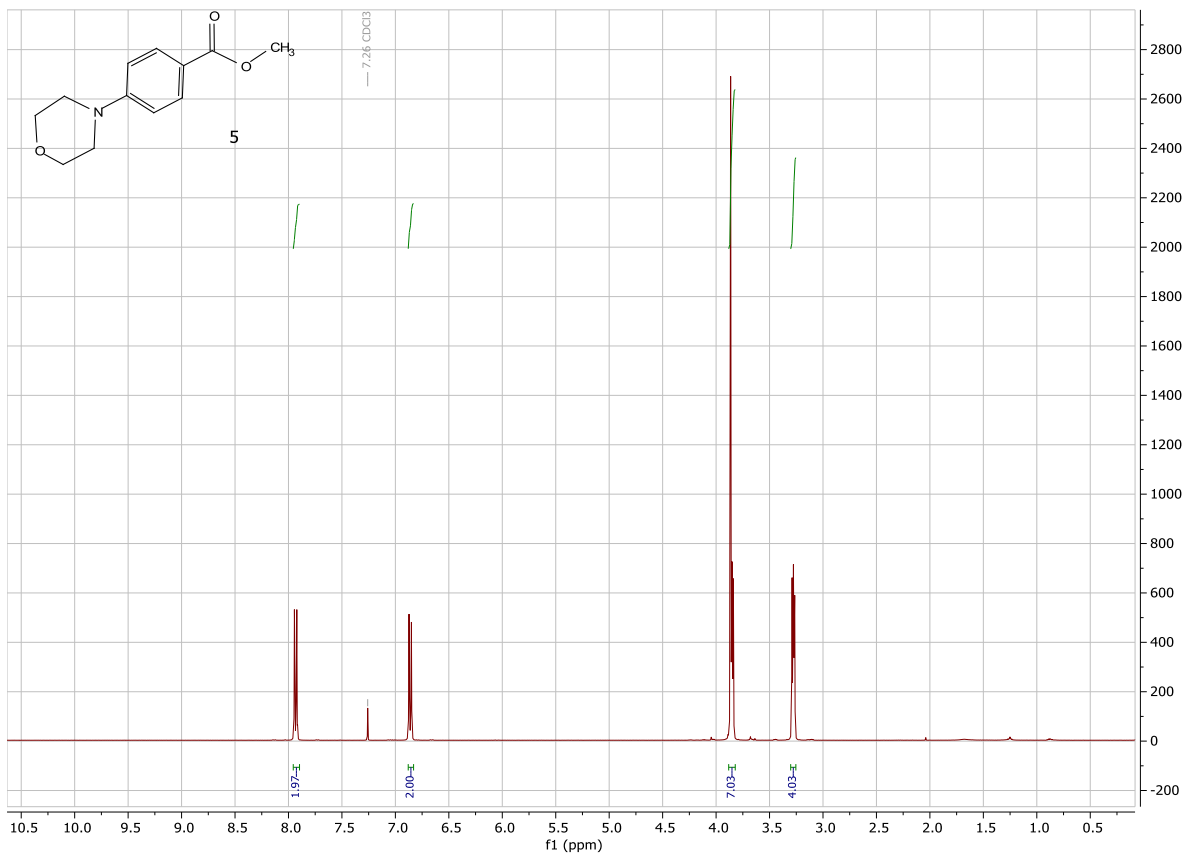
- and Sulfonamides Using Borrowing Hydrogen Methodology. *J. Am. Chem. Soc.* **131**, 1766-1774 (2009).
- 19 Sandtorv, A. H. & Stuart, D. R. Metal-free Synthesis of Aryl Amines: Beyond Nucleophilic Aromatic Substitution. *Angew. Chem. Int. Ed.* **55**, 15812-15815 (2016).
- 20 Urgaonkar, S., Xu, J.-H. & Verkade, J. G. Application of a New Bicyclic Triaminophosphine Ligand in Pd-Catalyzed Buchwald–Hartwig Amination Reactions of Aryl Chlorides, Bromides, and Iodides. *J. Org. Chem.* **68**, 8416-8423 (2003).
- 21 Lin, S.-X., Sun, G.-J. & Kang, Q. A visible-light-activated rhodium complex in enantioselective conjugate addition of α -amino radicals with Michael acceptors. *Chem. Commun.* **53**, 7665-7668 (2017).
- 22 Wolfe, J. P. & Buchwald, S. L. Scope and Limitations of the Pd/BINAP-Catalyzed Amination of Aryl Bromides. *J. Org. Chem.* **65**, 1144-1157 (2000).
- 23 Xie, X., Zhang, T. Y. & Zhang, Z. Synthesis of Bulky and Electron-Rich MOP-type Ligands and Their Applications in Palladium-Catalyzed C–N Bond Formation. *J. Org. Chem.* **71**, 6522-6529 (2006).
- 24 Liu, K.-J., Zeng, X.-L., Zhang, Y., Wang, Y., Xiao, X.-S., Yue, H., Wang, M., Tang, Z. & He, W.-M. Palladium-Catalyzed Reductive Coupling of Nitroarenes with Phenols-leading to N-Cyclohexylanilines. *Synthesis* **50**, 4637-4644 (2018).
- 25 Suárez-Pantiga, S., Hernández-Ruiz, R., Virumbrales, C., Pedrosa, M. R. & Sanz, R. Reductive Molybdenum-Catalyzed Direct Amination of Boronic Acids with Nitro Compounds. *Angew. Chem. Int. Ed.* **58**, 2129-2133 (2019).
- 26 Desmarets, C., Schneider, R. & Fort, Y. Nickel(0)/Dihydroimidazol-2-ylidene Complex Catalyzed Coupling of Aryl Chlorides and Amines. *J. Org. Chem.* **67**, 3029-3036 (2002).
- 27 Wolfe, J. P., Tomori, H., Sadighi, J. P., Yin, J. & Buchwald, S. L. Simple, Efficient Catalyst System for the Palladium-Catalyzed Amination of Aryl Chlorides, Bromides, and Triflates. *J. Org. Chem.* **65**, 1158-1174 (2000).
- 28 Yoshida, H., Morishita, T. & Ohshita, J. Direct Access to Anthranilic Acid Derivatives via CO₂ Incorporation Reaction Using Arynes. *Org. Lett.* **10**, 3845-3847 (2008).
- 29 Brenner, E., Schneider, R. & Fort, Y. Nickel-catalysed couplings of aryl chlorides with secondary amines and piperazines. *Tetrahedron* **55**, 12829-12842 (1999).

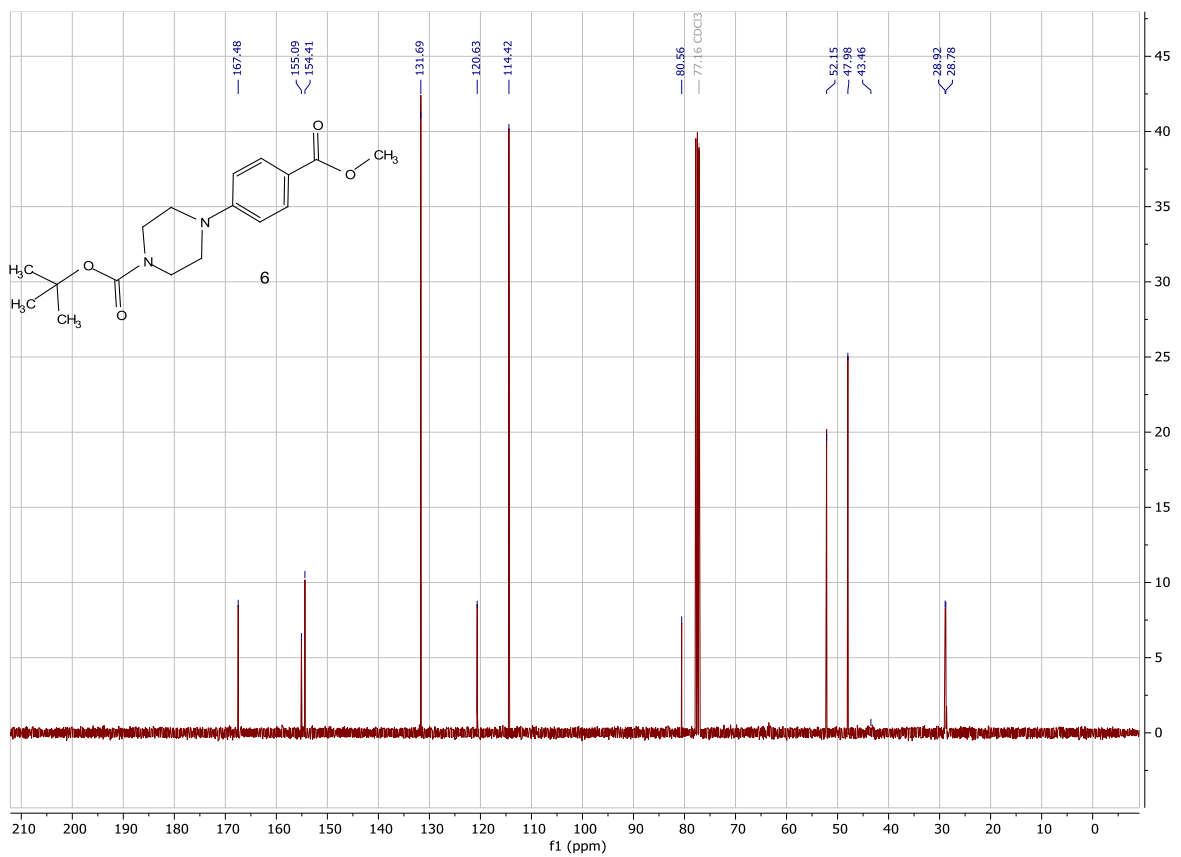
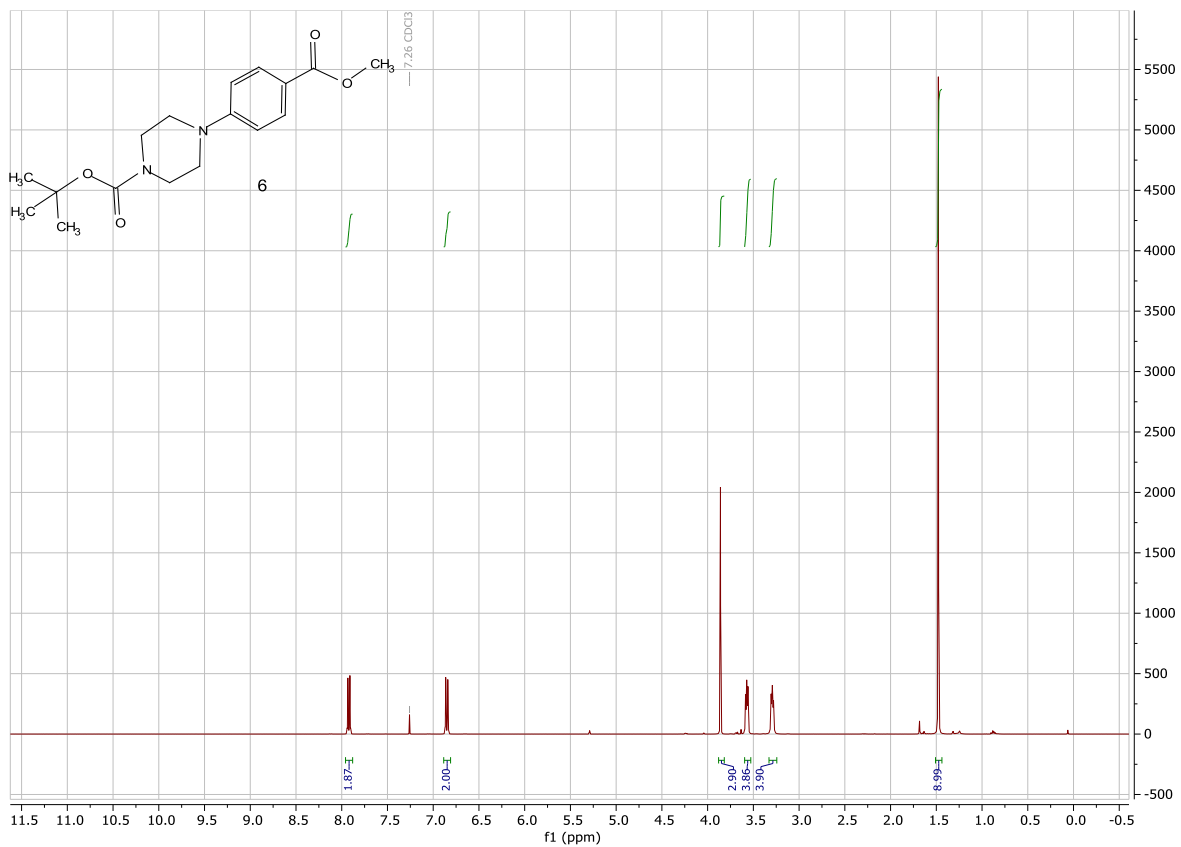
- 30 Johnson, T. C., Elbert, Bryony L., Farley, A. J. M., Gorman, T. W., Genicot, C., Lallemand, B., Pasau, P., Flasz, J., Castro, J. L., MacCoss, M., Dixon, D. J., Paton, R. S., Schofield, C. J., Smith, M. D. & Willis, M. C. Direct sulfonylation of anilines mediated by visible light. *Chem. Sci.* **9**, 629-633 (2018).
- 31 Hollmann, D., Bähn, S., Tillack, A., Parton, R., Altink, R. & Beller, M. A novel salt-free ruthenium-catalyzed alkylation of aryl amines. *Tetrahedron Lett.* **49**, 5742-5745 (2008).
- 32 Ju, Y. & Varma, R. S. An Efficient and Simple Aqueous N-Heterocyclization of Aniline Derivatives: Microwave-Assisted Synthesis of N-Aryl Azacycloalkanes. *Org. Lett.* **7**, 2409-2411 (2005).
- 33 Lim, S., Song, D., Jeon, S., Kim, Y., Kim, H., Lee, S., Cho, H., Lee, B. C., Kim, S. E., Kim, K. & Lee, E. Cobalt-Catalyzed C–F Bond Borylation of Aryl Fluorides. *Org. Lett.* **20**, 7249-7252 (2018).
- 34 Wolfe, J. P. & Buchwald, S. L. Palladium-Catalyzed Amination of Aryl Triflates. *J. Org. Chem.* **62**, 1264-1267 (1997).
- 35 Lakshminarayana, N., Prasad, Y. R., Gharat, L., Thomas, A., Narayanan, S., Raghuram, A., Srinivasan, C. V. & Gopalan, B. Synthesis and evaluation of some novel dibenzo[b,d]furan carboxylic acids as potential anti-diabetic agents. *Eur. J. Med. Chem.* **45**, 3709-3718 (2010).
- 36 Charles, M. D., Schultz, P. & Buchwald, S. L. Efficient Pd-Catalyzed Amination of Heteroaryl Halides. *Org. Lett.* **7**, 3965-3968 (2005).
- 37 Maiti, D., Fors, B. P., Henderson, J. L., Nakamura, Y. & Buchwald, S. L. Palladium-catalyzed coupling of functionalized primary and secondary amines with aryl and heteroaryl halides: two ligands suffice in most cases. *Chem. Sci.* **2**, 57-68 (2011).

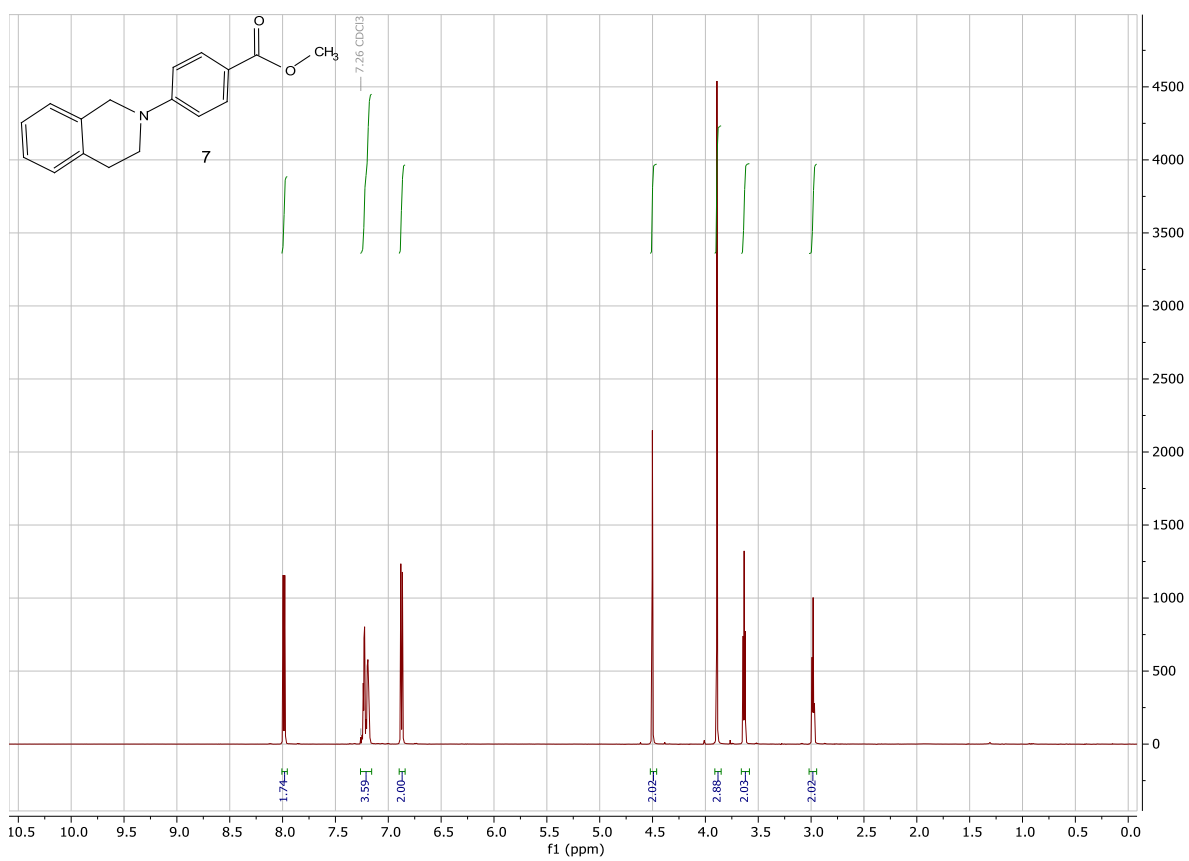
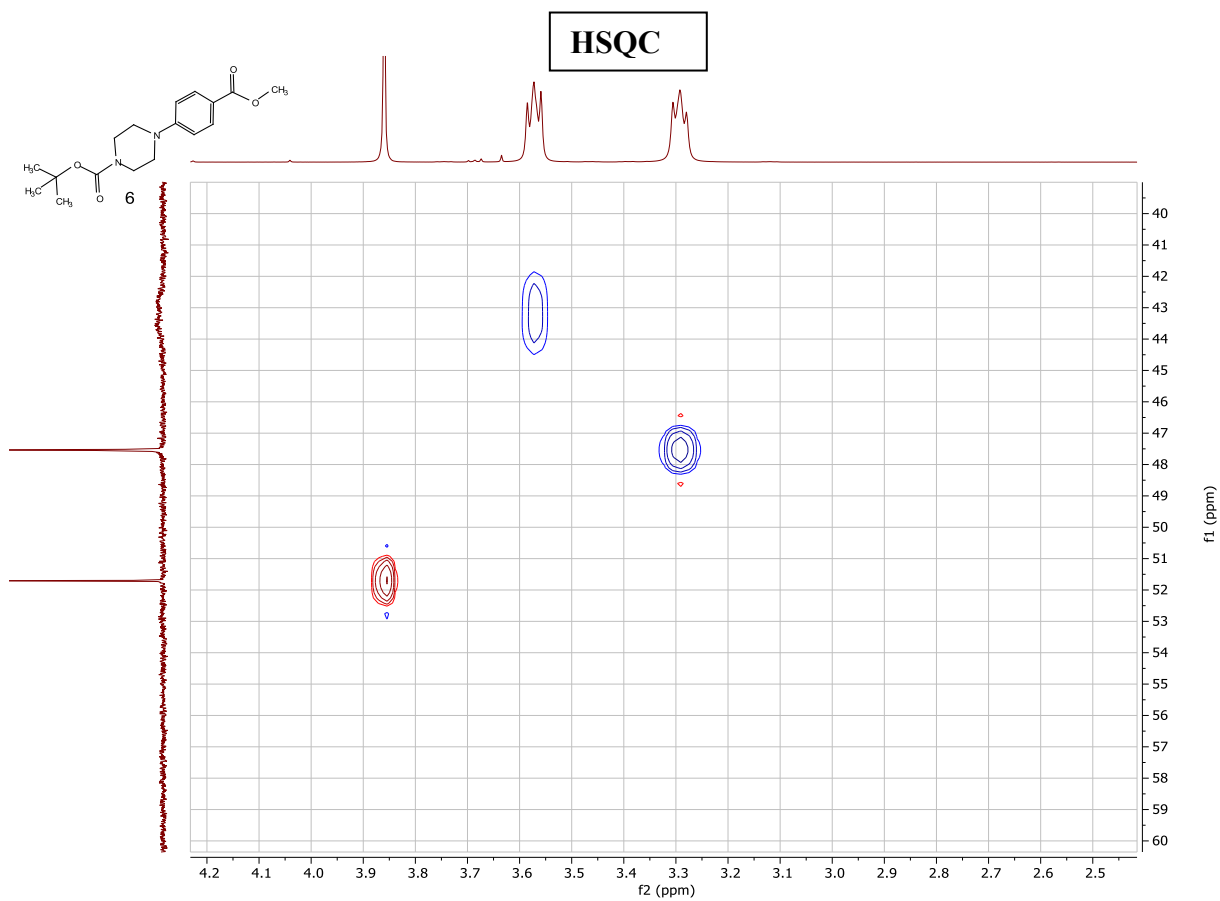
12. Copies of NMR spectra

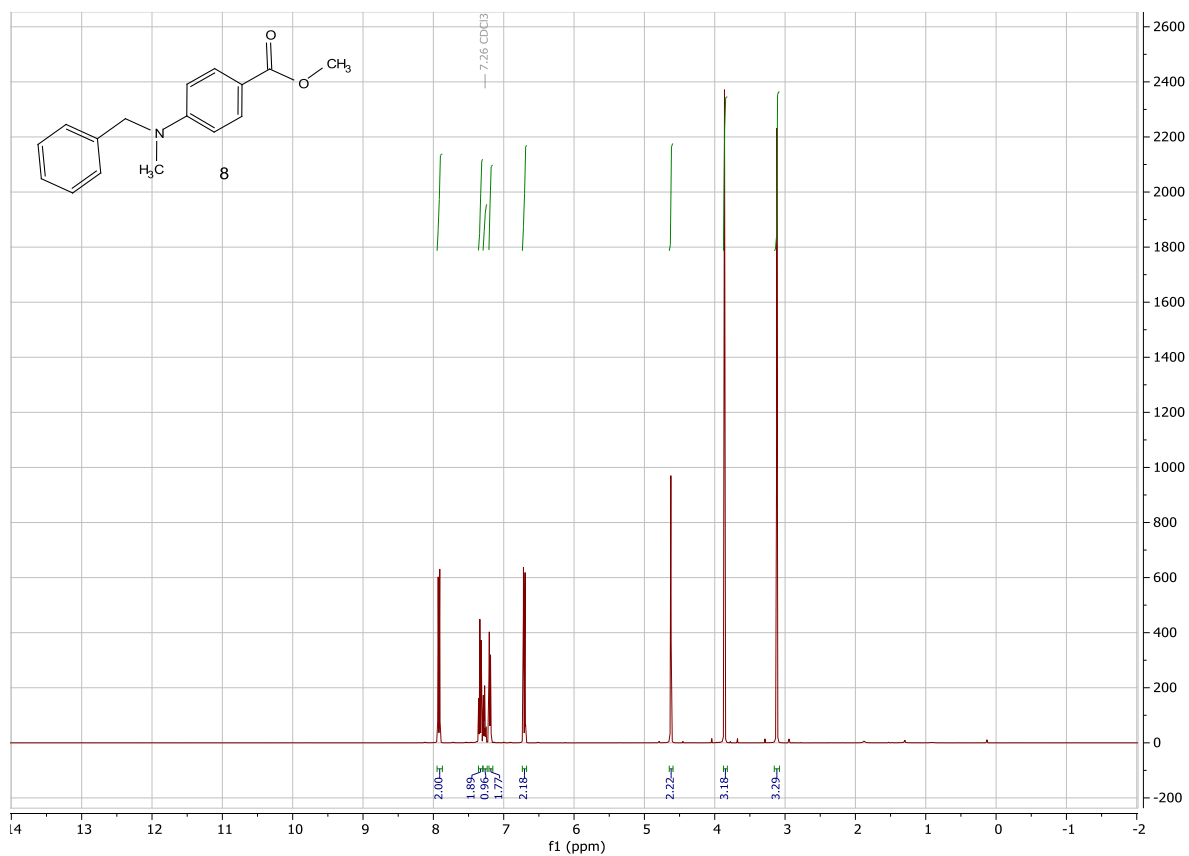
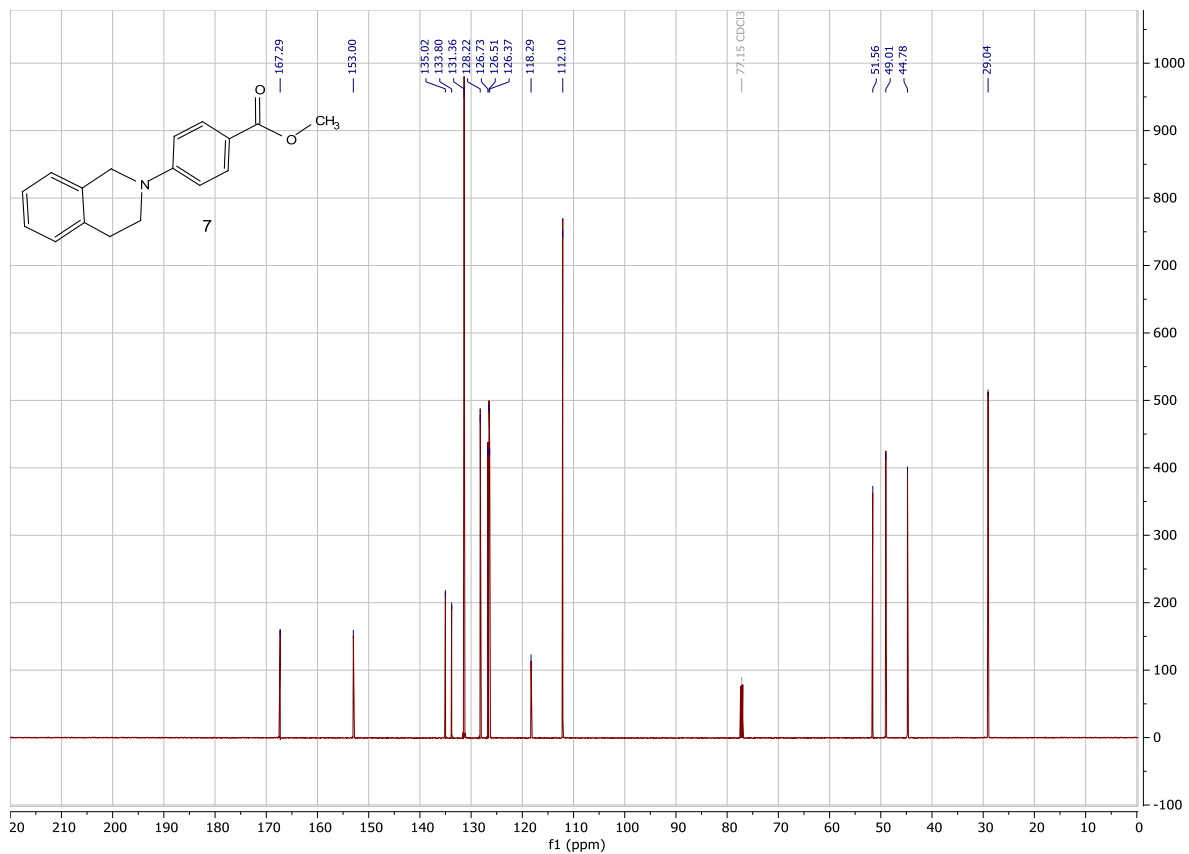


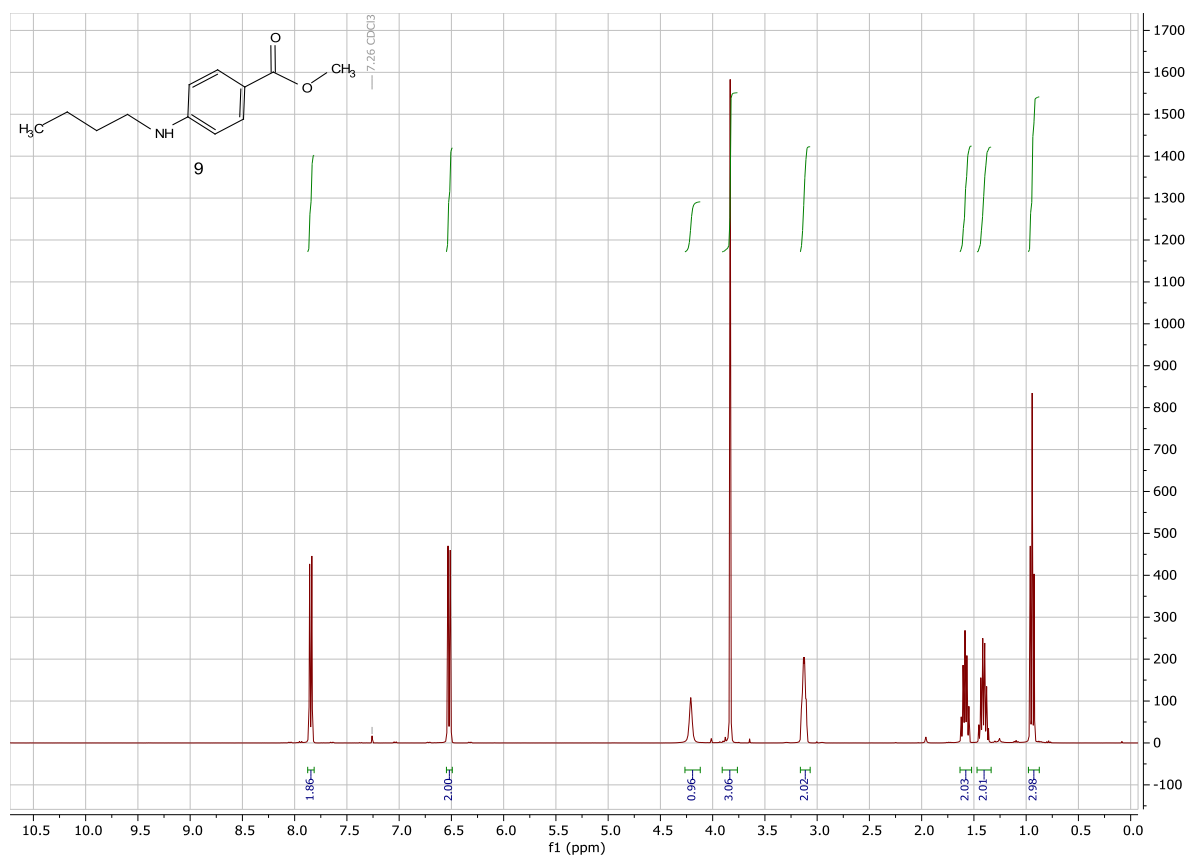
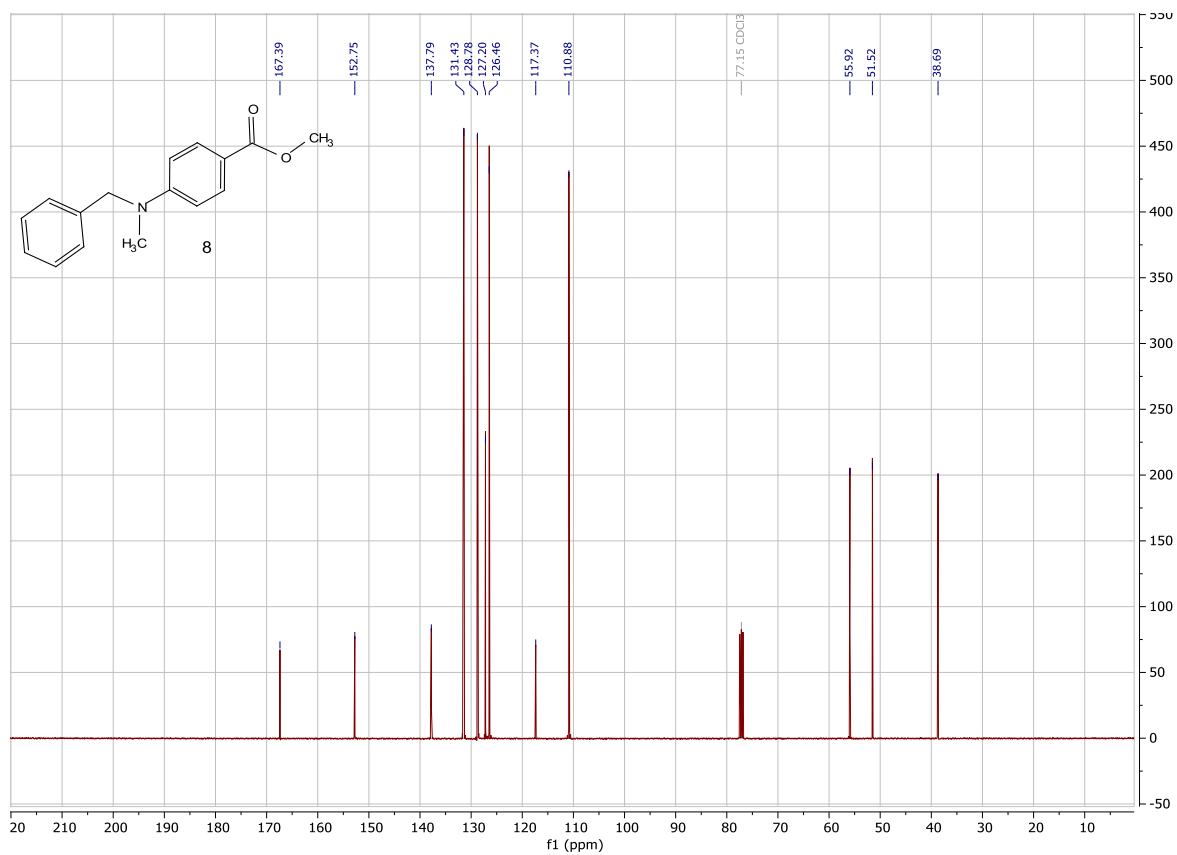


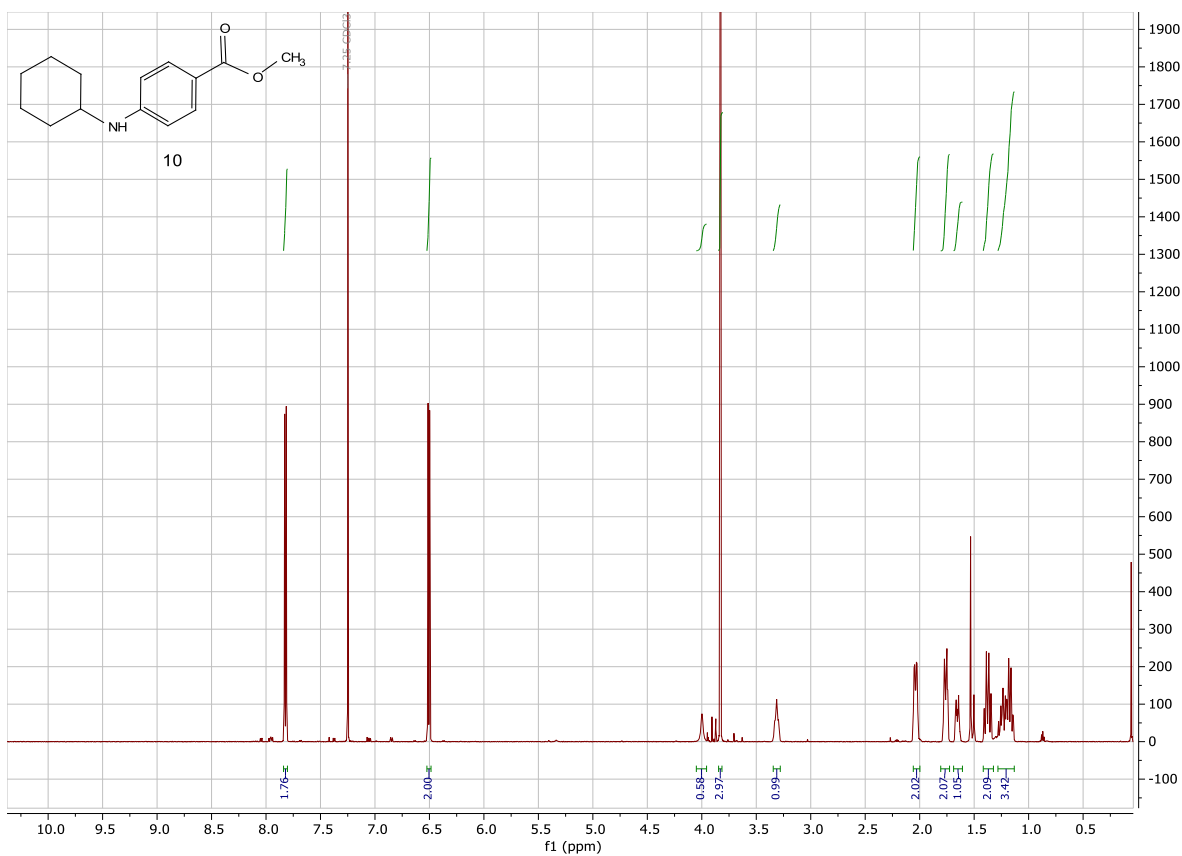
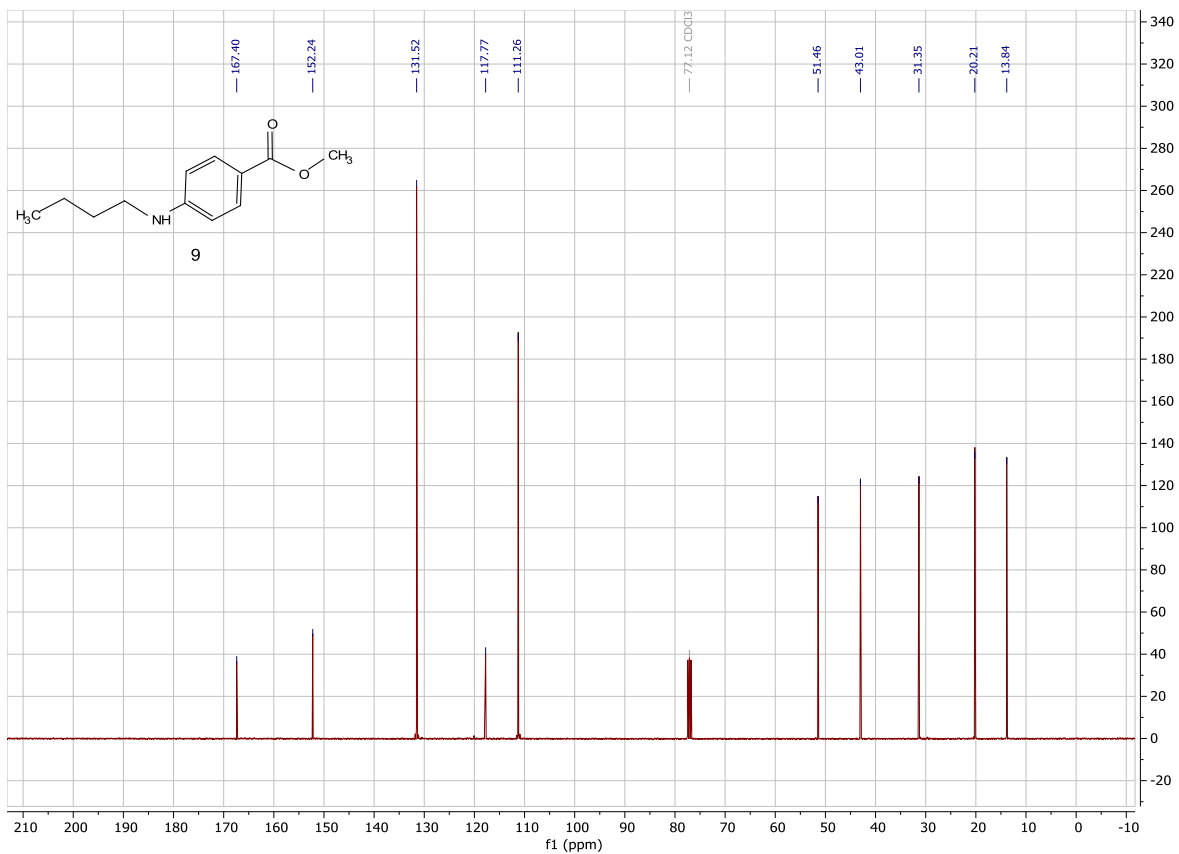


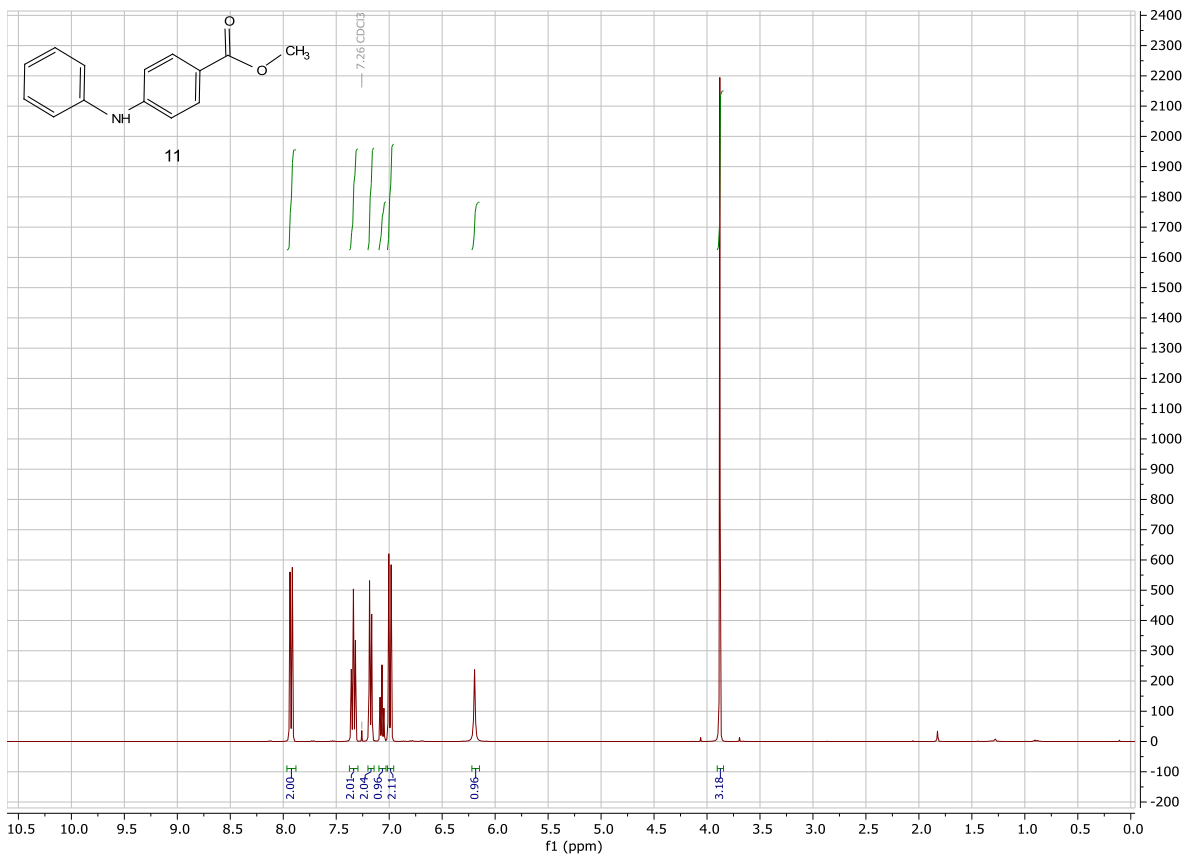
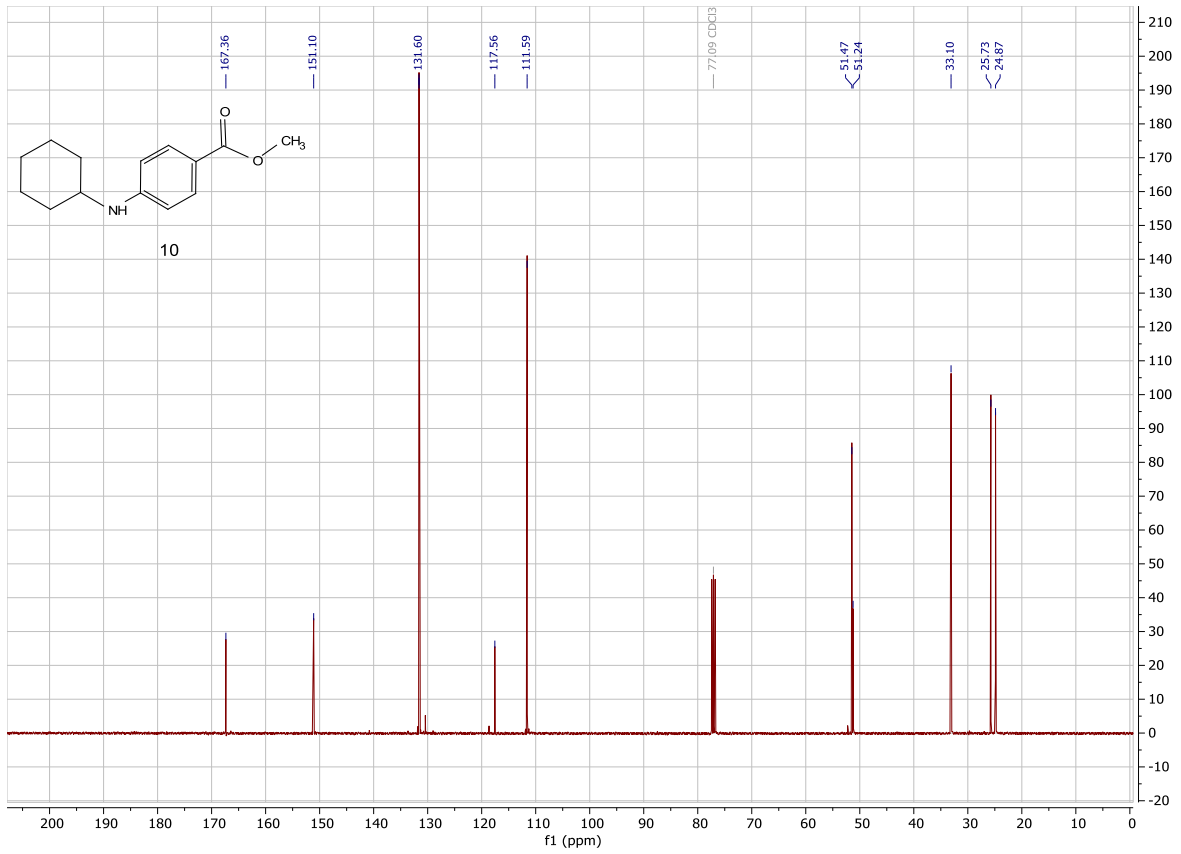


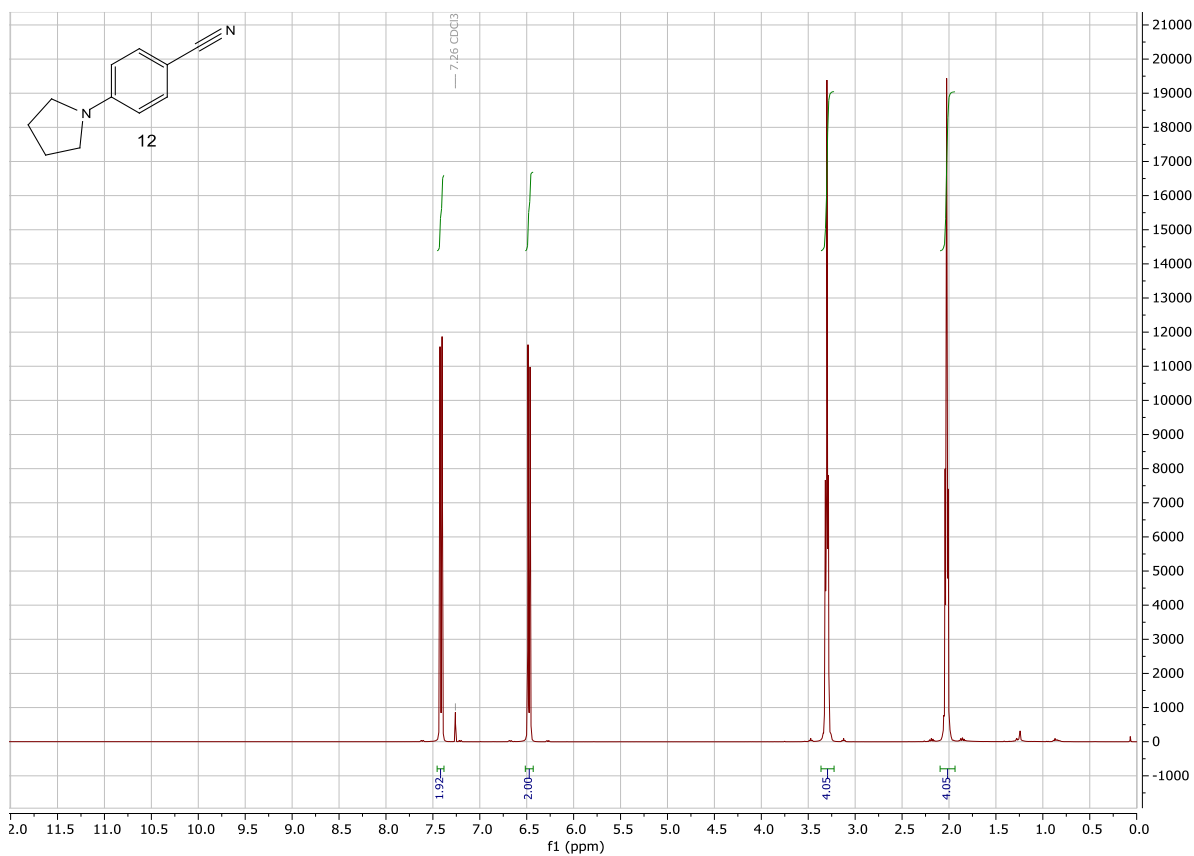
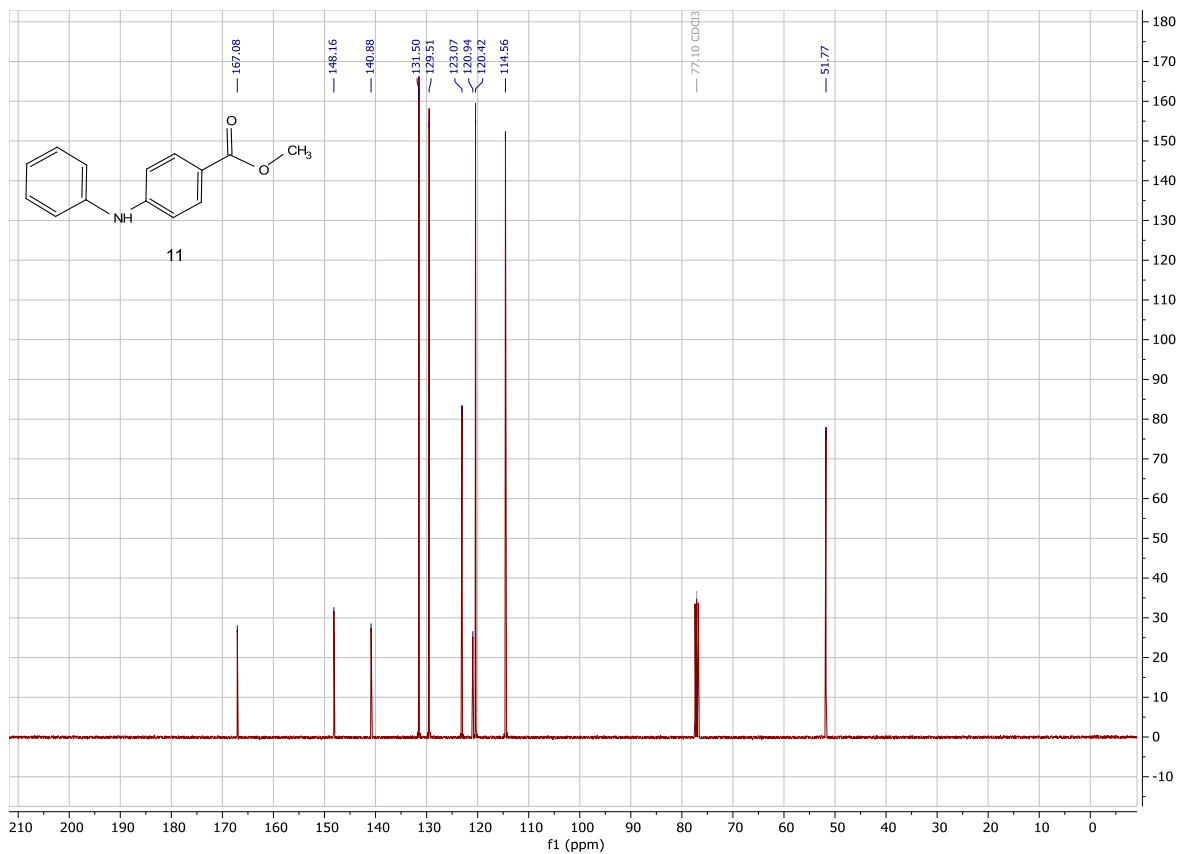


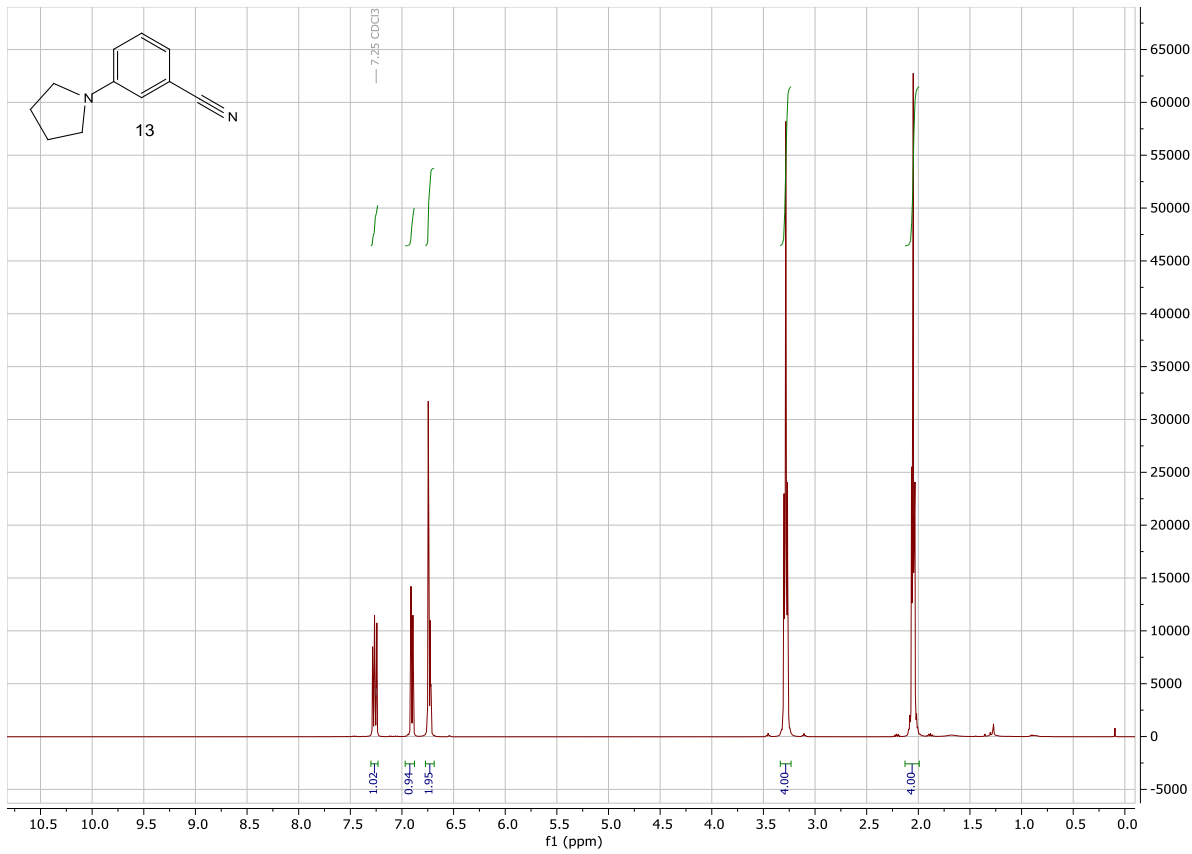
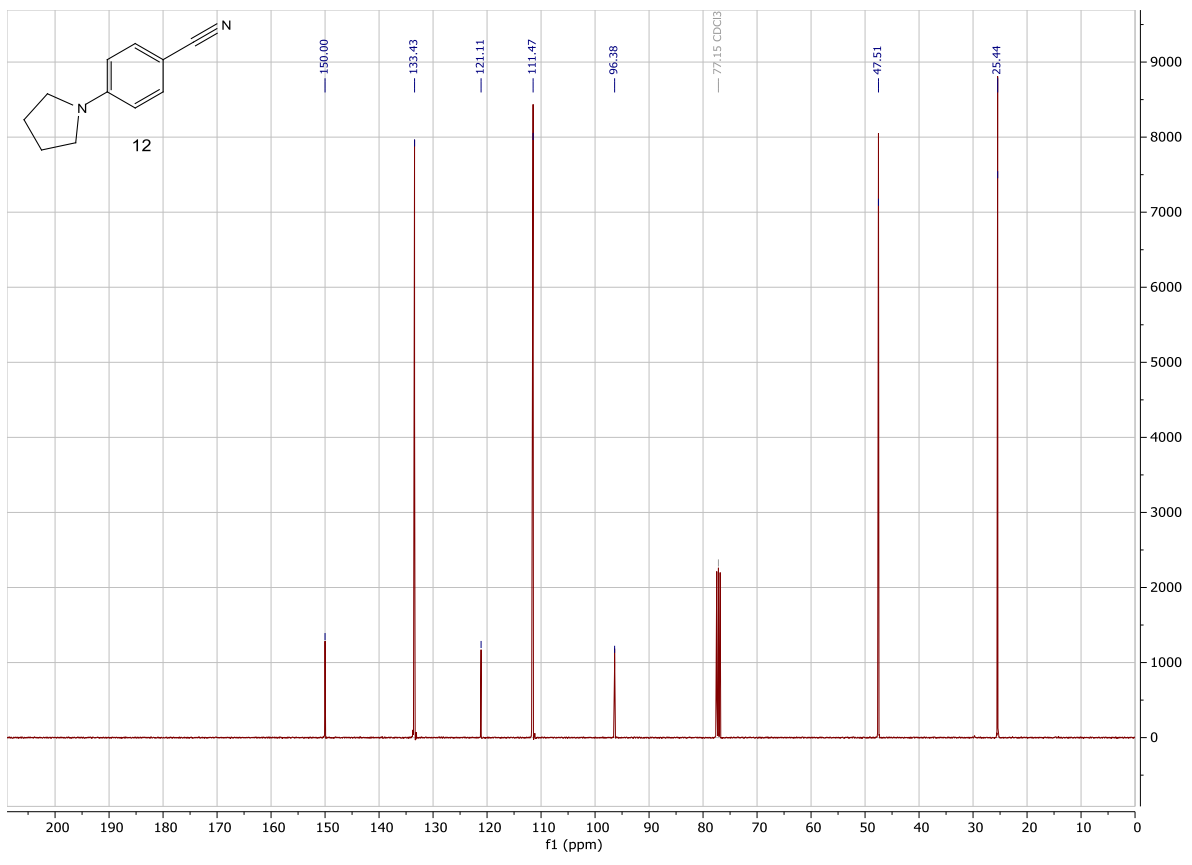


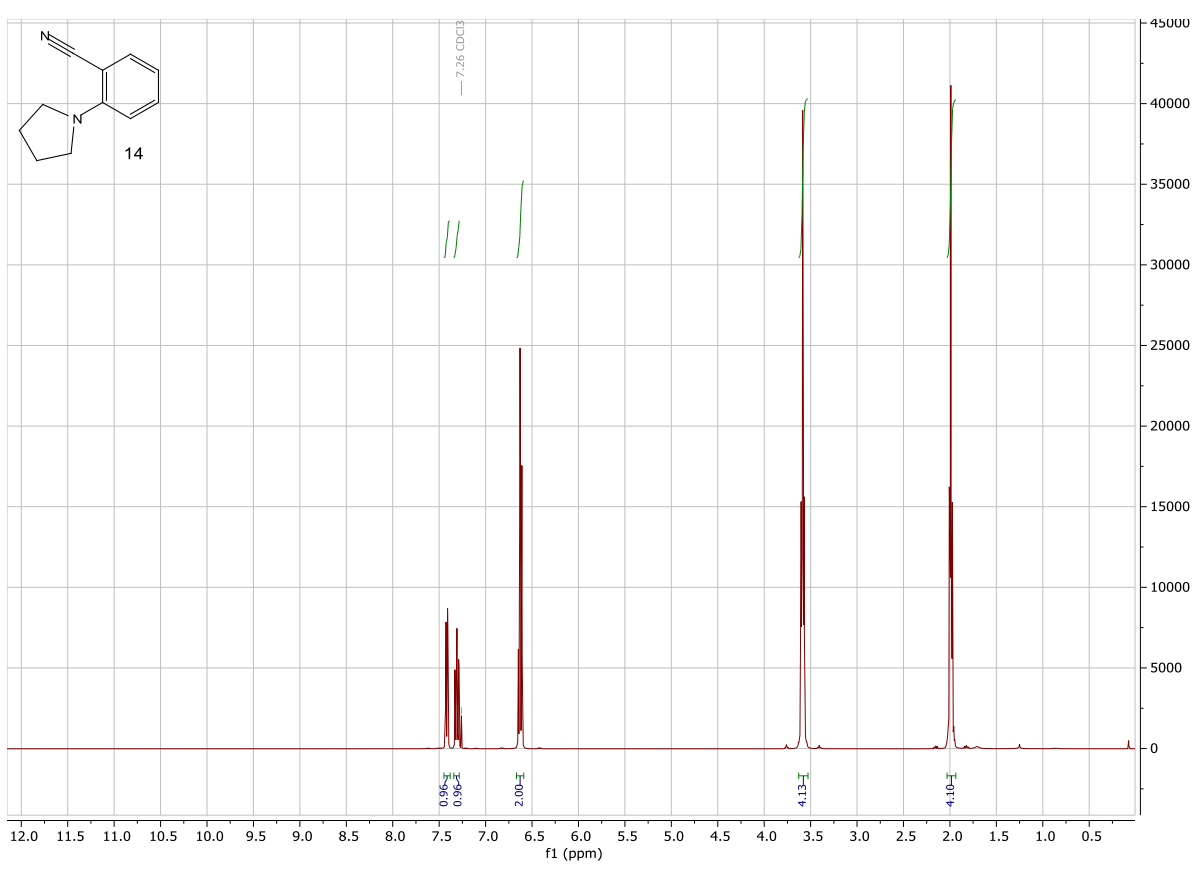
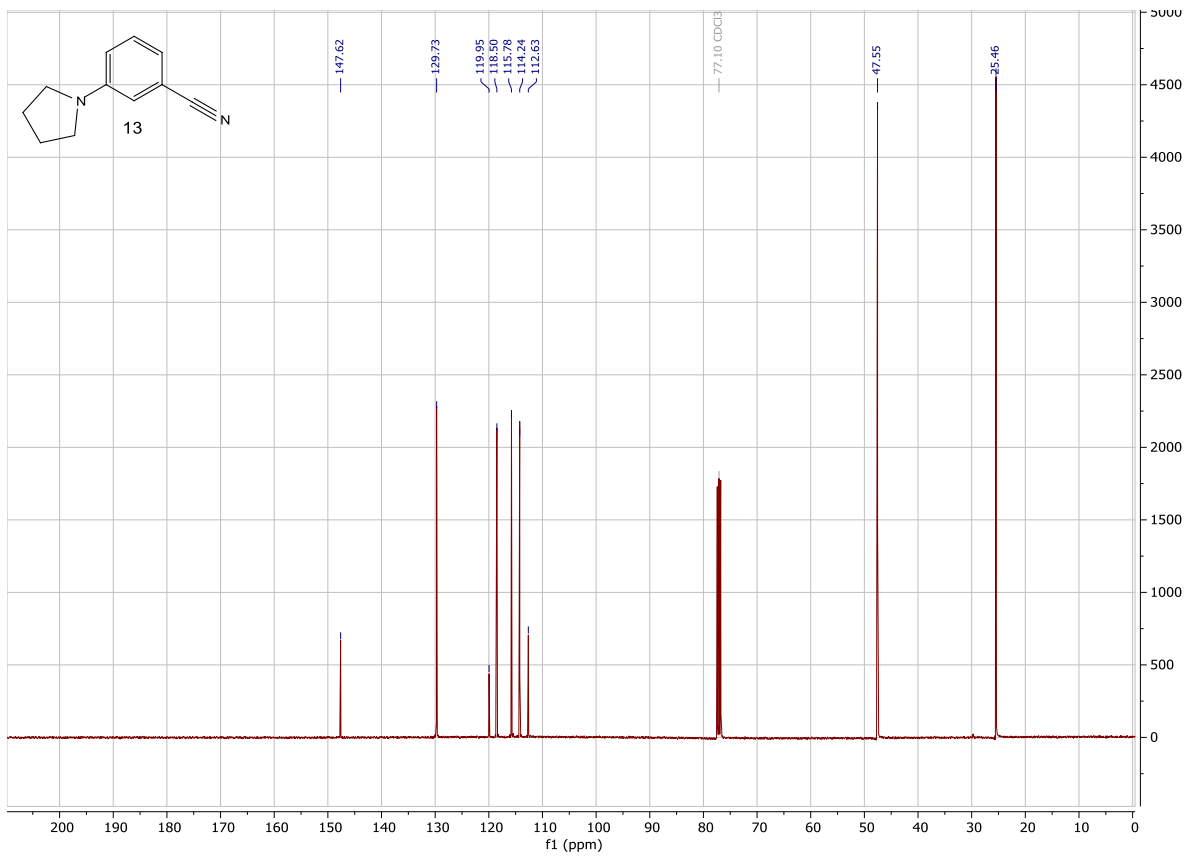


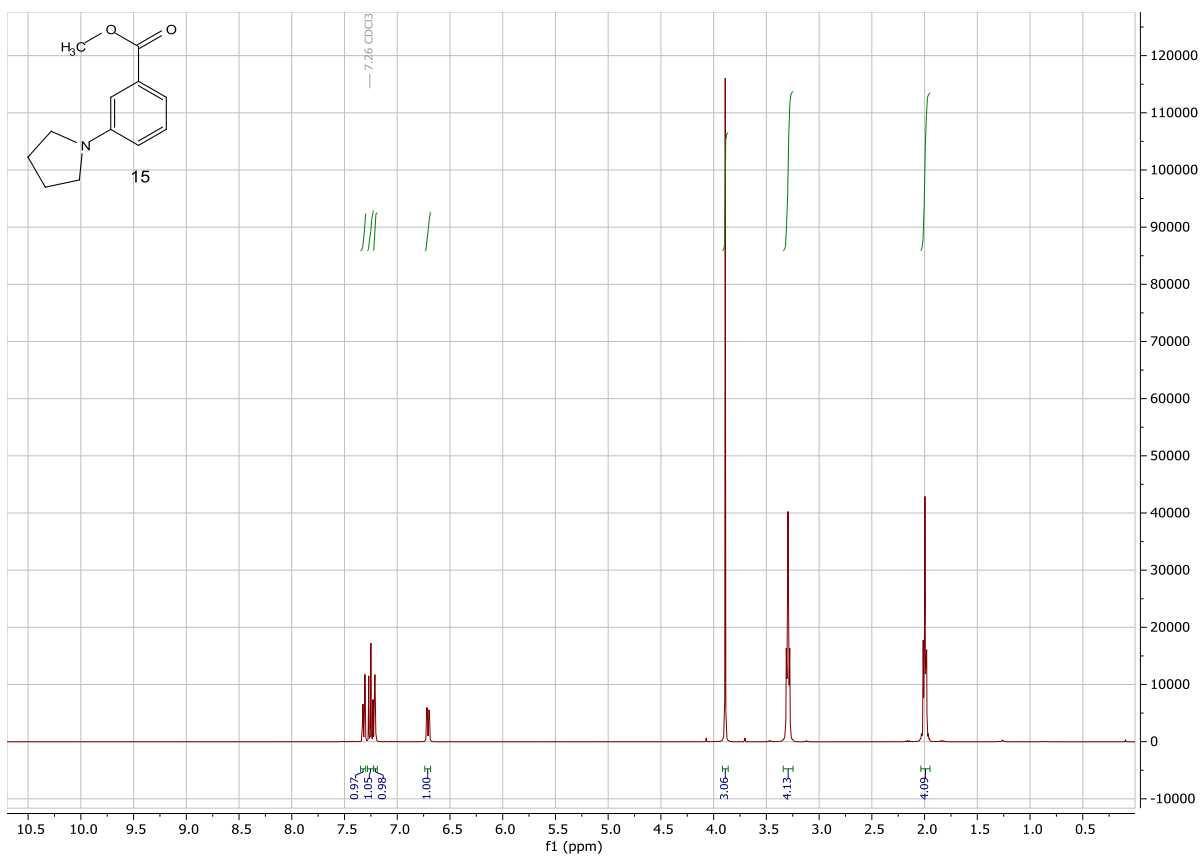
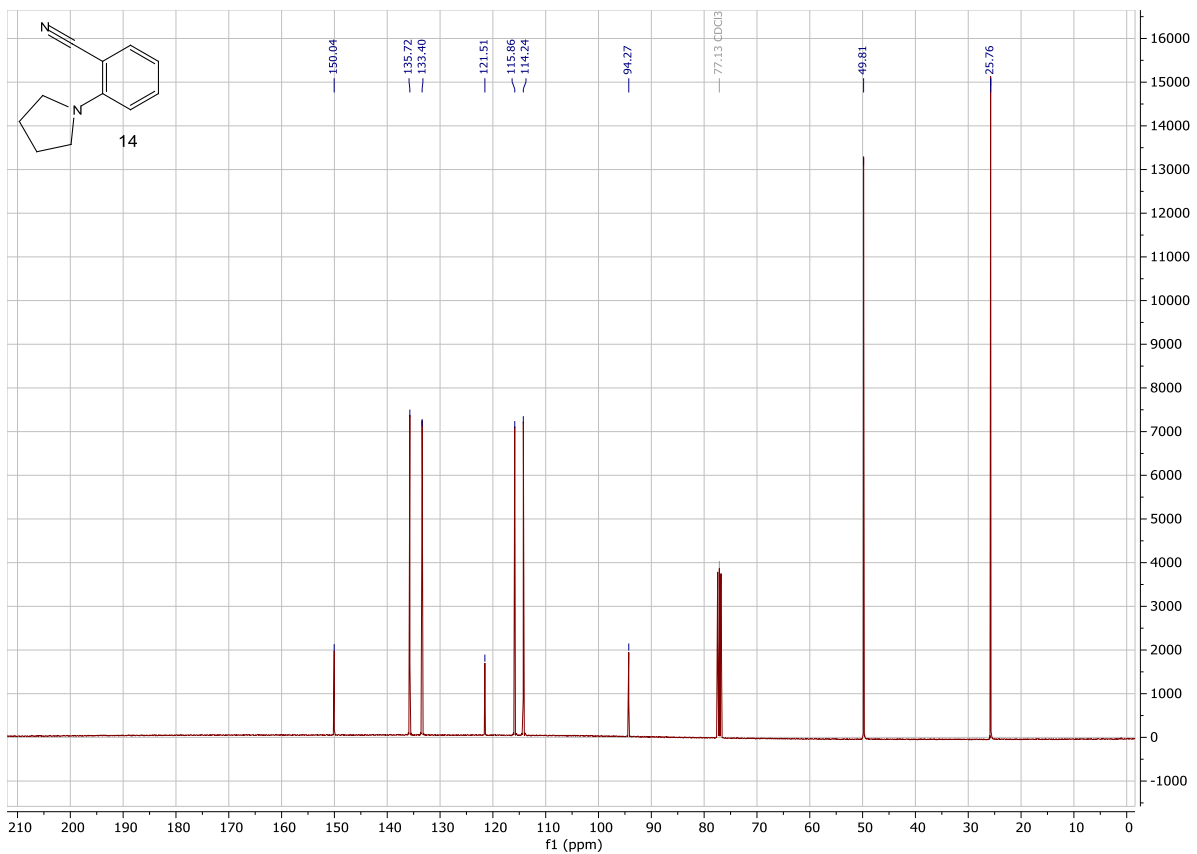


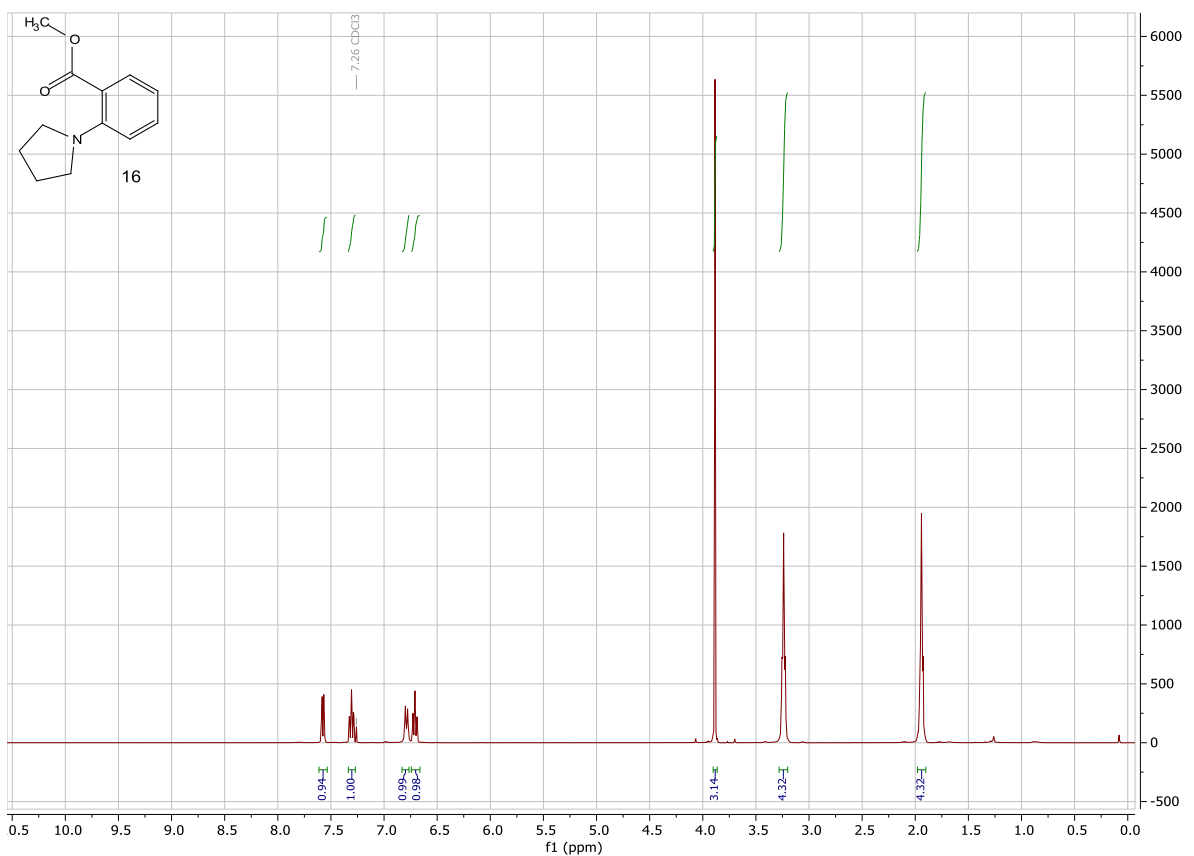
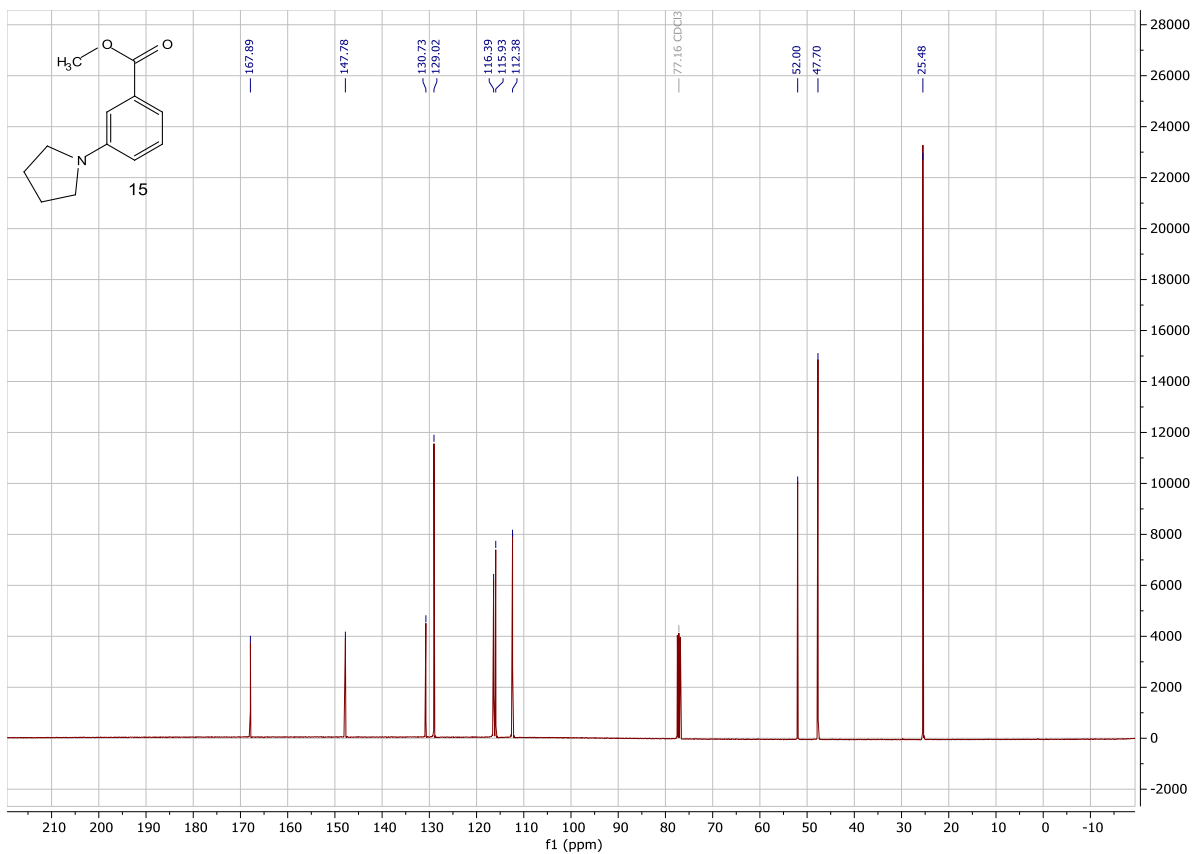


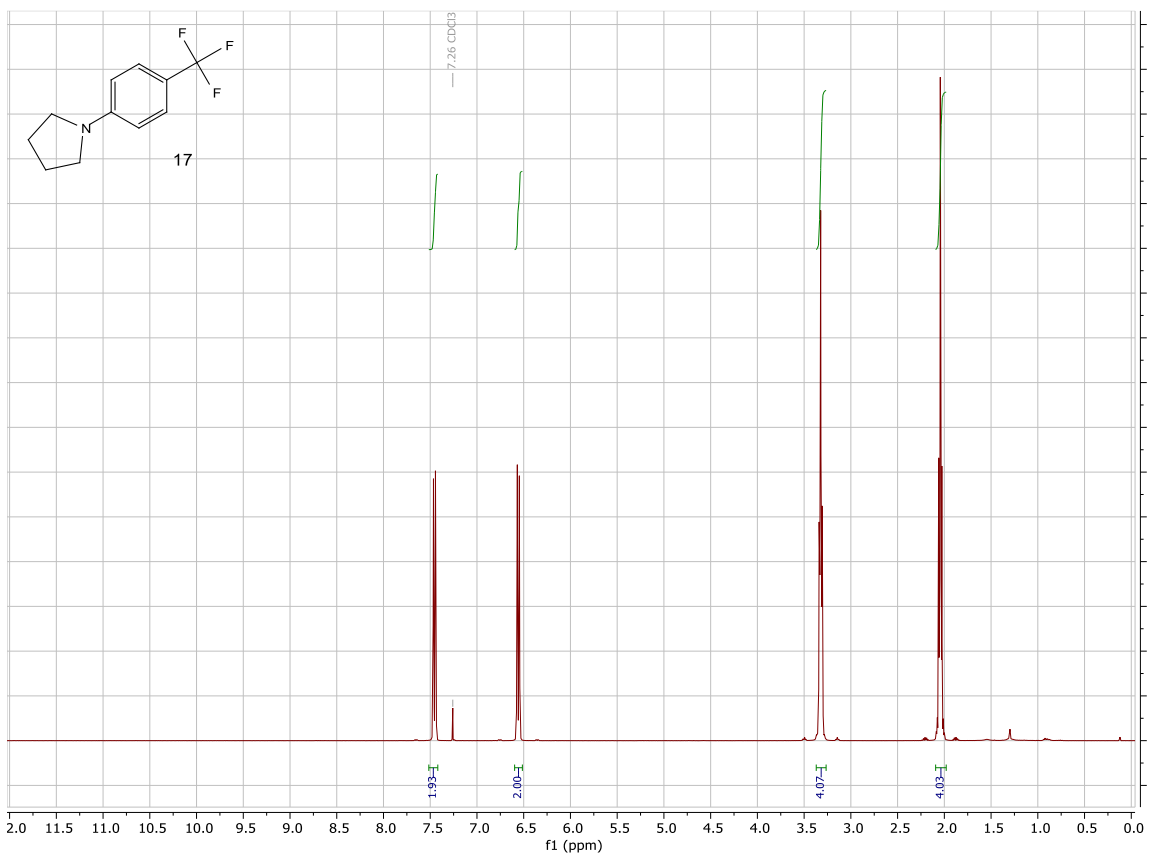
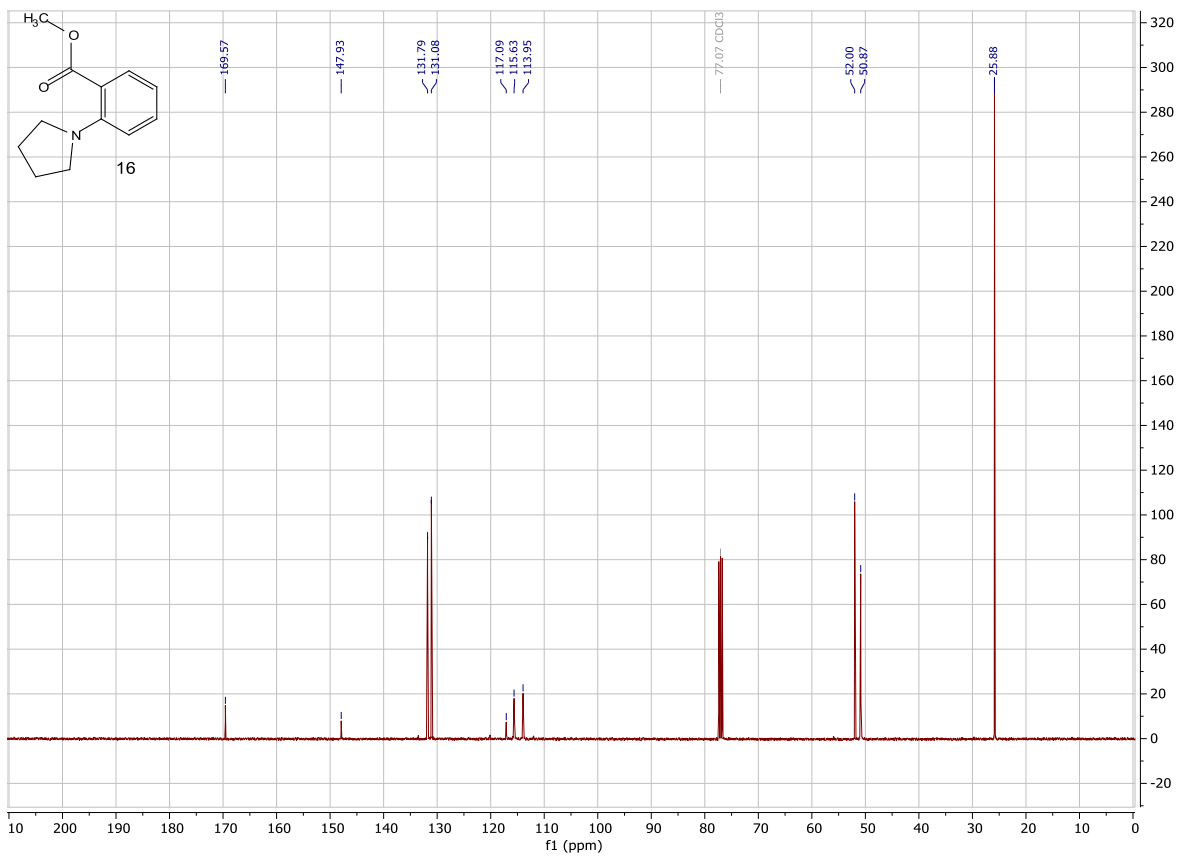


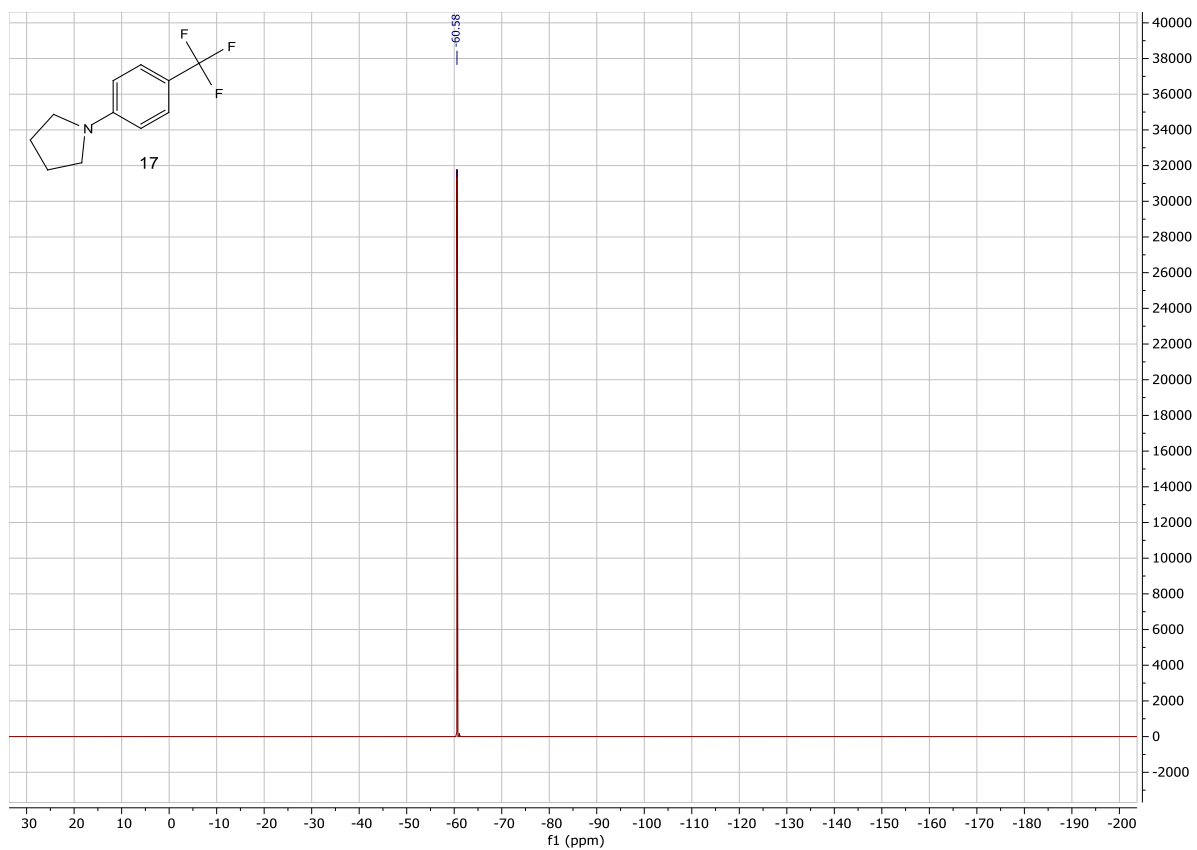
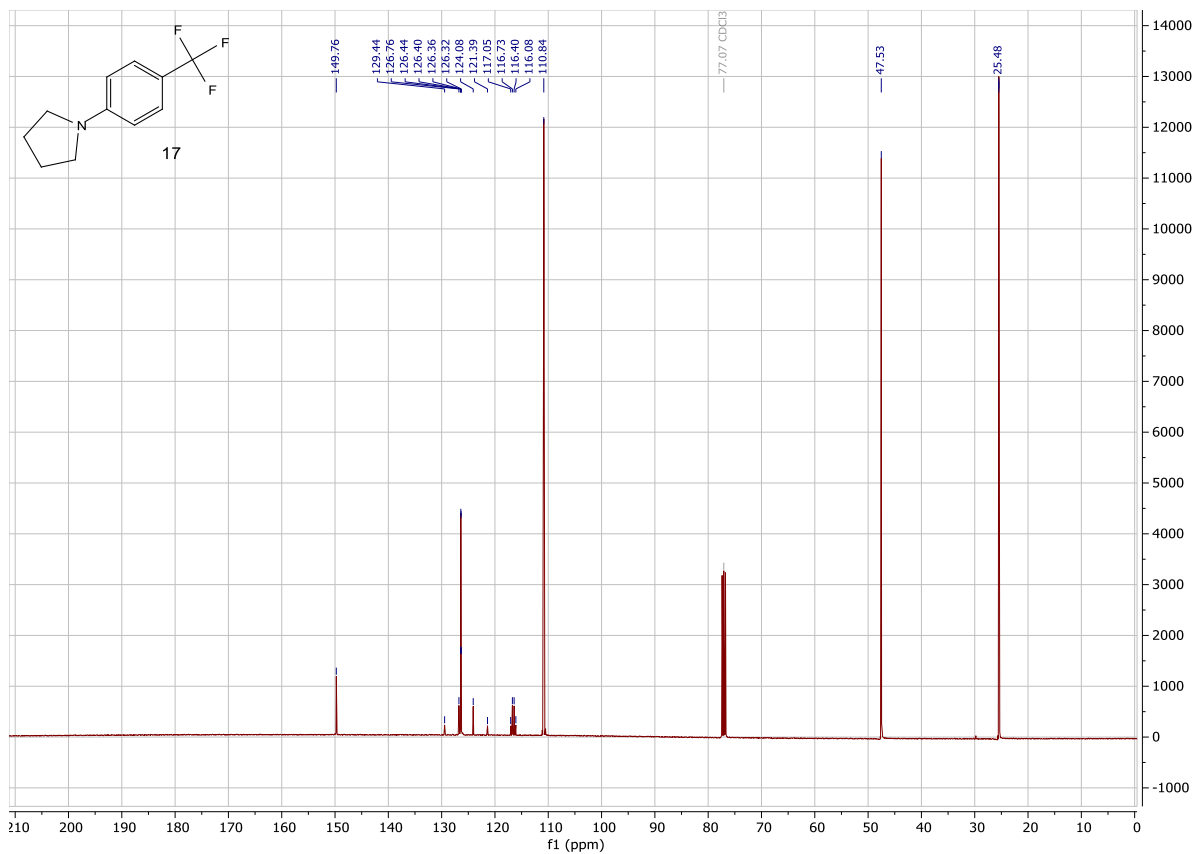


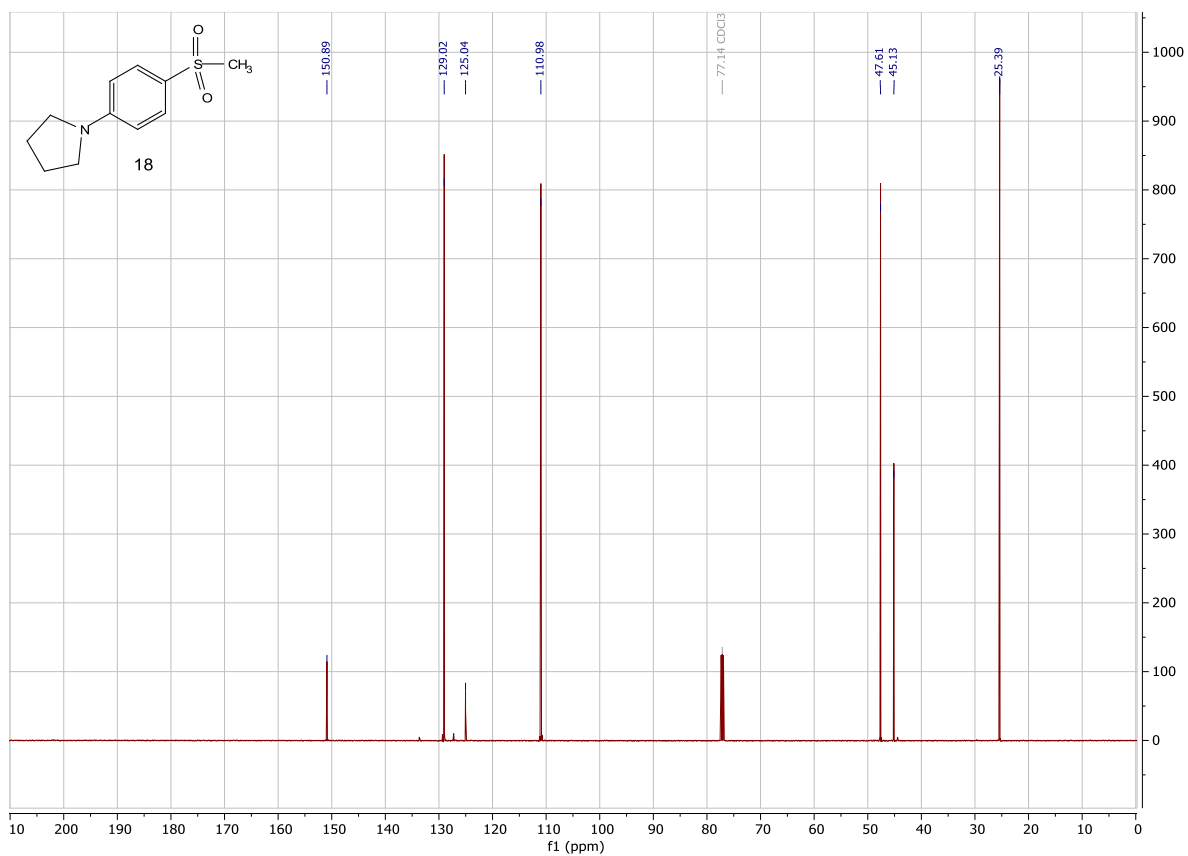
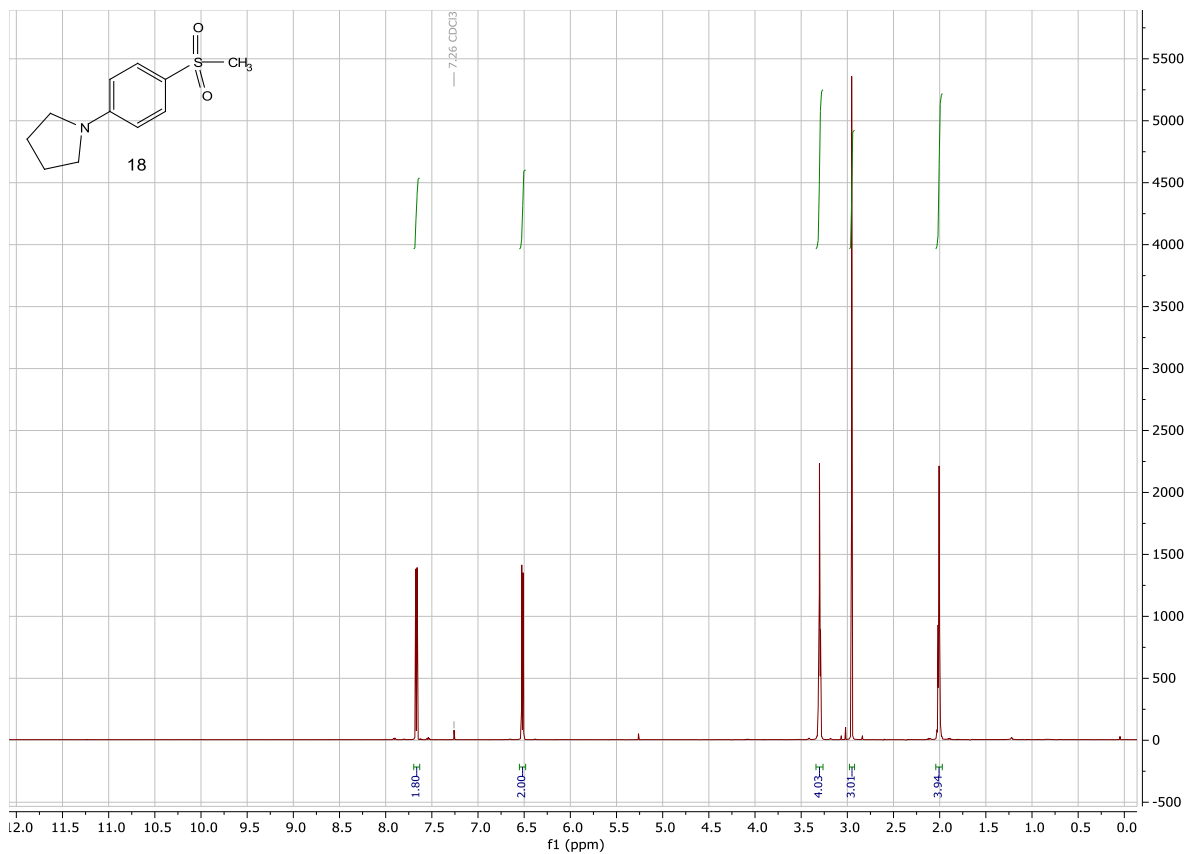


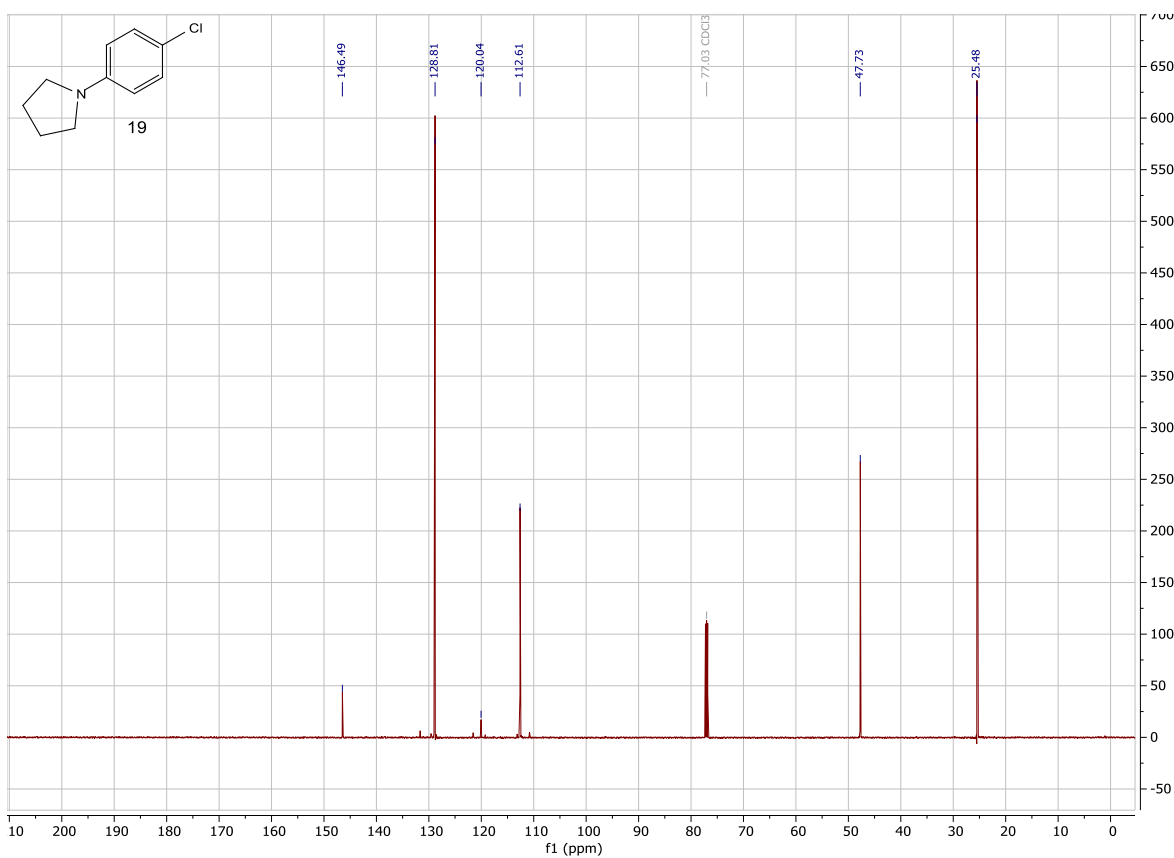
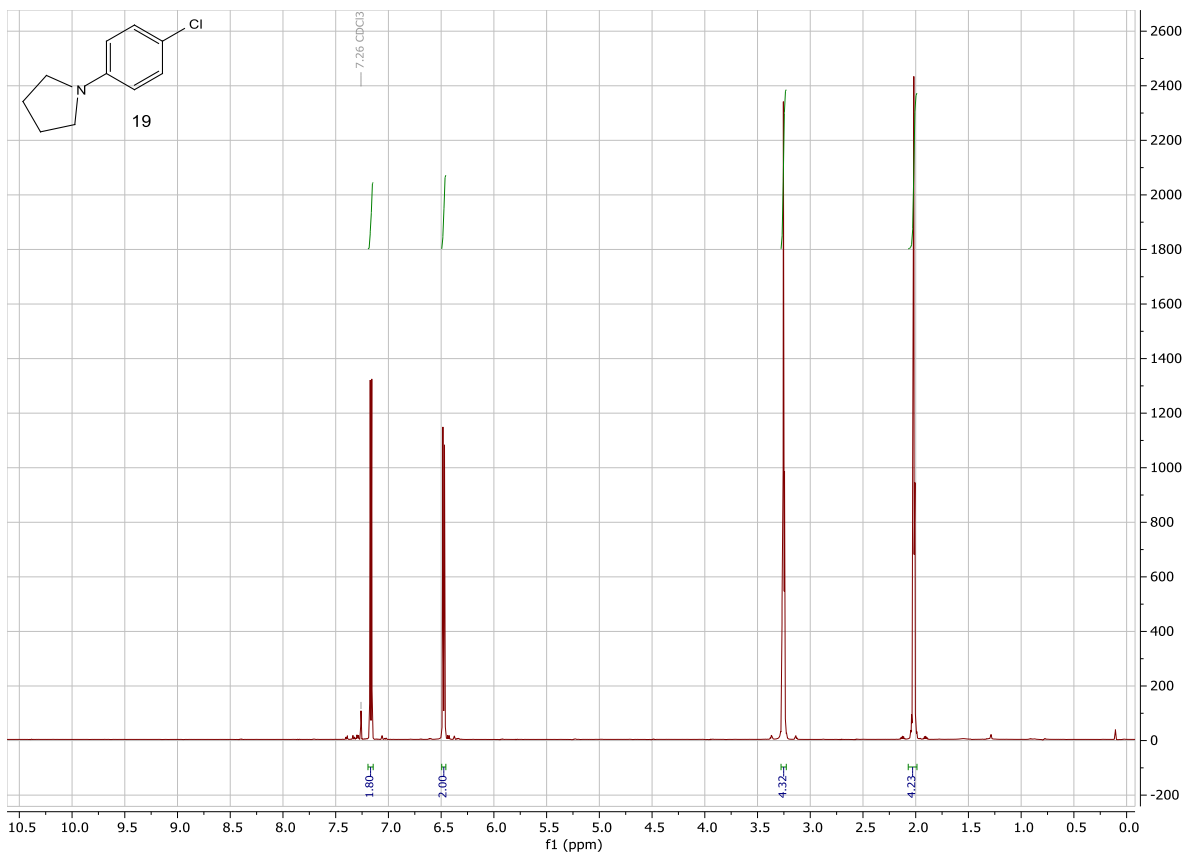


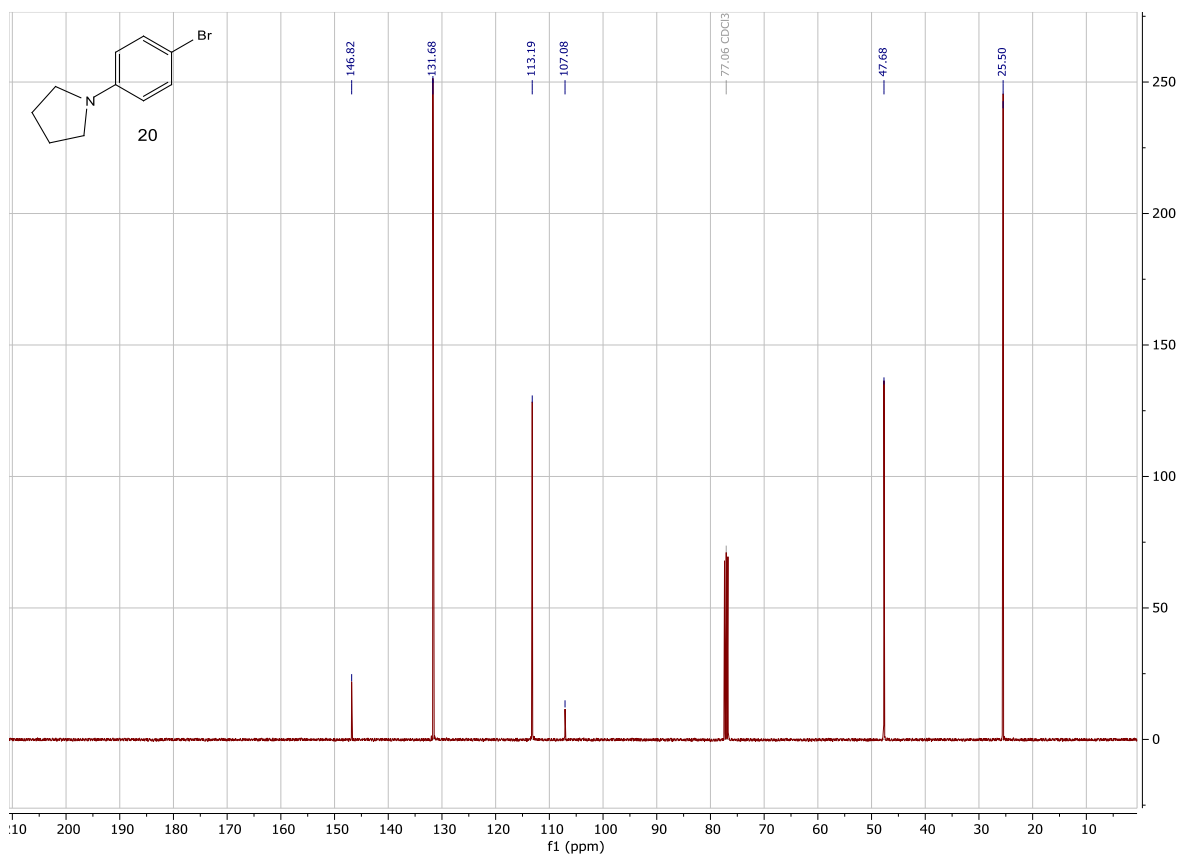
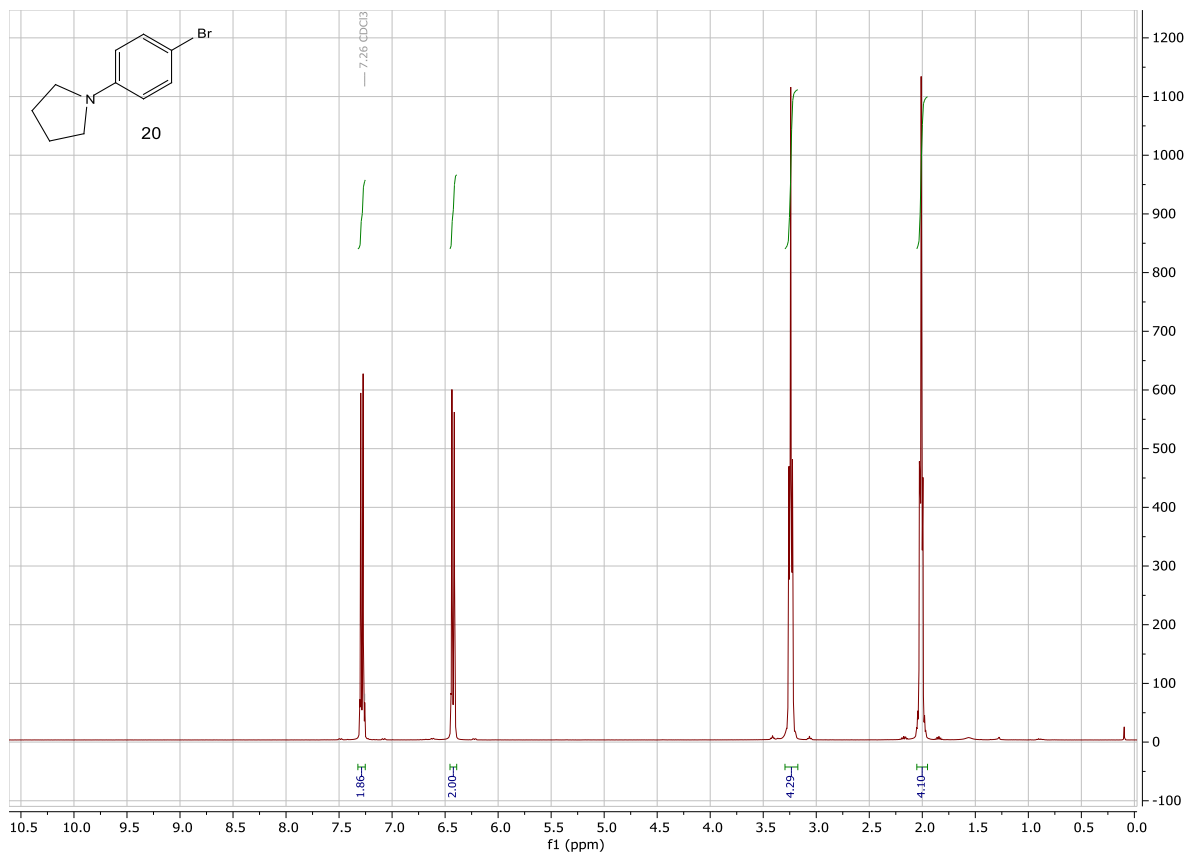


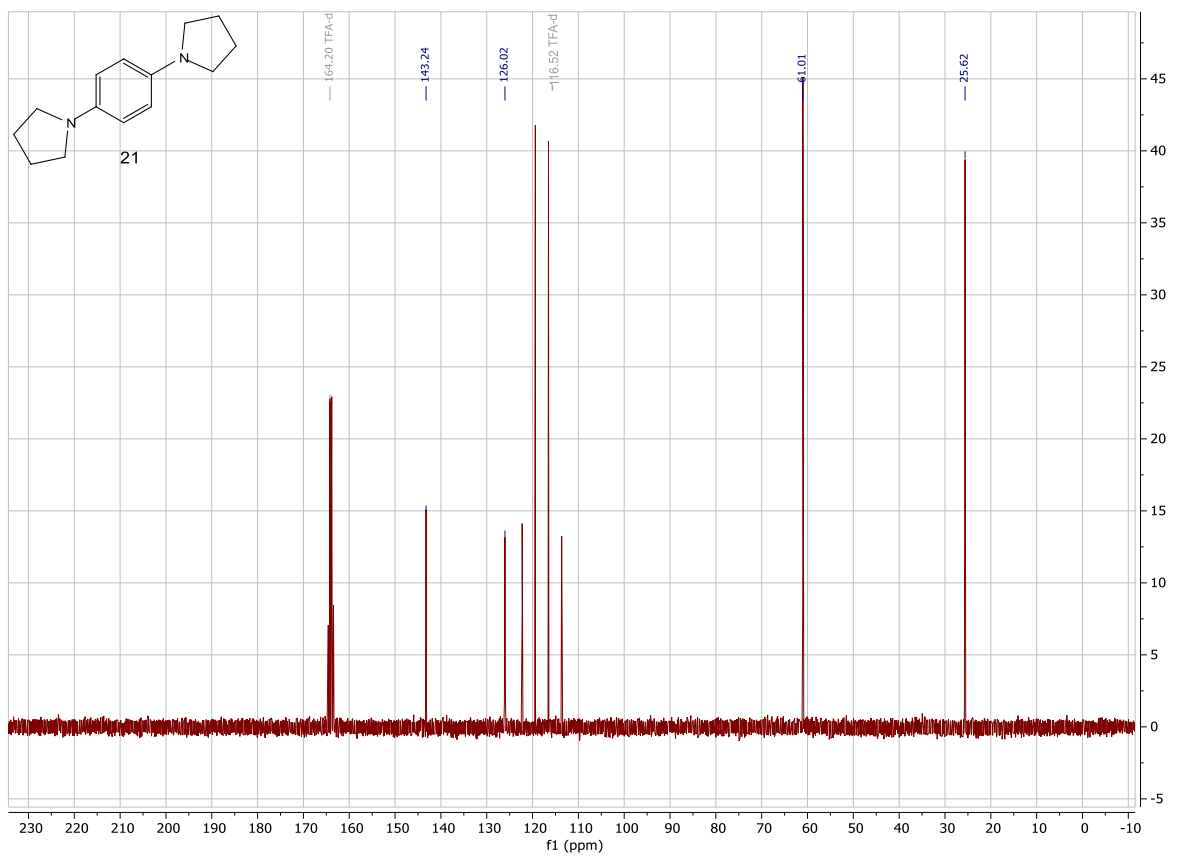
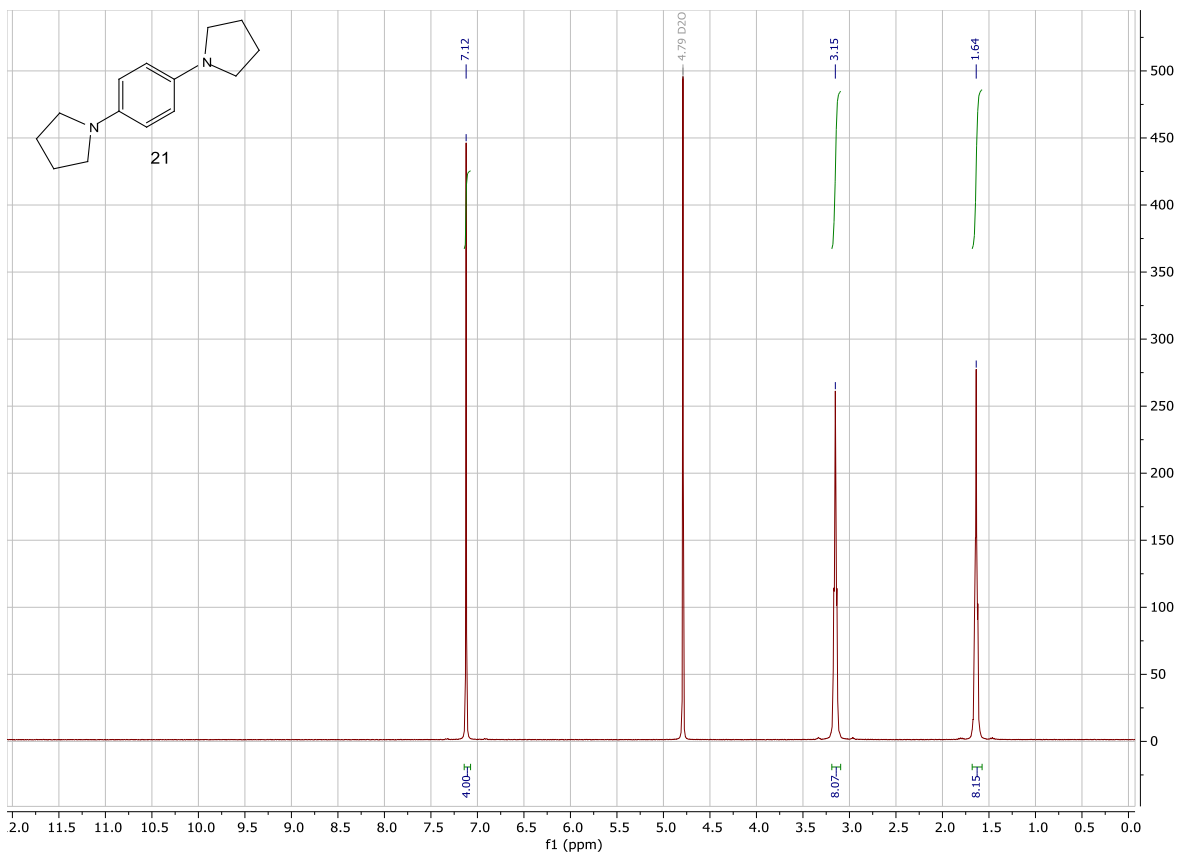


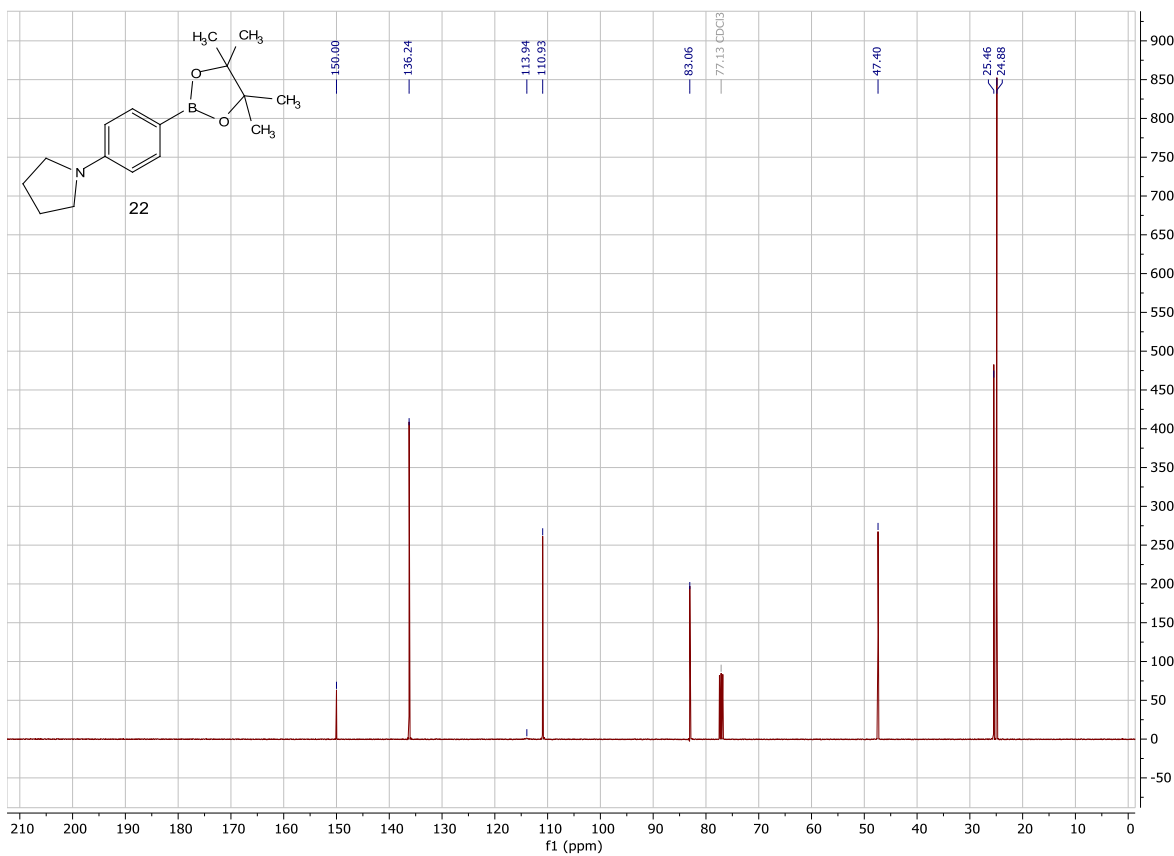
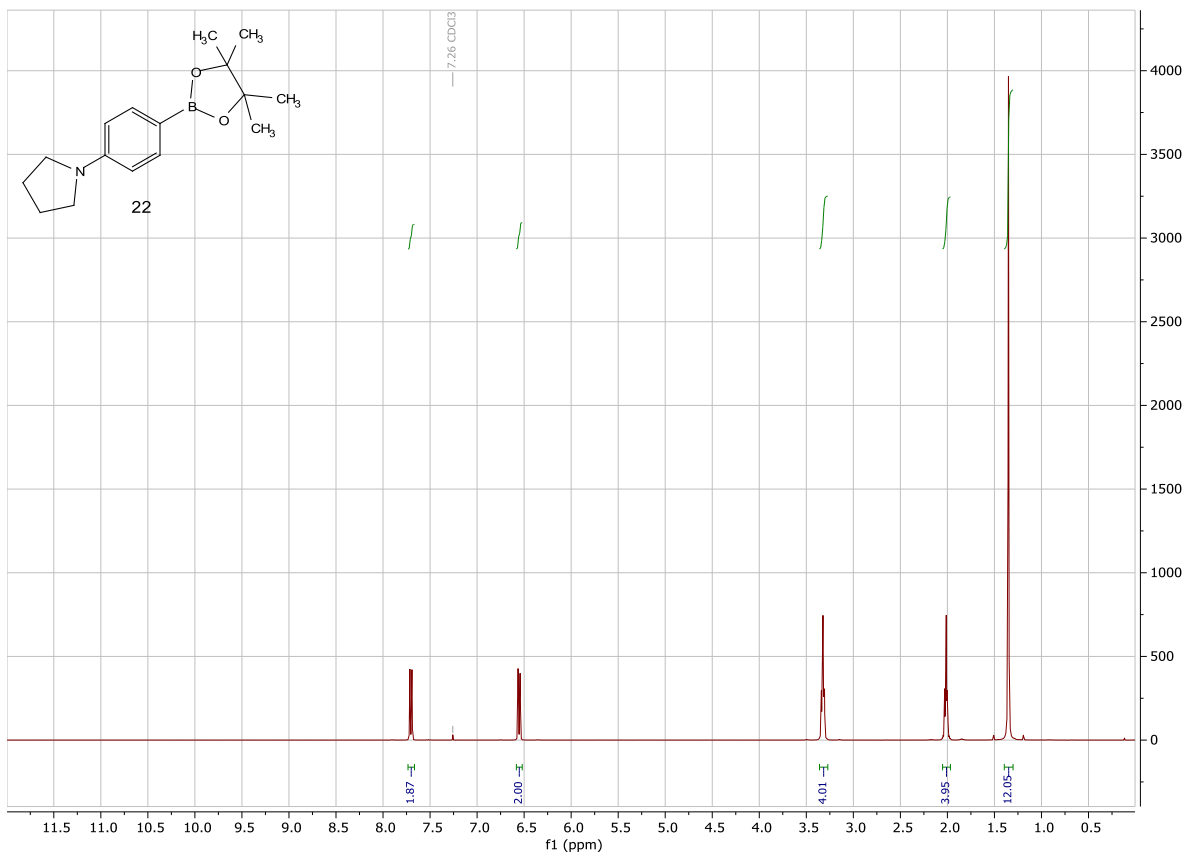


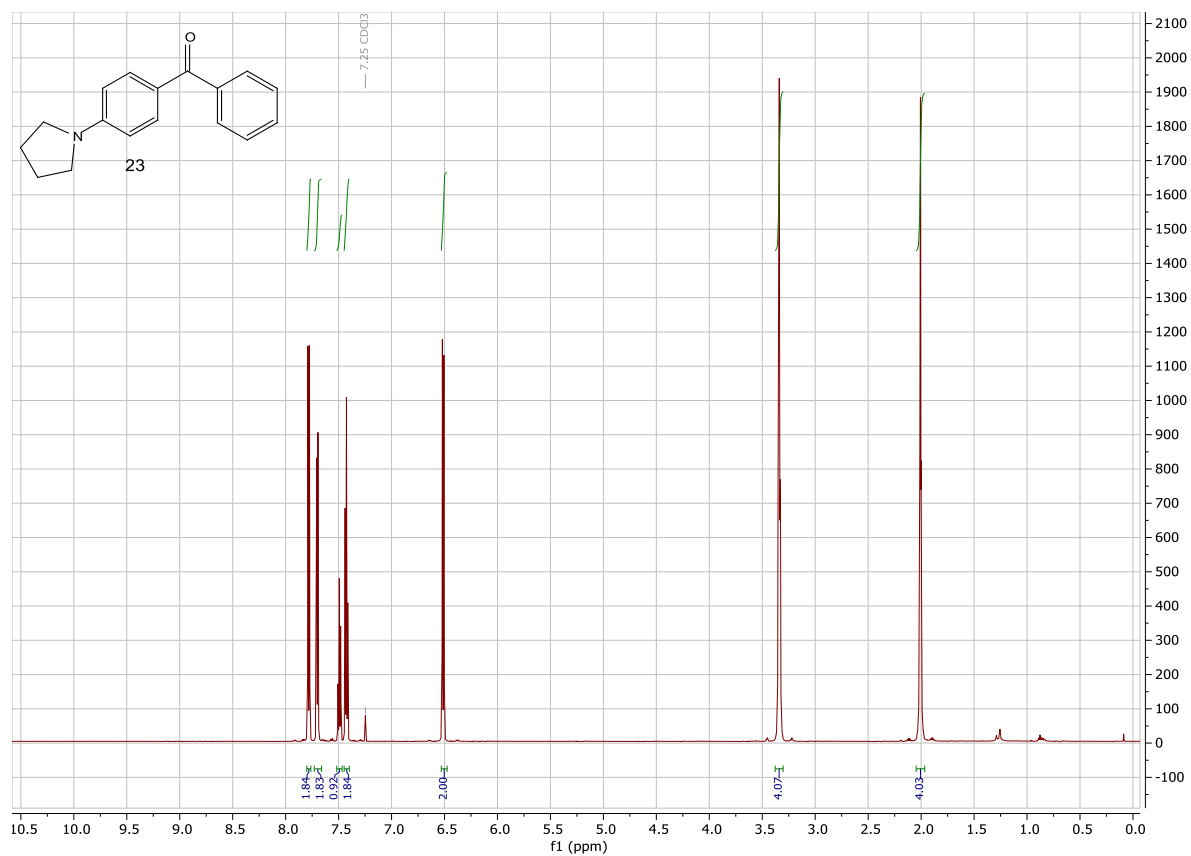
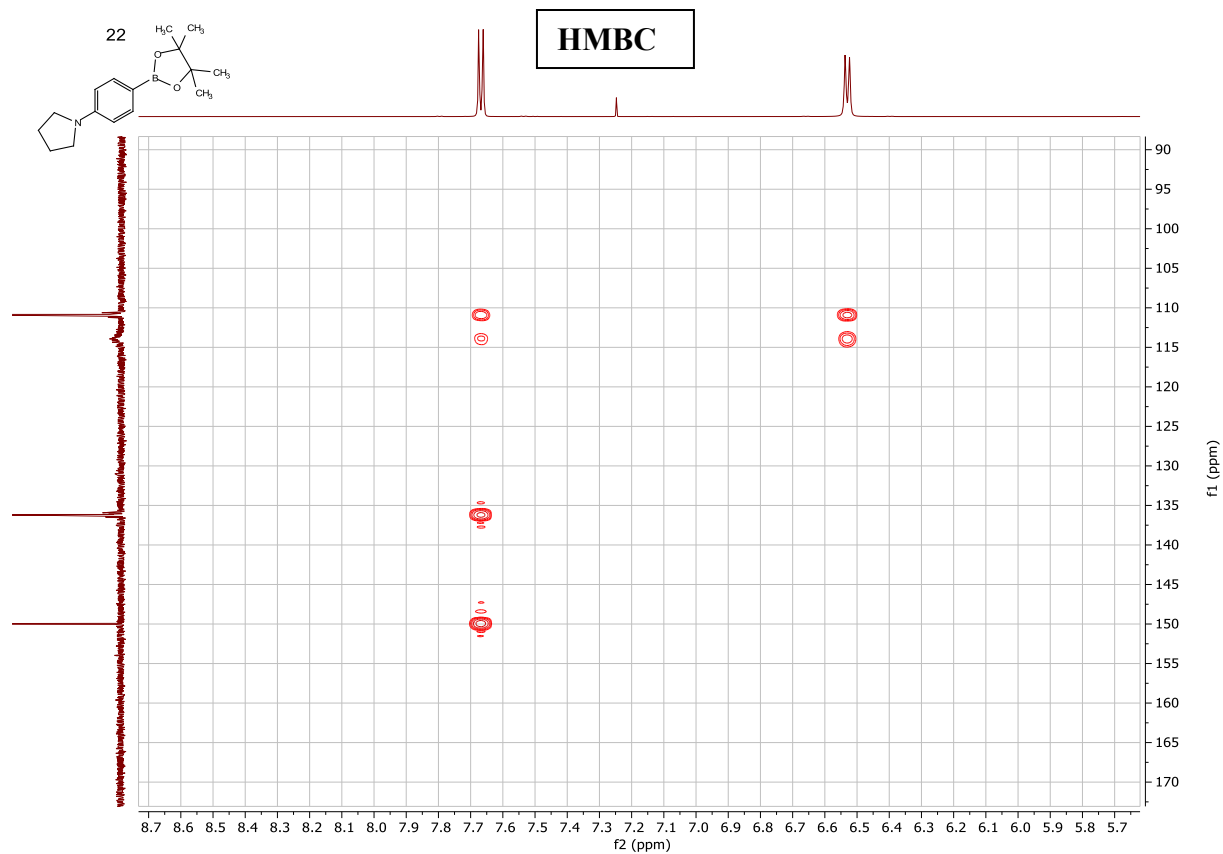


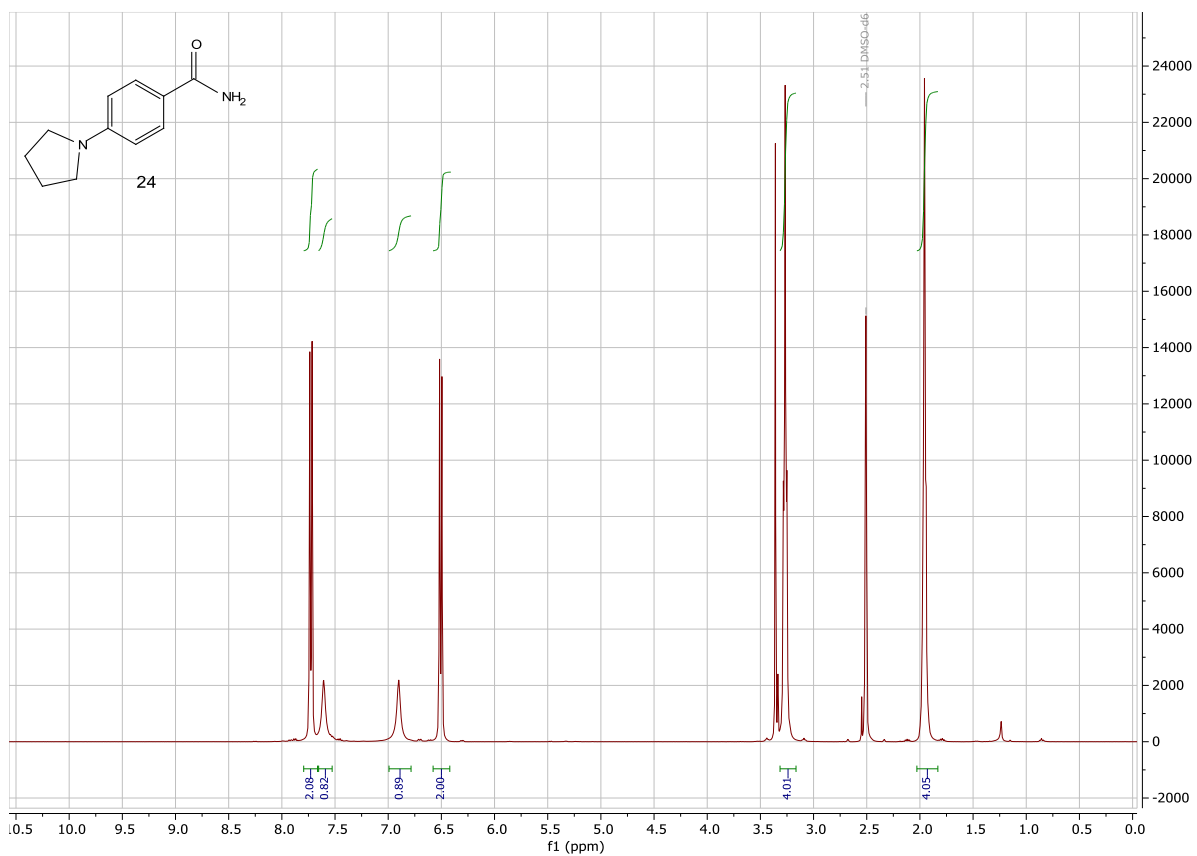
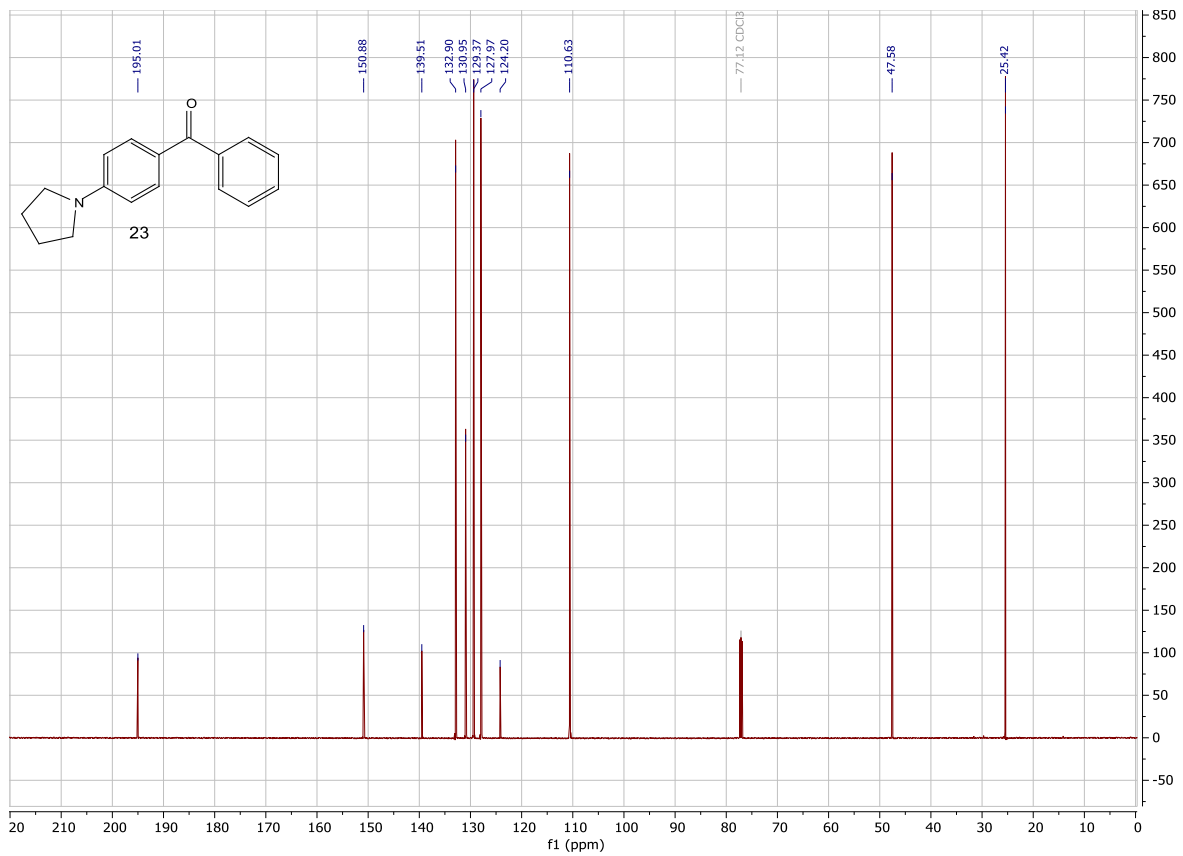


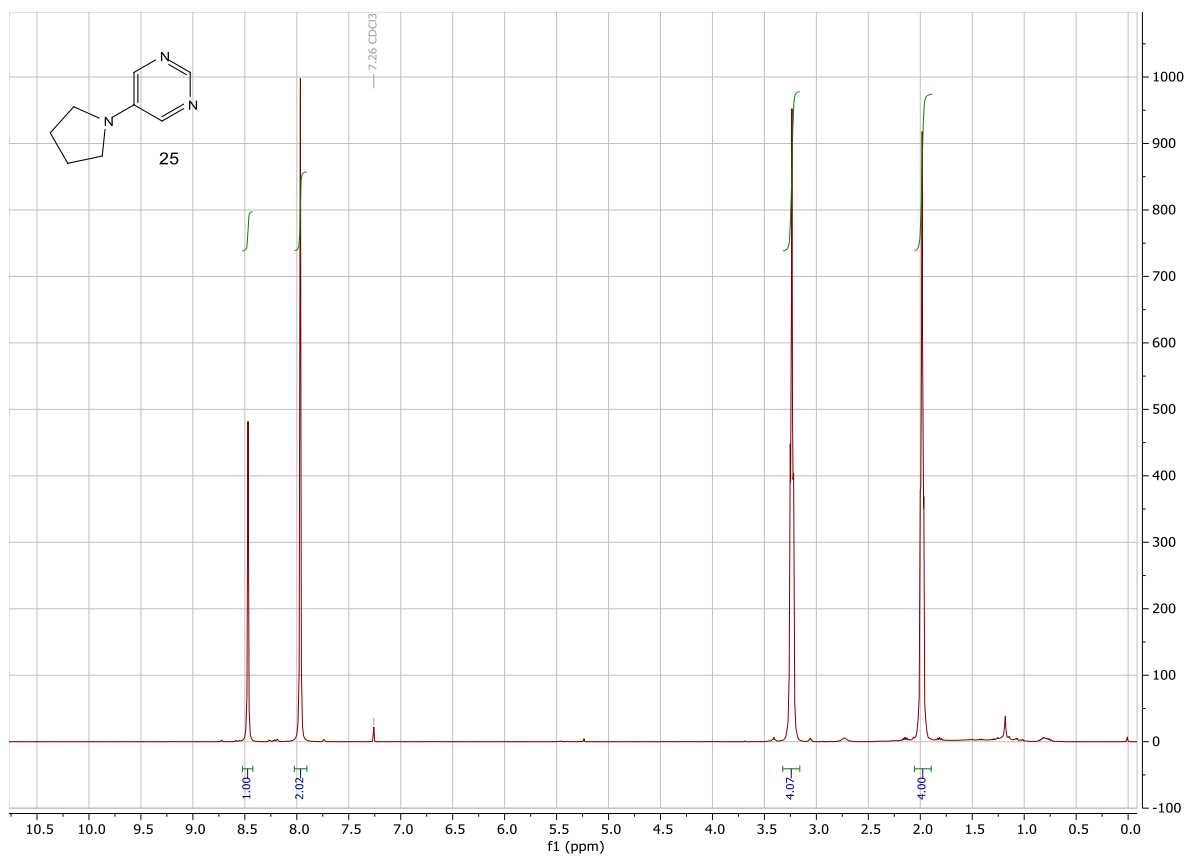
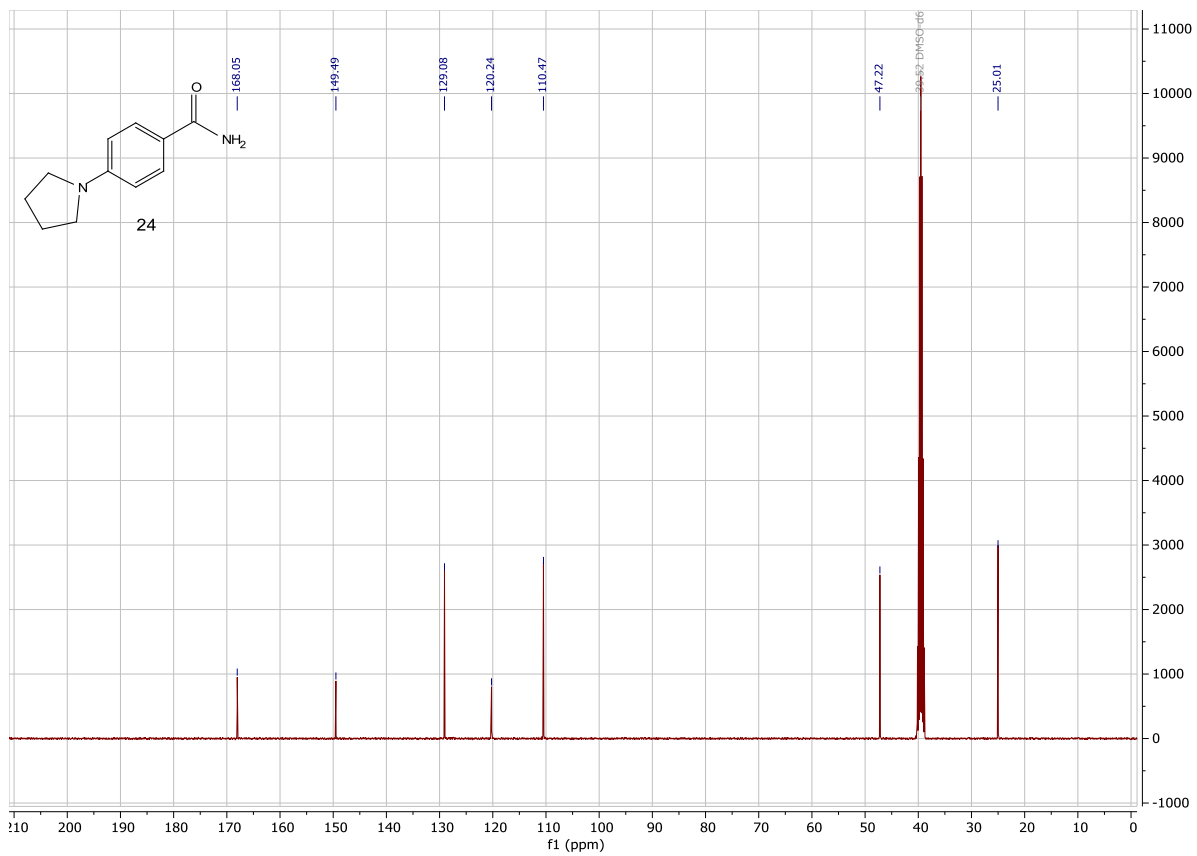


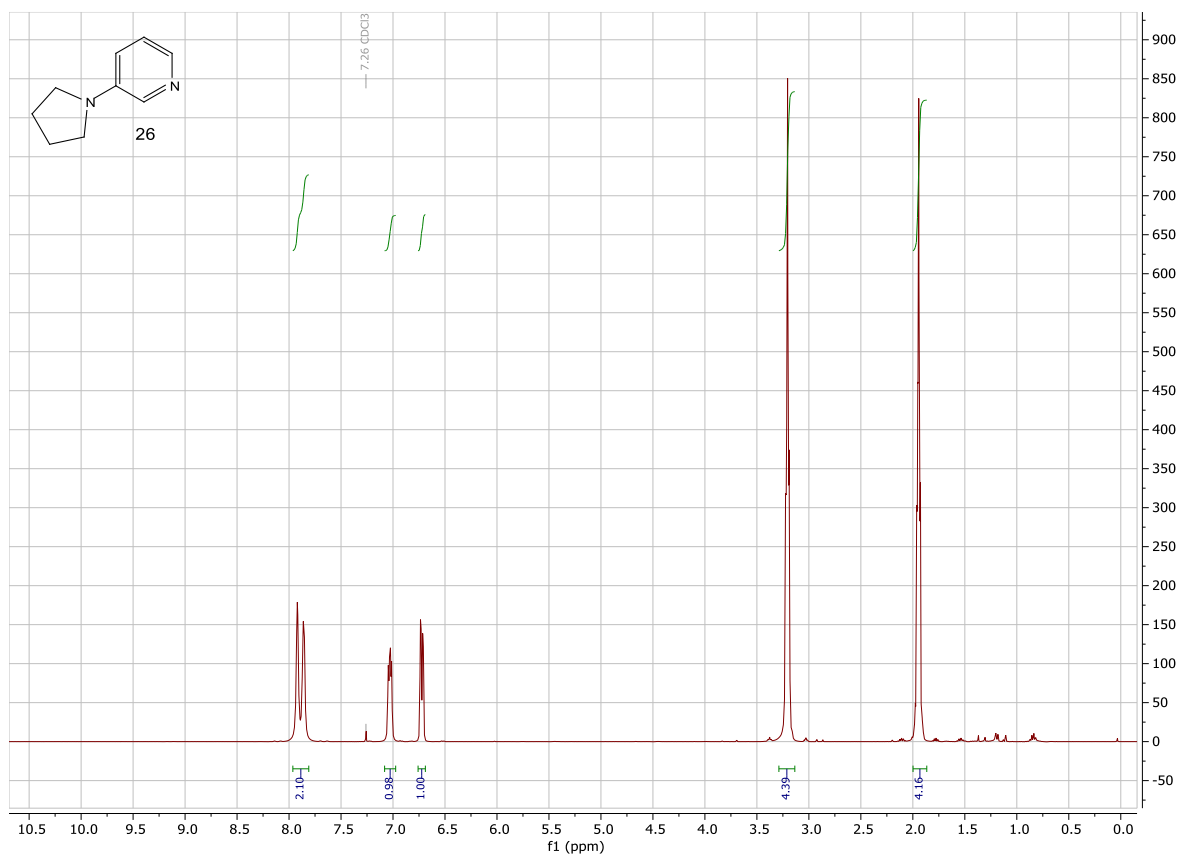
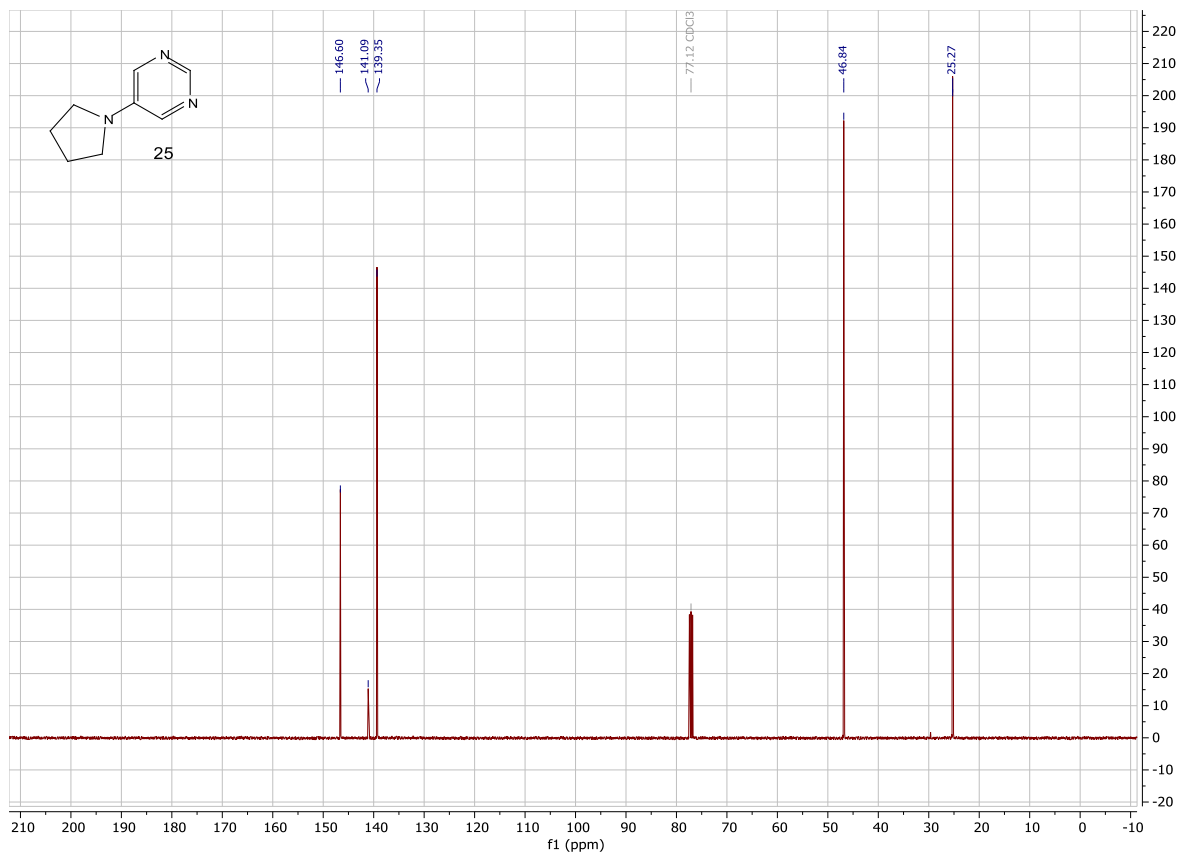


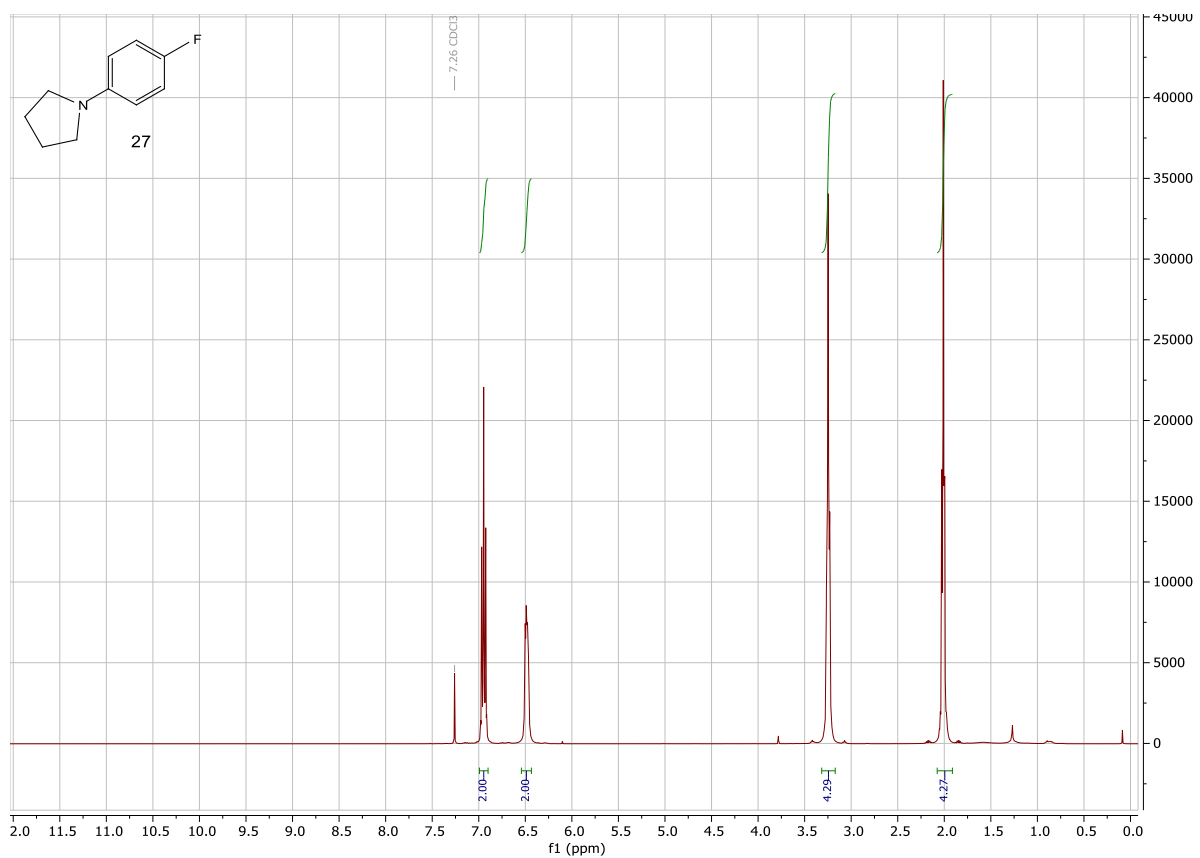
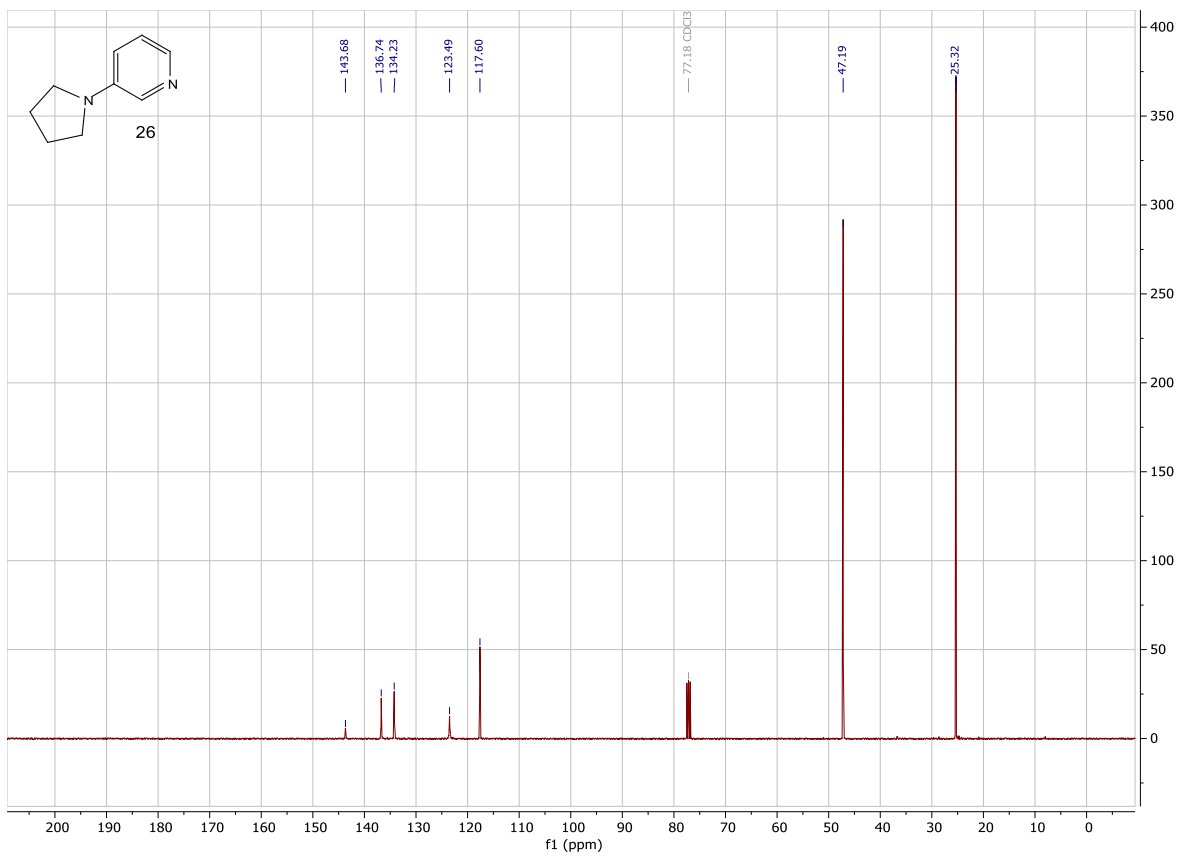


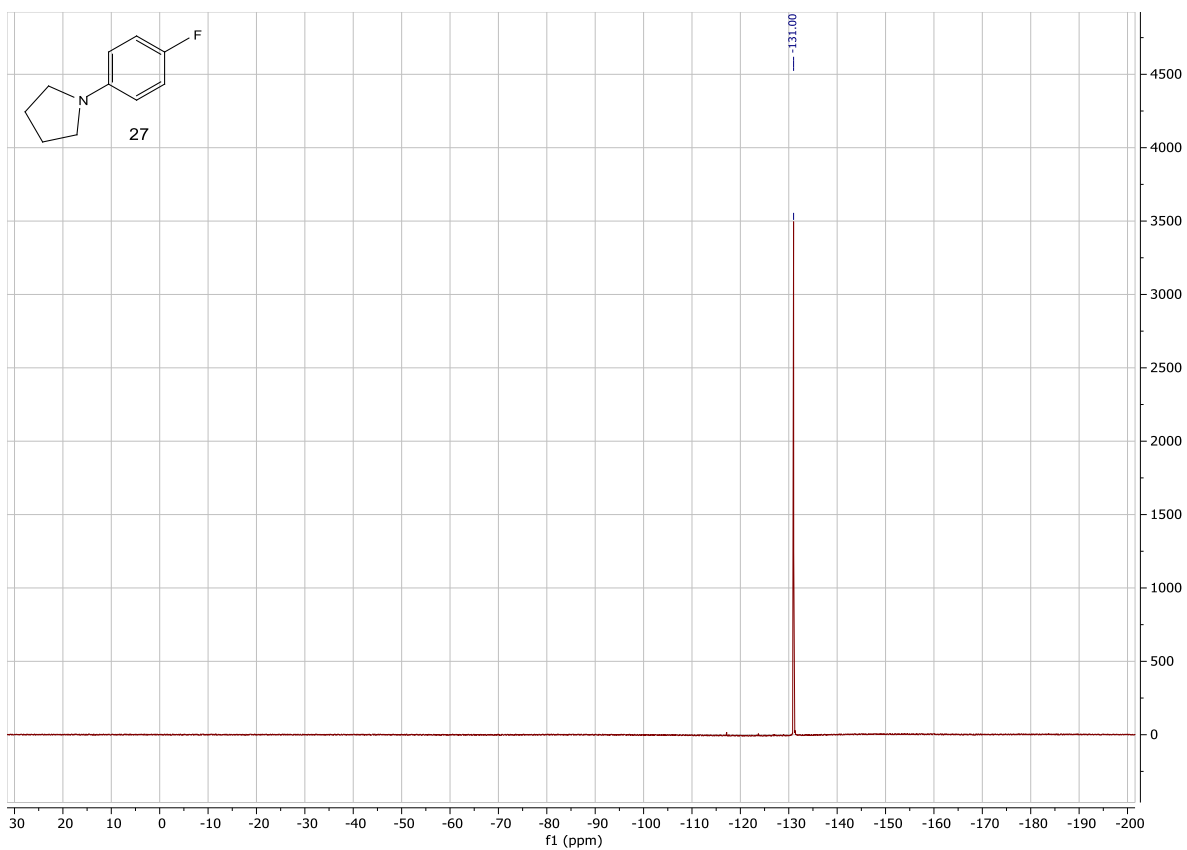
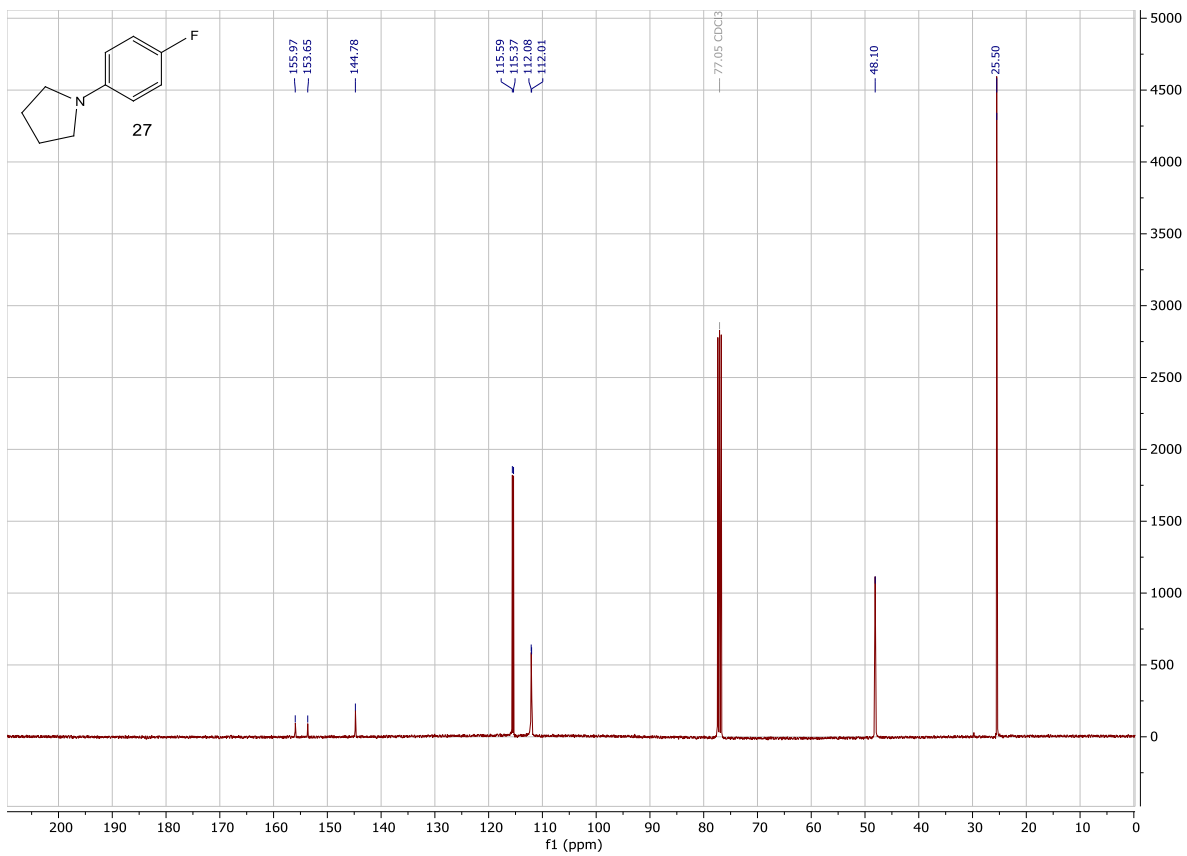


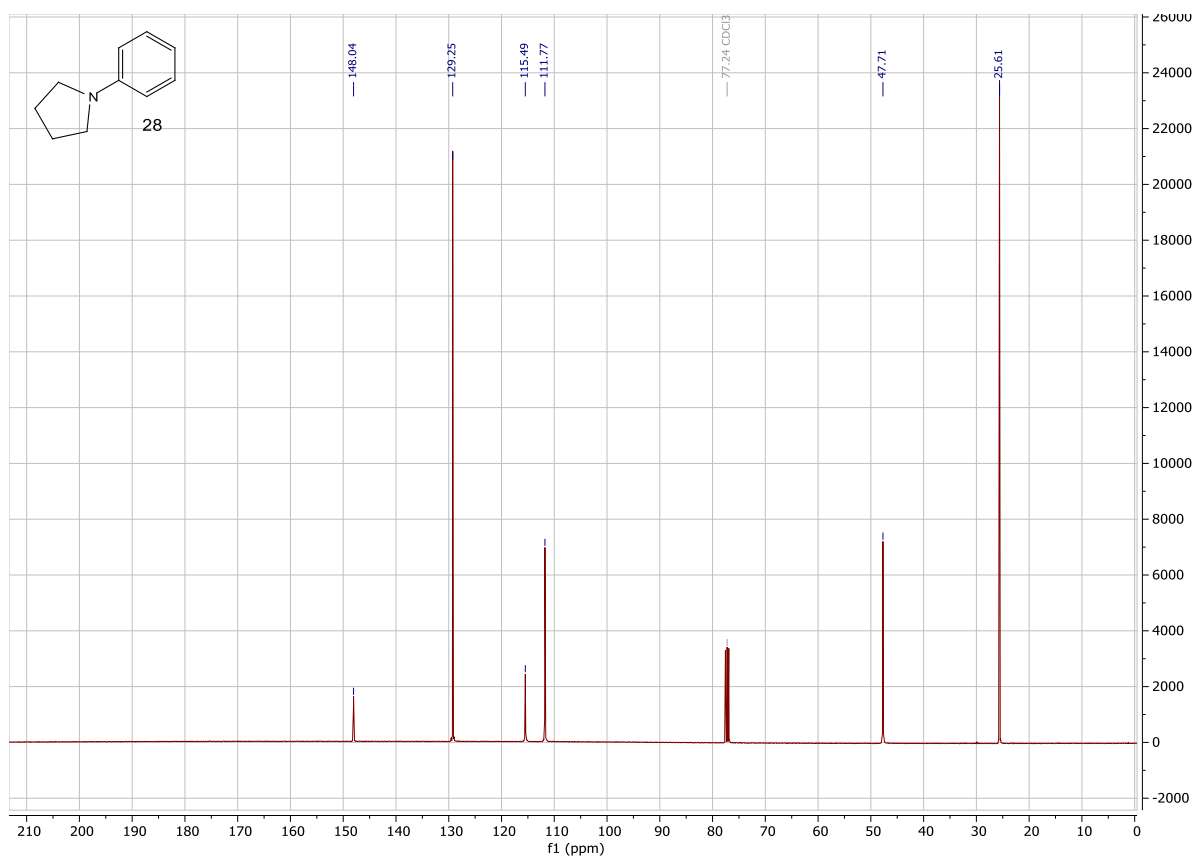
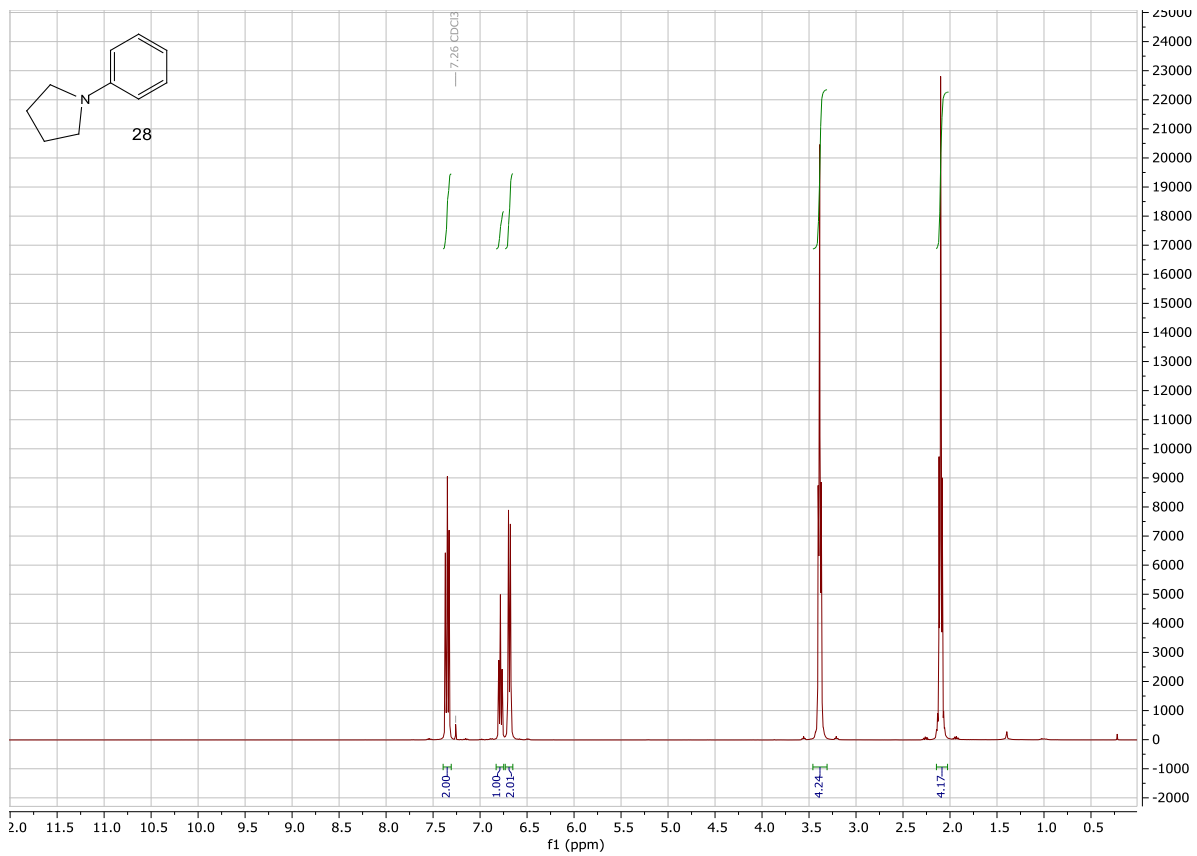


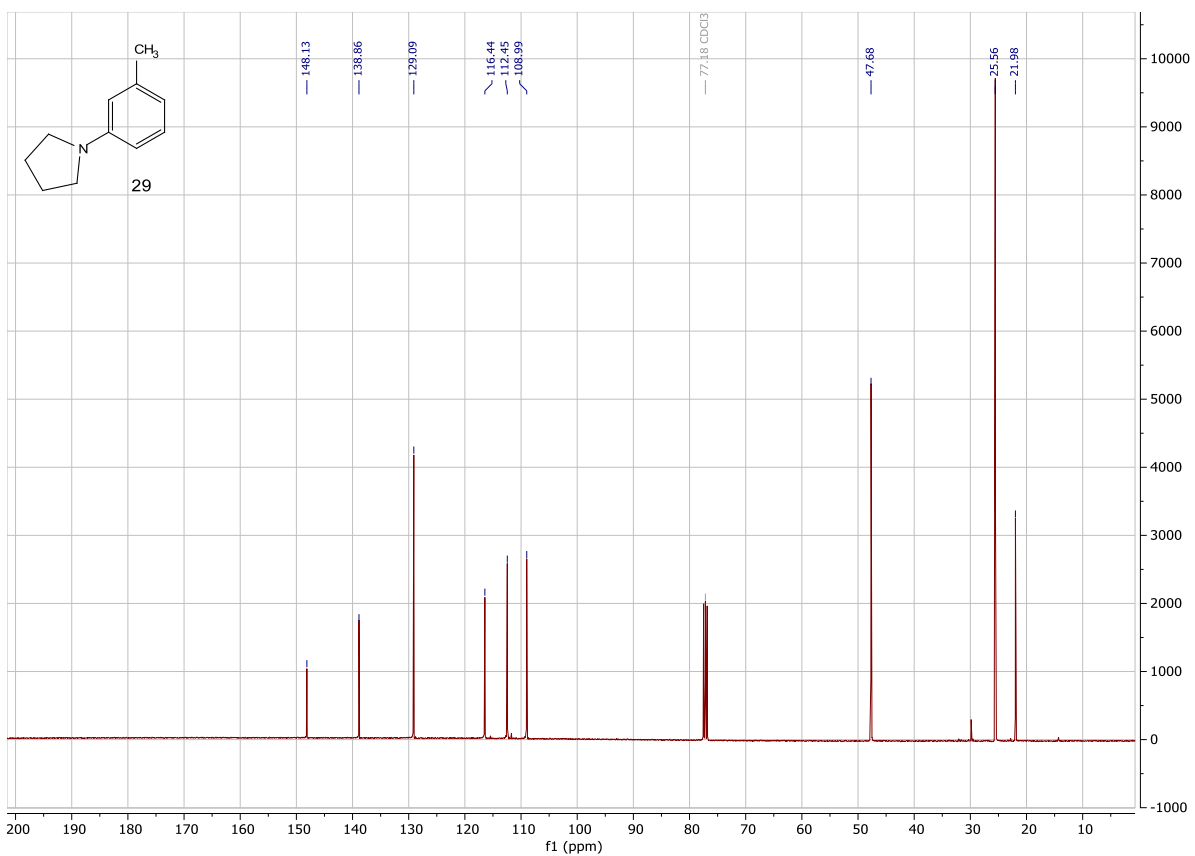
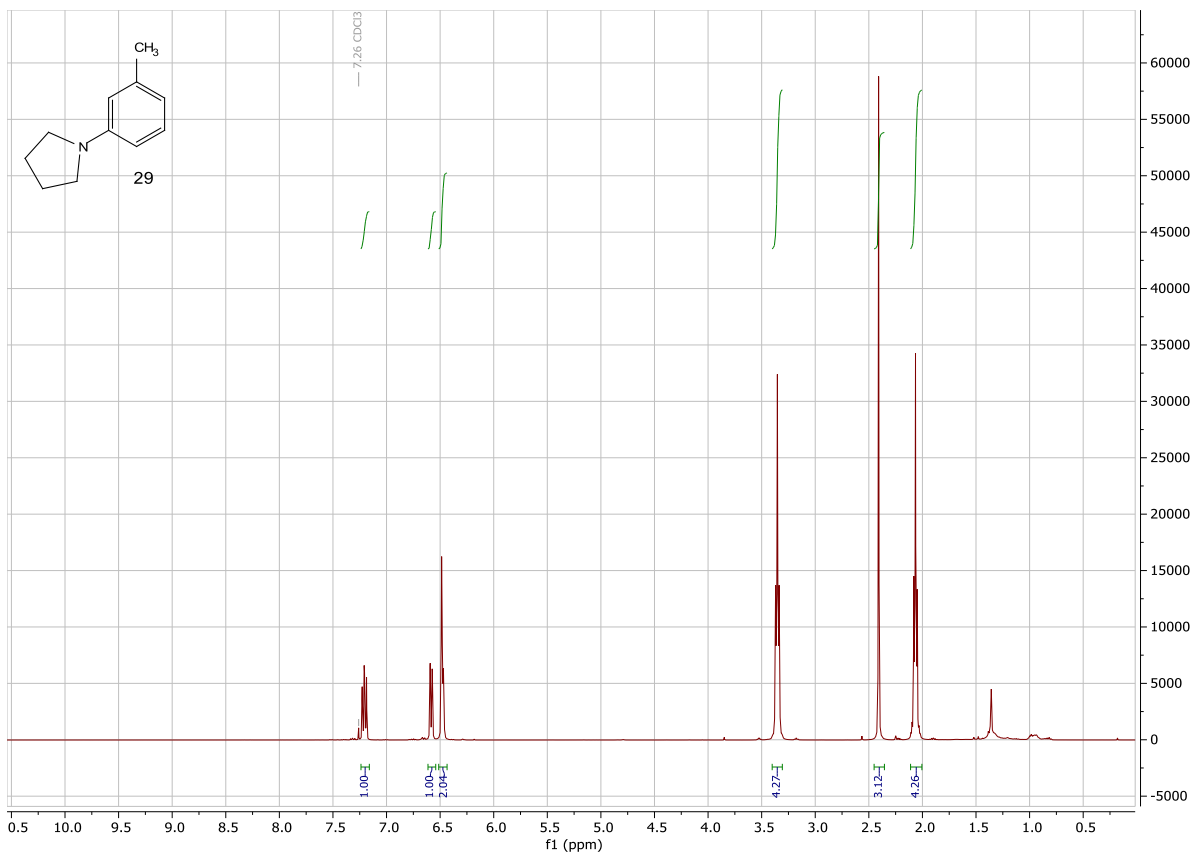


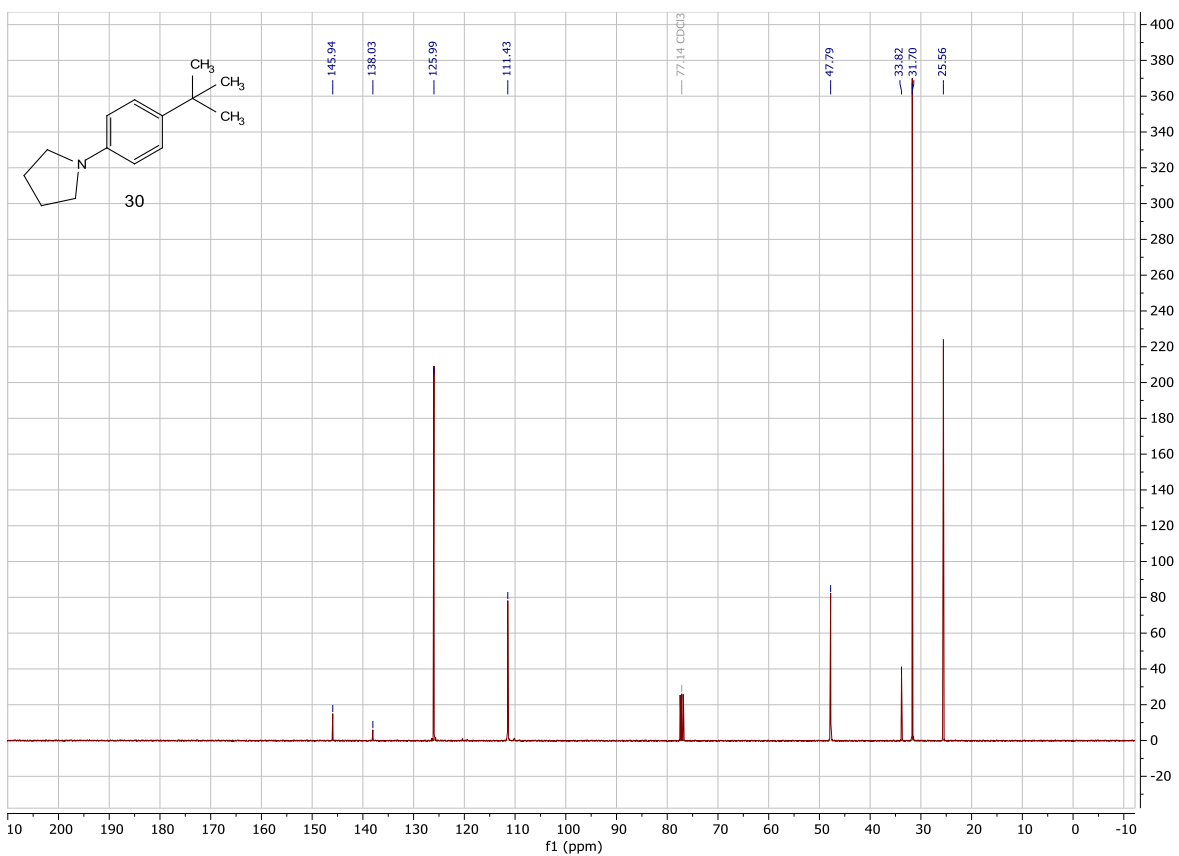
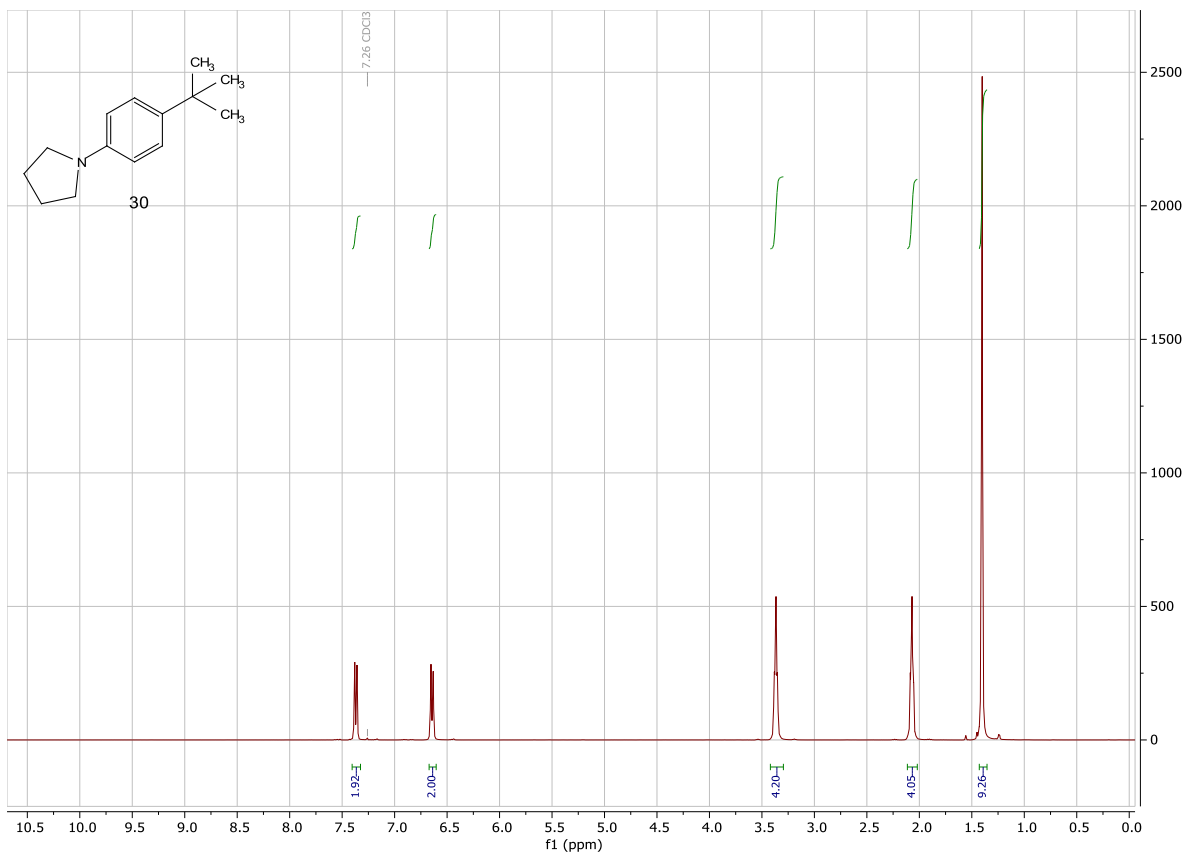


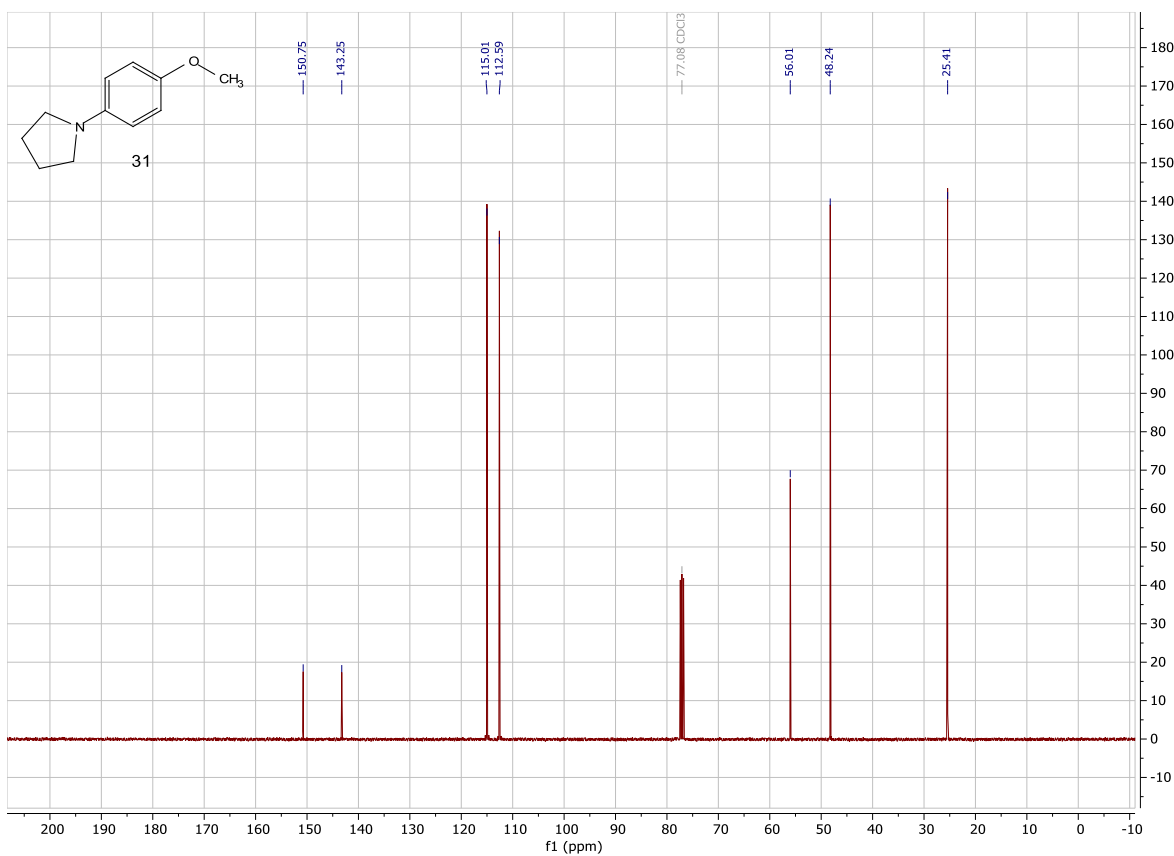
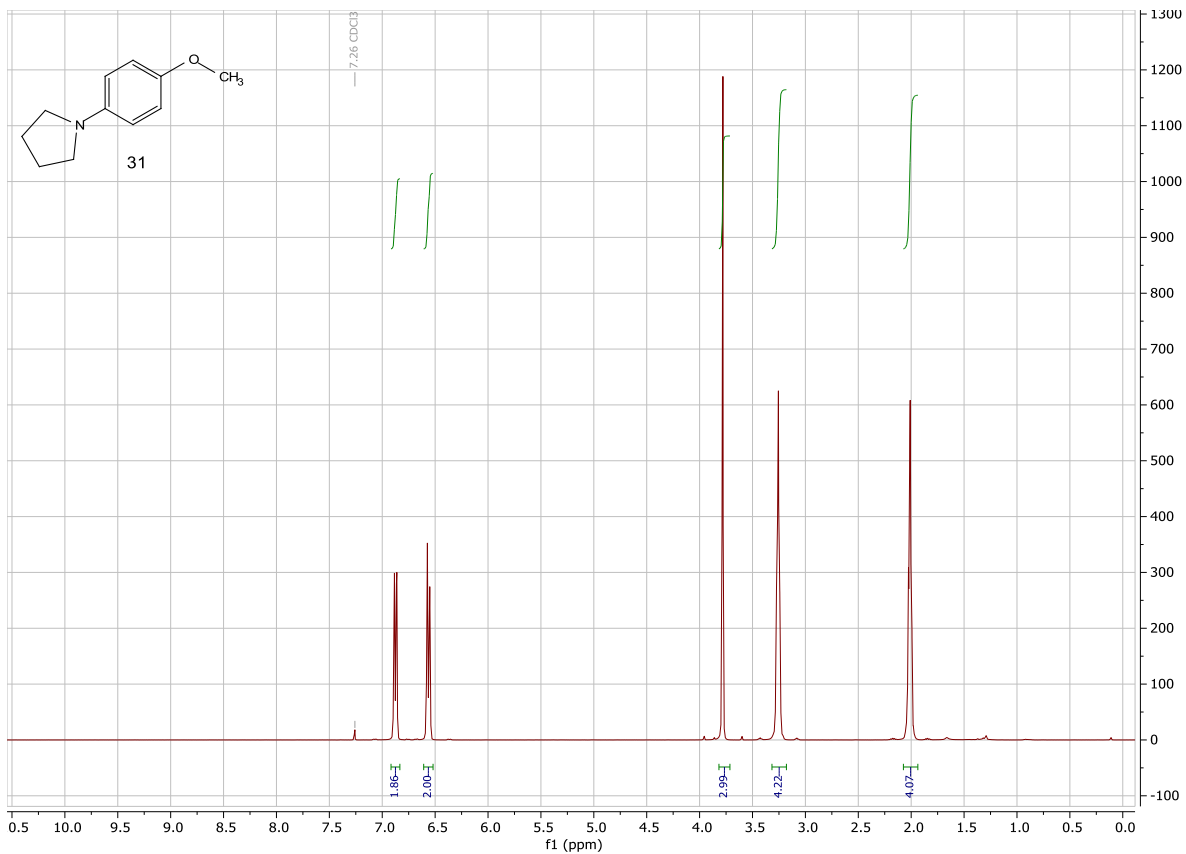












SI.pdf (8.70 MiB)

[view on ChemRxiv](#) • [download file](#)
